博士論文

論文題目　Homeostasis, Plasticity, and Memory : A Consequence of Enzyme-Limited Competition
(恒常性、可塑性、記憶 : 酵素競合律速から生まれる生命の普遍性)

氏名　畠山　哲央

Homeostasis, Plasticity, and Memory : A Consequence of Enzyme-Limited Competition

(恒常性、可塑性、記憶： 酵素競合律速から生まれる生命の普遍性)

Tetsuhiro S. Hatakeyama
畠山　哲央

February 2014

Everything needs to change, so everything can stay the same.
— Giuseppe Tomasi di Lampedusa, *The Leopard*

Contents

Part I

Introduction

Chapter 1

General Introduction

1.1 How to Understand Life?

"What is life?"

All of us may have ever thought such question at least once and none of us can have ever perfectly answered such question even once. Although this question has provoked endless discussions, the answer is still in controversy. We do not have the perfect answer, which anybody will agree with. Probably we will not reach the perfect answer in the future. It is because we are also living organisms, so that an answer to the question potentially has to include our own identity. Therefore, an answer to the opening question, i.e., a definition of life, is apt to become subjective. Because a definition of life is subjective, a definition of biology, that is, how should understand life, cannot but include a subjective part. When different persons say the word "biology", the implication may be greatly different by person.

In contrast, academic activities are always under pressure to be objective. Of course, the biology is no exception, too. Such pressures are not brought by transcendent existence, but players in biological fields make pressure each other. If there are two biologists, they will have different definitions of life, and they will press each other to reduce the gap between their own definitions. This repetition may underlie foundation of today's biology.

Then, where will we arrive at the end of such repetition? Is there a perfect answer at the end of this repeat? As suspected, there may not be a perfect answer. If that is the case, what meaning will such repetition have? Although there is no perfect answer, there may be universal characters and/or universal

rules which are common among anybody's own sense of life. To unveil such universal features will also be a key to fill the gap between subjective biologies and objective biology, and which itself can be the goal. It is because I believe that there is universality of life that I have written this doctoral thesis.

What should we do to uncover universal features of life? A great number of people have endeavored to unveil the essence of life, nonetheless we have not yet been able to uncover it. To discuss the issue, we should rethink concepts and failures of modern biologies.

First of all, we should think about a question: is the essence of the life "materials" or "phenomena"? Even if we used the same definition of life, biology could be a completely different academic activity, when we take a different viewpoint. As an example, consider the case that we assumed a self-reproduction property as a definition of the life. If we regard "materials" as the essence of life, then we the principle of life is uncovered when we identify molecules (e.g., nucleic acids, proteins, and lipids) relating to self-replication. In contrast, if we assume "phenomenon" as the essence, unveiling features of self-reproduction is the only way to understand life, where we do not have to care about materials constructing actual organisms. Hence, we will rethink about modern biologies based on the viewpoint mentioned above.

Today, molecular biology is the most prosperous discipline in all of biologies (Alberts et al., 2008). A principle of the molecular biology is to understand all of biological phenomena by reducing them into a molecule level. One of the reasons why molecular biology has succeeded today, is that molecules (e.g., DNAs, proteins) are visible. To visualize such molecules, a number of important studies have been accomplished, and the molecular biology has blossomed with such studies. Also, another reason of the success is explicitness of the principle. Most large motivation, which drives the molecular biology to progress, is to catalogize all of biological molecules, which relate to all of the biological phenomena. Even if biologists have their own definitions of life which are different from others, they can progress such catalogization, i.e., if molecular biologists find new biomolecules one after another, finally, perfect catalogue of biomolecules, including the molecular set related with the basis of life, will be completed.

When such perfect molecular catalogue is obtained, can we understand all of life? It is in suspect. Even if we stood in the viewpoint that the essence of life is molecules, we should find a combination of biomolecules, which is

directly relevant to the basis of life. Can we list up all of such combinations? It will be impossible.

First, because the catalogue contains thousands of biomolecules, a combinatorial explosion occurs when we choose a combination of key molecules. Thus, it is practically impossible to find an exact combination relating to the essential condition of life. Moreover, the molecular list will contain a lot of possible combinations. So, some of such combinations may partially correspond to each other while some of that may be completely different from others. As we know some different types of organisms (e.g., prokaryotes and eukaryotes), almost certainly we can find plural sets. Furthermore, if we find the extraterrestrial biological entity consisted of different molecules from well-known list of biomolecules, molecular biologists cannot identify such biological entity as a living organism.

Although catalogization of biomolecules is important as a foundation of progress in biology, we cannot uncover directly the essence of life from such catalogue unless there is the molecule of vital force.

Then, should we directly deal with a set of biomolecules rather than a single molecular species?

In synthetic biology, one focuses on how to combine molecules (Andrianantoandro et al., 2006). In contrast to main activity in the molecular biology that seeks for and identifies biomolecules, the main theme of the synthetic biology is reconstruction of some biological functions by mixing several molecular species in a test tube.

By this reconstruction, can we resolve the question, what is life? The answer is no. Some synthetic biologists have frequently quoted a text left by Feynman : "What I cannot create, I do not understand", and they have explicated that "if we create an organism, we can understand life" (Alberts, 2011). However, the converse is not necessarily true. If we take the contraposition, the true text will become "If I understand, I can create." Moreover, needless to say, we can create something without understanding, i.e., if we do not understand mechanism of human beings, we can make a baby. Here, even if we create a perfect organism, it is possible that a new black box will emerge in front of us.

By reconstruction, we can know a required molecular set for a biological function. However, it is only one set from all of possible combinations of biomolecules. There are many cases that a biological function consists of different mechanisms and different molecules in different organisms, though

the function seems to be same. For example, a circadian rhythm can be found in a wide range of organisms from unicellular bacteria to human, and its behaviors seem to be common. Constituent molecules, however, are different in different species (Bell-Pedersen et al., 2005). Therefore, even if we find one combination of biomolecules for the basis of life, we cannot understand what life is only by one example of such combinations. Furthermore, there is no assurance that the extraterrestrial biological entity uses the same molecular set of us.

In this regard, however, I do not think that the synthetic biology is meaningless. The synthetic biology is useful to separate a complicated bacterial system into several small and simple parts. Synthesis of such parts will facilitate us to understand a particular biological function. For example, when we succeed in reconstructing an artificial system with self-replication property, it will become easy to understand a mechanism of self-replication.

One of the reasons for the failure in the molecular biology and the synthetic biology is to deal with the essence of life as materials. Then, when we treat the essence of life as phenomena, can we unveil the secret of life? Alife (artificial life) is academic activity under such philosophy, with the intention to discuss about all possible life-forms without being restricted by actual organisms in the earth (Langton, 1989, 1992, 1994). Studies in the Alife community focus on reconstructing programs with biological functions mainly on a computer to understand universal features of life. At first glance, this approach can avoid some difficulties as describing above. There is, however, a critical problem.

To discuss this problem, we will discuss about Pocket Monsters, which is a Japanese game software (Pokémon, 1996). In Pocket Monsters, players take care of some artificial creatures called Pokémon and pit such creatures against other player's creatures. On the software, Pokémon grows with defeating enemies, metamorphoses into a different form (such transformation is called "evolution" in this software). When male Pokémon mates with female, it reproduces itself. In this time, a child receives a genetic information from his (or her) parents with a complicated heredity system. Such behaviors are similar with those observed in a real organism. However, most people may not recognize Pokémon as life, because, Pokémon's behaviors are merely imitations of actual organisms and its mechanisms are different from these in real life substantially, in spite of the similarity in the behavior.

Alife studies take a great risk to imitate organisms like Pokémon, because

Alife can be developed without being restricted by real organisms since our definitions of life are too subjective.

From the discussions above, we come to know that it is risky for understanding of life to deal with the essence of life as either materials or phenomena. Then, what kind of approach should we choose?

As discussed above, different organisms often use different materials for the same biological function. For example, prokaryotes and eukaryotes use different molecules and different mechanisms for self-reproduction, and extraterrestrial biological entities may use other molecules and other mechanism. Then, if materials are different, is a phenomenon in concern also different? It is not necessarily the case. To undergo cell division, a cell must duplicate its heredity informations, double its contents including its membrane, and split into two finally. Although composed materials are different among species, the above requirements should be satisfied and mechanisms for such requirements should be provided to achieve self-renewal ability. To satisfy such requirements, organisms are expected to follow common universal rules and laws.

Fumio Oosawa advocated a theory called "loose coupling" from his researches of a motor protein (Oosawa, 2000; Oosawa and Hayashi, 1986). This theory means that outputs from biological machines do not show one-to-one relationship against the same input, which is in strong contrast to artificial machines. This is because biological machines have several internal states and use internal and external noises. Of course, it does not mean that outputs of biomolecules are arbitrary, but there are loose rules.

This loose coupling thesis from materials to phenomenon may also be applied to a connection from phenomenon to materials in general, i.e., correspondence between constitutive materials and mechanisms of a biological function is not uniquely determined. Of course, it does not mean that any phenomenon can be generated from any materials, and there are some rules that loosely determine the connection. Such loose coupling may introduce a constitutive difficulty to one-side approaches either from only material or phenomenon to understand life. However, loose coupling between phenomenon and material has a positive side to understand life. If phenomenon and materials are loosely coupled, underlying rules between such coupling is expected to obey general laws, following thermodynamics, dynamical systems theory, network theory, and so fourth, rather than special rules for each case. The study in a molecular motor by Oosawa and his colleagues will provide an

example. He demonstrated that the dynamics of a molecular motor can be explained as an analogy to Feynman's ratchet whose function is governed by the law of thermodynamics (Vale and Oosawa, 1990). In contrast, if a coupling is tight, materials should be finely tuned for the phenomenon, which will be determined by specific rules and mechanisms for individual phenomena. For example, to understand a feature or a structure of an artificial machine, we will need to understand a function of individual screws and gears. In contrast, the loose coupling between phenomenon and materials will facilitate our generic understanding of similar phenomenon in different organisms, and we except that rules underlying such loose coupling will be universal among all of the living things.

Now even though, there are no perfect definitions of life which can be satisfied by all of the people, there can be universal laws commonly shared by anybody's definitions of life. If we understand such universal rules, we can reconstruct a possible living being from materials completely different from those adopted by the present living organisms we know. At this time, we may realize true intention of Feynman's phrase, "What I cannot create, I do not understand."

Understanding the universal rules underlying the loose coupling is a different kind of biology, whose example I would like to demonstrate an ultimate goal of the present doctoral thesis. At least, I hope that this thesis contributes to understand of a class of universality in common to certain biological topics. This direction could commonly be shared by researches in systems biology and quantitative biology. Unfortunately, majority in the field aim at just quantitative or complicated version of molecular or synthetic biology. Thus, if we should name this motivation, "universal biology", advocated by Kunihiko Kaneko (and also by Sakyo Komatsu in science fiction of about 40 years ago (Komatsu, 1972)), will be appropriate, probably.

1.2 Topics in the Present Thesis

Before we discuss spacific topics in the present thesis, we should return to the opening question, "what is life." We will quote the wikipedia as an example of answer to this question (Wikipedia, 2013). In the wikipedia, definitions of life are described below:

1. Homeostasis: Regulation of the internal environment to maintain a

constant state; for example, electrolyte concentration or sweating to reduce temperature.

2. Organization: Being structurally composed of one or more cells — the basic units of life.

3. Metabolism: Transformation of energy by converting chemicals and energy into cellular components (anabolism) and decomposing organic matter (catabolism). Living things require energy to maintain internal organization (homeostasis) and to produce the other phenomena associated with life.

4. Growth: Maintenance of a higher rate of anabolism than catabolism. A growing organism increases in size in all of its parts, rather than simply accumulating matter.

5. Adaptation: The ability to change over time in response to the environment. This ability is fundamental to the process of evolution and is determined by the organism's heredity, diet, and external factors.

6. Response to stimuli: A response can take many forms, from the contraction of a unicellular organism to external chemicals, to complex reactions involving all the senses of multicellular organisms. A response is often expressed by motion; for example, the leaves of a plant turning toward the sun (phototropism), and chemotaxis.

7. Reproduction: The ability to produce new individual organisms, either asexually from a single parent organism, or sexually from two parent organisms.

Although the above list is not well ordered, it may gain a broad consensus. Most of such criteria are required for self-sustainment. For example, "adaptation" and "homeostasis" are required not to change the state of an organism itself against changes in external environments, whereas "response to stimuli" is required to change substantially some part of an organism while keeping most part of it constant. "Growth" and "reproduction" contribute to a long term self-sustainment by making clones. Doubtlessly, the self-sustainment is one of the essence of life.

The self-sustainment is achieved across multi-layers of biological systems. The first layer is "from molecules to cells". In this layer, a cell state is

kept constant by partially changing molecular states (e.g., state of a single molecule, proportion of concentrations of molecules). The second layer is "from cells to individuals". In this layer, an individual state is kept constant by partly changing cellular states. Further, there is a layer "from individuals to ecosystems." In the present thesis, we mainly discuss the layer "from molecules to cells" while it is partly related with the layer "from cells to individuals."

For self-sustainment, it is important to keep internal states constant against changes in external environments. This property is called as homeostasis (or robustness). Body temperature regulation is the most famous example of homeostasis (Benzinger, 1969). If body temperature increases too much, the organisms will come to death state because of disruption in a balance of speeds of biochemical reactions and of denaturing of biomolecules. To avoid it, some homeothermic animals sweat to decrease their body temperature by heat of evaporation. Such functions to keep its own condition constant is homeostasis.

In contrast, to use changes in external environments often provide large advantages for subsistence, and sometimes facilitate to avoid risks of death. Thus, organisms should alter their internal states against changes in external conditions. Such property is called as plasticity. Chemotaxis may be thought as one example of plasticity (Adler, 1966; Bargmann and Horvitz, 1991; Gerisch, 1982). It is a cellular function by which cells approach attractants and escape from repellants, and is observed in variety of organisms from bacteria to eukaryotes. If organisms had no chemotaxis, they could not find new food efficiently when food is depleted, and would be starved finally. Moreover, when a poison is administrated, they would fail to escape from the poison. Thus, without plasticity to respond to external change, self-sustainment would be hard to be achieved.

It is important to unclear the mechanism of each homeostasis and plasticity, for the understanding of life (Kaneko, 2006). Note that homeostasis implies resistance to change and plasticity implies feasibility to change. They seem to be incompatible at first glance. How organisms can achieve both of the two conflicting features is a principal problem.

As described above, adaptation to changes in external environments is important for self-sustainment, and external environments have various timescales, from sub-seconds to hours, days, and years. Thus, it is also important for

self-sustainment to control a timescale of internal chemical reactions in the cell. Although a timescale of the ordinary biochemical reactions is known as a sub-second order (Phillips et al., 2010), changes in external environments have a much longer timescale. Moreover, repeated and continuous changes may occur more frequently than one-time transient change. To cope with such frequent changes, it will be more effective to prepare such cellular state that can adapt to such changes in a fast timescale. For it, cellular state needs to store informations of such frequent experiences, preserved in a much longer timescale. This is memory in the cell. In spite of importance and universality of such cellular memory, however, detailed mechanisms for it is not unveiled.

The main claim in this doctor thesis is that homeostasis, plasticity, and memory in a cell can be achieved as universal features of enzymatic reactions. First we will discuss about universality in biochemical reactions and introduce a new concept called "enzyme-limited competition" in Chapter 2. In Chapters 3 and 4, we will discuss a mechanism of homeostasis and plasticity of circadian clocks and show how these two features are compatible. In Chapters 5 and 6, we will show that a timescale of enzymatic reactions can be prolonged by enzyme-limited competition and such reactions can work as cellular memory. Finally, we will summarize all topics coherently and about a plan of future works.

Chapter 2

Biological Universality as a Consequence of the Enzymatic Reaction

2.1 Universality of Enzymatic Reactions

To understand a biological function at a "from molecules to cells" layer, we should study universality in biochemical reactions in a cell. For biochemical reactions, it is important to clarify a function of enzymes (catalysts). Here, enzymes can facilitate slow reactions with high activation energies. If activation energies for the whole reactions in the cell are too low, distribution of concentrations of biomolecules in the cell may approach a thermal equilibrium state soon, and it is difficult to maintain a highly organized state as actual organisms. On the other hand, if activation energies for the whole reactions are too high, internal reactions progress more slowly than changes in external environments, and cells never show any vivid behaviors. It is like a stone. Enzymes work like a switch between the above two states. When the amount of enzymes is sufficient, biochemical reactions progress without any delay, whereas for low enzyme concentrations, biochemical reactions progress too slowly. Schrödinger proposed in his book "What Is Life?" that living matter maintains negative entropy to avoid a disordered state (Schrödinger, 1944), and such spontaneous order formation in a cell can be achieved only in the presence of enzymes. This is also consistent with the project for synthesizing artificial cell by Szostak and others, where encapsulated catalyst is

a key issue for a complex protocol to emerge (Szostak et al., 2001). They described that it is important for evolving of complexity of a protocell to emerge a catalyst (ribozyme). Hence we first focus on universal characteristics of enzymatic reactions. Note that following discussions can only adapt to living matters which use chemical reactions as an elemental ingredient, and might not adapt to other types of life form.

2.1.1 Michaelis-Menten kinetics (and Hill kinetics)

Kinetics of the catalytic reactions are roughly divided into two types. The first type is a mass-action kinetics. An example of reactions schemes is described below:

$$C + S \xrightarrow{k} C + P \tag{2.1}$$

and its differential equations are described below:

$$\begin{aligned} \frac{d[S]}{dt} &= -k[C][S] \\ \frac{d[P]}{dt} &= k[C][S] \end{aligned} \tag{2.2}$$

where S and P are a substrate and product, respectively. C is a catalyst, and $[x]$ is a concentration of x. It is a slight extrapolation from the equilibrium thermodynamics, but is reasonable by considering that reaction speeds depend only on collision probability. It has been confirmed in many experiments. Note that when multiple substrates react, the above equations are altered as follows:

$$\begin{aligned} C + nS &\xrightarrow{k} C + P \\ \frac{d[S]}{dt} &= -nk[C][S]^n \\ \frac{d[P]}{dt} &= k[C][S]^n \end{aligned}$$

When a catalyst and substrate make a reaction intermediate, there is an appropriate description of reaction dynamics, that is Michaelis-Menten kinetics (Michaelis and Menten, 1913). An example of reaction scheme is

described below:

$$C + S \underset{k_-}{\overset{k_+}{\rightleftarrows}} CS \xrightarrow{k} C + P \tag{2.3}$$

The above scheme can be described as the following equations:

$$\frac{d[S]}{dt} = -k_+[C][S] + k_-[CS] \tag{2.4}$$

$$\frac{d[CS]}{dt} = k_+[C][S] - k_-[CS] - k[CS] \tag{2.5}$$

$$\frac{d[P]}{dt} = k[CS] \tag{2.6}$$

where, CS is a complex between the catalyst and the substrate. Here, if k_+ and k_- are larger than k, i.e., association and dissociation reactions are faster than the catalytic reaction, concentrations of S and CS will reach stationary concentrations quickly and dynamics of these concentrations will be able to be eliminated adiabatically. By using a conservation concentration of the catalyst ($[C]_{total} = [C] + [CS]$), the above equations can be described below:

$$\frac{d[P]}{dt} = \frac{k[C]_{total}[S]}{K_d + [S]} \tag{2.7}$$

where, K_d is a dissociation constant, described as $K_d = (k_- + k)/k_+$. When multiple substrates react, the equation is altered to:

$$\frac{d[P]}{dt} = \frac{k[C]_{total}[S]^n}{K_d^n + [S]^n} \tag{2.8}$$

This equation is called as Hill kinetics (Hill, 1910).

Almost enzymatic reaction dynamics in the cell follows the Michaelis-Menten kinetics or the Hill kinetics because ordinarily association and dissociation reactions are faster than catalytic reaction. In the Michaelis-Menten form, the maximum speed of such reactions follows a concentration of the enzyme and not a concentration of the substrate, as the concentration of the substrate is too increased. This is because an active site of an enzyme is reshaped by interactions with substrates in the modified lock-and-key model (the induced-fit model) (Koshland, 1958) and such reshaping reaction should be slower than binding reactions. In contrast, reactions with a metal-catalyst follows the mass-action kinetics. This is because the metal-catalysts have a

360-degree active sites. Thus, the maximum speed of these reactions follow a concentration of the substrates.

How broad is the universality of such Micaelis-Menten kinetics in the living matters (not only for present organisms but also for the whole possible living being including extraterrestrial biological entities)? To consider this problem, we should think how the basis of Michaelis-Menten kinetics, such as assumptions that a catalyst is occupied by a single substrate and make a complex, and association and dissociation between a catalyst and a substrate are faster than the catalytic reaction ($k_+, k_- \ll k$), will be achieved in the origin of life and through evolution of enzyme.

Hypotheses on the origin of life can be roughly divided into two types, "information first" and "metabolism first." "Information-first hypothesis" assumes that genetic information and a robust hereditary system emerge first and then complex metabolic systems evolve. "Metabolism first hypothesis" assumes that a metabolic system, which is loosely inherited, appears first and then a robust hereditary system evolves later. For the robust hereditary system, a reliable replication machinery for information molecules will be required in order to avoid error catastrophe. Moreover, for the loosely-inherited metabolic system, catalysts also need high specificity to synthesize molecules with high catalytic activity preferentially, because synthesis of a molecule with low catalytic activity (called a cheater) will decline the reproduction rate of cells. Although it is still open which hypothesis is plausible, both hypotheses will need evolution of catalysts to have higher specificity.

To achieve high specificity, a catalyst generally has some regulatory sites with an active site which is relatively small. Such small active site will provide an one-on-one binding between a substrate and a catalyst, because the substrate bound to the active site occupies the catalyst and prevents other substrates from binding to such catalyst. Thus, the substrate and the catalyst will make a catalytic-reaction intermediate before making product. Therefore, the kinetics of such catalyst with higher specificity will not follow the simple mass-action kinetics. Once an active site of a catalyst is occupied by a substrate, then the catalyst cannot bind to other substrates. Hence the reaction rate will be saturated as the substrate is much more abundant than catalyst. This is in contrast with most metal-catalyst where many active sites exist on the metal surface.

Moreover, to evolve higher specificity, catalyst often shows a slower conformational change after binding to a substrate for achieving the conforma-

tional proofreading (Savir and Tlusty, 2007). For example, it is known that ribozyme structure is changed by binding with a substrate (Cochrane and Strobel, 2008) and a substrate-dependent conformational change increases fidelity (Bergeron and Perreault, 2005). The slower conformational change leads to $k_+, k_- \ll k$, the requirement for Michaelis-Menten kinetics. Such scenario may be independent of material of catalyst. Therefore, the Michaelis-Menten kinetics can be universally adapted to a wide class of living matters.

2.1.2 Chemical modification and multimerization

The organisms use many kind of post-translational modifications of proteins, e.g, phosphorylation, methylation, and acetylation, and it known that information molecules (DNA) are also chemically modified in particular methylated (Bird, 2007). Such chemical modifications are observed in various biological functions of actual organisms, e.g., metabolisms, signal transductions (Cohen, 2000), and epigenetic regulations by changing states of information molecules (Bird, 2007; Jablonka et al., 1992). Are these modification universal? To discuss this problem, we should rethink about some features of such modifications.

First, chemical modifications can easily increase the variety of species of molecules. Recent comprehensive analysis of the human genome revealed that the number of genes in human is approximately 21000 at most (Pennisi, 2012). On the other hand, the number of genes in *Escherichia coli* is approximately 4300 (Blattner et al., 1997). Thus, the number of genes in human is five times as large as that in *E.coli*. At a glance, this number seems too low to control complicated biological functions in human. However, the typical number of phosphorylation sites in a protein (n) shows a significant increase from $n \leq 7$ in prokaryotes to $n \geq 150$ in eukaryotes (Gnad et al., 2007; Thomson and Gunawardena, 2009). The number of combinations of on/off controls of phosphorylations in proteins may increase a variety of biomolecules at an accelerated rate with progression of evolution. Of course organisms may not use all possible combinations, but post-translational modifications may be one of the most important reasons why eukaryotes can control complex dynamics with a relatively small number of genes.

One of the reasons why relatively small number of genes is used in eukaryotes may be due to the increase in a cost of maintaining information molecules. If all of molecules in a organism are directly coded by information molecules, a large amount of information molecules may be necessary. Cost

for maintaining such molecules would increase terribly because proofreading machinery is also needed to correct possible errors in polymerized reactions. When organisms evolve to gain a new biological function, they will require a number of new biomolecules. At that time, if such new biomolecules are directly coded by information molecules, direct maintenance will become hard and cost for maintenance throughout evolution will be heavy. Thus, use of the chemical modification to increase the number of molecular species will be advantage for the organism. Indeed, all of the living organisms use chemical modifications of their components (Gnad et al., 2007) and it is thought to contribute to avoid the explosion of a size of information molecules.

Next, chemical modifications can alter a timescale of reactions independently of the timescale of syntheses of biomolecules and that of changes in information molecules. If chemical modifications progresses with a faster timescale than the timescale of syntheses of biomolecules, it will be advantageous for a fast adaptation against changes in external environments, since the adaptation is possible without new synthesis of a biomolecule.

Moreover, fast chemical modifications can also regulate syntheses of biomolecules. If the number of biomolecules is suddenly increased or decreased externally, such fast regulation in syntheses of biomolecules can work to bring back the number of biomolecules to the original level in a fast timescale. In contrast, if timescales of both syntheses of biomolecules and regulations of such syntheses are of the same order, the slow negative feedback will often lead to oscillation like air conditioner with ineffective thermal feedback (Alon, 2007) and a homeostatic response will not be achieved.

If chemical modifications progresses with a faster timescale than a timescale of the evolution and with a slower timescale than that of ordinary molecular syntheses and degradations, such modifications may work as a memory, which may be advantageous for a long-term adaptation. Hence such altered timescales are important for organisms to achieve homeostasis, plasticity, and memory.

Organisms which have faster timescale than syntheses of biomolecules can adapt to sudden changes in environments and can easily enter a new ecological niche. Moreover, having longer timescale than bimolecular syntheses will help organisms to prosper under changing environments over a long time. Therefore, when the living matters evolve, they will have various different timescales in their bodies. Thus, using the chemical modifications is one of the most reasonable solution, though they may use different functional groups from actual organisms.

Furthermore, it also important that chemical modifications can change physical properties of biomolecules. For example, a phosphate group adds a negative charge to the substrate, and it is known that such effect works in a metabolism by inhibiting diffusion of a glucose from a membrane (Alberts et al., 2008). In the origin of life, it is important to cohere biomolecules into higher concentration, and such chemical modifications may work effectively to agglutinate molecules. To sum-up, chemical modifications are adapted to a wide class of organisms, due to the above advantages for life processes.

Multimerizations of biomolecules can work in the same way as chemical modifications. Furthermore, multimerizatons is expected to be advantageous for organisms for other reasons (Lynch, 2012). One potential advantage of protein multimerizations is the increase of structural size of the protein. With this increase, the encounter rate for reactions is increased while resulting decrease in surface-area to volume ratio reduce the vulnerability of the protein leading to denaturation. Furthermore, such multimerizaion also increases opportunities for allosteric regulation of its activity. It is suggested that variation in the multimeric states of proteins can readily arise from stochastic transitions from a monomer to a multimer, resulting from the joint processes of mutation and random genetic drift (Lynch, 2013). In contrast, the number of phosphorylation sites increase gradually along with the evolution (Gnad et al., 2007). The effective number of molecular species can be increased combinatorially by introducing a few number of chemical modifications in a biomolecules.

2.2 Enzyme-Limited Competition

So far we have discussed that the Michaelis-Menten equations and the multiple modifications in biomolecules are prevalent in the living organisms. It often comes to the case that multiple modifications are catalyzed by a single catalyst. Actually, in the existing organisms, it is known that the same protein kinase phosphorylates various proteins. In this case, if the number of a catalyst is not much larger than that of substrates, competition for a limited catalyst should follow, i.e., when the amount of a catalyst (enzyme) is less than that of substrates, substrates will compete for a catalyst. We call such situation as “enzyme-limited competition (ELC).”

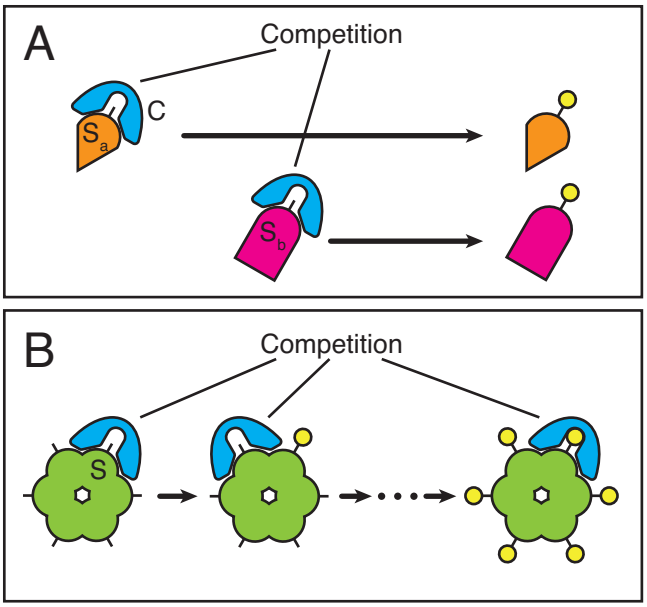

Figure 2.1: The schematic representation of (A) a parallel ELC and (B) a sequential ELC. (A) S_a and S_b are different substrates with a modification site, which is modified by the same catalyst C. (B) S is a substrate with multiple modification sites, which are modified by the same catalyst C in a step-by-step manner.

There could be two types of enzyme-limited competition, a parallel ELC and a sequential ELC (see Fig.2.1). In the former, parallel reactions with different substrate species in the same spaces are catalyzed by the same enzyme, and in the latter, successive reactions with the same substrate species with different modification forms are catalyzed by the same enzyme.

Earlier studies have mainly focused on the parallel ELC, in which different substrate species compete for a same catalyst. A scheme of the parallel ELC is presented in Fig.2.1A. Parallel ELC provides a switch by mutual inhibition between two reactions via the competition for a common enzyme (Thattai and Shraiman, 2003), while catalytic reaction with two substrates sharing the same catalyst provides both of negative and positive correlations between their products (Cookson et al., 2011; Mather et al., 2013, 2010). In the living organisms, the parallel ELC is thought to be metabolic of carbon sources (Thattai and Shraiman, 2003). The parallel ELC can mainly produce functions of an ultrasensitivity and a switch.

In contrast, in the present thesis, we will mainly focus on a sequential ELC, in which the same substrates with a different number of modified sites compete for the same catalyst (Fig.2.1B). Multimerizations of biomolecules will increases the likelihood of the sequential ELC, because modification sites in different subunits in the same multimertic protein will be catalyzed by the same enzyme. In this case, the behavior of modification dynamics is critically different from the parallel ELC, because an increase in the abundances of some substrate directly induces a decrease in the abundance of other substrates, and vice versa. Actually, from the next chapter, we will discuss two salient features by the sequential ELC, i.e., temperature compensation of circadian clocks and cellular memory.

The ELC may have many applications other than above two examples. Molecular networks in the organism (e.g., metabolic and signaling networks) arguably have rate-limiting steps. For example, three steps are rate-limiting in glycolysis (Alberts et al., 2008), i.e., first (hexokinase), third (phosphofructokinase 1), and tenth steps (pyruvate kinase), and RAF phosphorylation is rate-limiting in RAS signaling (Hibino et al., 2011). Although such rate-limiting steps are thought to be important to determine dynamics of whole biological networks because they can alter the slowest timescale in networks drastically, little attention has been given to problems why they are rate-limiting and how they are controlled. To think these problems, we should notice to the ELC. In the upper stream of a rate-limiting step, some molecules must be accumulated owing to slowing down at the rate-limiting step. In this

case, such accumulated molecules will compete for the rate-limiting catalyst. Conversely, there may be cases that a rate-limiting step is achieved by the ELC. Thus, the ELC is thought to be ubiquitous as well as the rate-limiting step and to be important to determine the whole dynamics of biological networks. Two examples in the present thesis would be helpful to understand multiple functions of the ELC.

Before describing examples of the sequential ELC, we will present its basic structure. The scheme is presented in Fig.2.1B and reactions are described below:

$$C + S_i \underset{k_{-i}}{\overset{k_{+i}}{\rightleftarrows}} CS_i \xrightarrow{k_i} C + S_{i+1}$$

where S_i and CS_i denote the substrates and a substrate-catalyst complex with i modified sites, respectively, and C denotes the catalyst. Here, differential equations that govern the dynamics of concentrations is derived by the same procedure as the Michaelis-Menten formulation. By denoting the concentration of free catalyst that does not form a complex as $[C]_{free}$, the model can be described as:

$$\begin{aligned}
[\dot{S}_0] &= -k_0 \frac{[C]_{free}[S_0]}{K_0 + [C]_{free}} \\
[\dot{S}_i] &= -k_i \frac{[C]_{free}[S_i]}{K_i + [C]_{free}} \\
&\quad + k_{i-1} \frac{[C]_{free}[S_{i-1}]}{K_{i-1} + [C]_{free}} \\
[\dot{S}_N] &= k_{N-1} \frac{[C]_{free}[S_{N-1}]}{K_{N-1} + [C]_{free}} \qquad (2.9)
\end{aligned}$$

$$[C]_{total} = \sum_{i=0}^{N} \frac{[C]_{free}[S_i]}{K_i + [C]_{free}} + [C]_{free} \qquad (2.10)$$

where $K_i (= k_i^- / k_i^+)$ are the dissociation constants between S_i and C.

In the following chapters, we will mainly deal with cases in which dissociation constants depend on the number of modified sites, i.e., $K_0 \neq K_1 \neq \cdots \neq K_{N-1} \neq K_N$. This is rather natural, because a single modification in a substrate can change the whole structure of the substrate, and such structural change must alter an affinity between the catalyst and the substrate. Indeed, the structures of proteins is known to change by a single phosphorylation,

while such structural change regulates their functions.

Part II

Biological Clock

Chapter 3

Generic Temperature Compensation Based on Enzyme-Limited Competition

Chapter Outline

Circadian clocks — ubiquitous in life forms ranging from bacteria to multicellular organisms — often exhibit intrinsic temperature compensation; the period of circadian oscillators is maintained constant over a range of physiological temperatures, despite the expected temperature dependence from the Arrhenius law for the reaction coefficient. Observations have shown that the amplitude of the oscillation depends on the temperature but the period does not—this suggests that although not every reaction step is temperature independent, the total system comprised of multiple reactions still exhibits compensation. Here we present a general mechanism for such temperature compensation. Consider a system with multiple activation energy barriers for reactions, with a common enzyme shared across several reaction steps. The steps with the highest activation energy rate-limit the cycle when the temperature is not high. If the total abundance of the enzyme is limited, the amount of free enzyme available to catalyze a specific reaction decreases as more substrates bind to the common enzyme. We show that this change in free enzyme abundance compensates for the Arrhenius-type temperature dependence of the reaction coefficients. Taking the example of circadian clocks with cyanobacterial proteins KaiABC, consisting of several phosphorylation

sites, we show that this temperature compensation mechanism is indeed valid. Specifically, if the activation energy for phosphorylation is larger than that for dephosphorylation, competition for KaiA shared among the phosphorylation reactions leads to temperature compensation. Moreover, taking a simpler model, we demonstrate the generality of the proposed compensation mechanism, suggesting relevance not only to circadian clocks but to other (bio)chemical oscillators as well.

3.1 Introduction

The circadian clock is one of the most remarkable cyclic behaviors ubiquitous to the known forms of life, ranging from the unicellular to the multicellular level—including prokaryotes. Because of its importance, the underlying chemical reactions have been the subject academic interest for a long time and have recently been elucidated experimentally. Thus, we now know that circadian clocks have three important features:
1. They persist in the absence of external cues with an approximately 24-h period, which is rather long compared with most chemical reactions.
2. They can be reset by exposure to external stimuli such as changes in illumination (dark/light) or temperature.
3. The period of the circadian clock is robustly maintained across a range of physiological temperatures. (temperature compensation) (Hastings and Sweeney, 1957; Pittendrigh, 1954) .

Generally, the rate of chemical reactions depends strongly on the temperature. Indeed, most biochemical reactions have an energy barrier that must be overcome with the aid of enzymes, and thus the rate can be expected to follow the Arrhenius law. For this reason, the period of chemical or biochemical oscillators can be expected to strongly depend on the temperature (Dutt and Mueller, 1993). However, this is not case: temperature-compensated biological circadian clocks are ubiquitous, which suggests some generic mechanism(s) behind it. Although the emergence of cyclic behavior with a capacity for entrainment is theoretically understood as being a result of the existence of a limit-cycle attractor in a class of dynamical systems described by chemical rate equations, this does not provide a mechanism that can explain temperature compensation.

Overall, there are two possibilities for such a mechanism: one is that compensation exists at each elementary step, and the other is that compensation

occurs at the system level—for the total set of enzymatic reactions. Recently, it was found that the rates of some elementary reaction steps in circadian clocks depend only slightly on temperature (Isojima et al., 2009; Terauchi et al., 2007), suggesting that the activation energy barrier of some reactions is rather low. This suggests element-level compensation. However, it is difficult to imagine that every reaction step is fully temperature-compensated at the single-molecule level. Indeed, if that were the case, temperature changes would not influence the oscillation of chemical concentrations at all. In contrast, it is known that the amplitude changes indeed depend on temperature (Liu et al., 1998; Majercak et al., 1999; Nakajima et al., 2005), even though the period does not. Furthermore, circadian clocks are known to entrain to external temperature cycles, and they can be reset by temperature cues (Liu et al., 1998; Merrow et al., 1999; Yoshida et al., 2009). Although temperature changes can influence the oscillation, the period is still robust.

Hence, it is necessary to search for a general logic that underlies the temperature compensation phenomenon at the system level. Indeed, several models have been proposed (Akman et al., 2008; Hong et al., 2007; Hong and Tyson, 1997; Kurosawa and Iwasa, 2005; Leloup and Goldbeter, 1997; Ruoff, 1992). In most of the system-level studies, several processes that are responsible for the period are considered, which cancel out each other's temperature dependence. This is a balance mechanism by which temperature compensation can be achieved. Such a mechanism, however, requires a fine-tuned set of parameters or, rather, an ad-hoc combination of processes for balancing. Considering the ubiquity of temperature compensation, a generic and robust mechanism that does not require tuning parameters is desirable.

Here we propose such a mechanism that has general validity for any biochemical oscillator consisting of several reaction processes catalyzed by enzymes. The mechanism can be briefly outlined as follows:

Biochemical clocks are comprised of multiple processes, such as phosphorylation and dephosphorylation, with each generally having a different activation energy barrier ΔE. The rate of such reactions, then, is given by $k[A]_{free}\exp(-\Delta E/T)$, where $[A]_{free}$ is the concentration of "free" enzyme available, and k is the rate constant. If the enzyme concentration were insensitive to temperature, the rate would just agree with the simple Arrhenius form, thus implying high temperature dependence. Now, consider a situation where several substrates share the same enzyme. At lower temperature, the reactions with higher activation energy will be slower and the substrates involved in these reactions will accumulate. Then, because they share the

same enzyme, competition for the enzyme will also increase. Accordingly, the concentration of available (free) enzyme decreases, and when it reaches a level satisfying $k[A]_{free}\exp(-\Delta E/T) \sim \tau_0^{-1}$, where τ_0 is the inherent time scale of the system (τ_0 is the basic reaction rate), these enzymatic reactions will be highly suppressed. The system spends most of its time under such conditions, which limits the rate. Thus, the Arrhenius-type temperature dependence is compensated for by the concentration of available enzyme as $[A]_{free}\exp(-\Delta E/T) \sim \tau_0 k \sim 1$.

Although this is a rather basic description, its validity may suggest that temperature compensation emerges in any general chemical oscillation consisting of steps, catalyzed by a common enzyme. Here, we first study the validity of this enzyme-limited temperature compensation mechanism for the specific case of the Kai protein clock model introduced by van Zon et al. (van Zon et al., 2007) to explain the circadian clock of KaiABC proteins in cyanobacteria, which was discovered by Kondo and his colleagues (Ishiura et al., 1998; Nakajima et al., 2005) Indeed, in this system, the period of circadian oscillation of Kai proteins is temperature compensated (Nakajima et al., 2005). Further, although some of the elementary components in this system, specifically, KaiC's ATPase activity and KaiC's phosphatase activity, were suggested to depend only slightly on temperature (Terauchi et al., 2007; Tomita et al., 2005), the origin of system-level temperature compensation has not yet been explained without imposing a balance mechanism. Here, we show numerically that system-level temperature compensation emerges due to competition for limited enzymes, without the need for tuning parameter values. Furthermore, we elucidate the conditions necessary for this temperature compensation to work. Then, based on this analysis, we illustrate the above mechanism with a simpler model consisting of a few catalytic reactions. Possible relations between our results and reported experimental findings for circadian clocks are also discussed.

3.2 Models

3.2.1 KaiC protein model

The Kai-protein-based circadian clock, discovered by Kondo's group, consists of KaiA, KaiB, KaiC proteins with ATP as an energy source (Nakajima et al., 2005). KaiC has a hexameric structure with six monomers, each with

two phosphorylation sites (Kageyama et al., 2003). It has both autokinase activity and autophosphatase activity, but the autophosphatase activity is usually stronger, and so it is spontaneously dephosphorylated (Nishiwaki et al., 2000; Xu et al., 2003). KaiA, in a dimer form (Kageyama et al., 2003), attaches to KaiC and thus increases its kinase activity, leading to phosphorylation of KaiC (Iwasaki et al., 2002; Xu et al., 2003), whereas KaiB inhibits the activity of KaiA (Williams et al., 2002; Xu et al., 2003). This phosphorylation/dephosphorylation process of the KaiABC proteins constitutes a circadian rhythm.

Here, we simplify the process, to focus on the temperature compensation of the period. We reduce the two phosphorylation residues to just one, because abundance of singly phosphorylated KaiC is strongly correlated with that of doubly phosphorylated KaiC (Rust et al., 2007) so that the phosphorylation of the two residues are equilibrated on a rather short time scale. Next, we do not include KaiB explicitly in our model, because changes in the concentration of KaiB affect the period only slightly (Nakajima et al., 2010). Note that although KaiB is necessary to generate circadian oscillations, the effect can be accounted for by introducing a parameter value for KaiA activity. Here, we adopt a slightly simplified version of the model introduced by van Zon et al. (van Zon et al., 2007) (See also (Brettschneider et al., 2010; Clodong et al., 2007; Johnson et al., 2008; Mehra et al., 2006; Yoda et al., 2007)).

First, each KaiC monomer has two states—active and inactive. Second, allosterically regulated KaiC hexamers in the active state can be phosphorylated, whereas those in the inactive state can be dephosphorylated. A phosphorylated KaiC monomer energetically prefers the inactive state, whereas a dephosphorylated KaiC has the opposite tendency. Here the flip-flop transition between active and inactive states occurs only from the fully phosphorylated or fully dephosphorylated states, as assumed in the concerted MWC model (Monod et al., 1965). No intermediate states are assumed. Hence, the reaction process exhibits a cyclic structure as in Fig.3.1.

Next, KaiA facilitates phosphorylation of active KaiC with an affinity that depends on the number of phosphorylated residues of each KaiC hexamer. KaiCs with a smaller phosphorylation number have stronger affinity to KaiA. This assumption is necessary for generating stable oscillations (van Zon et al., 2007). Then, the reactions are given by

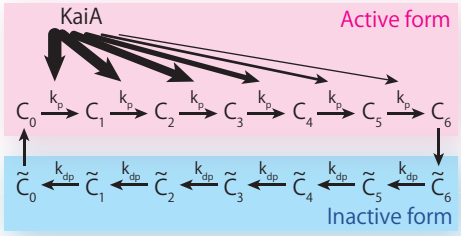

Figure 3.1: A simplified model of circadian clock involving KaiAC proteins based on van Zon et al. (van Zon et al., 2007). A KaiC hexamer, with six phosphorylation sites, can also take either an active or inactive state. The active form of KaiC is phosphorylated by KaiA at rate k_p, whereas in the inactive state, dephosphorylation progresses without any enzymes at the rate k_{dp}. Affinity between active KaiC and KaiA reduces as the number of phosphorylated sites of KaiC increases (represented by the width of arrows).

$$C_6 \xrightarrow{f} \tilde{C}_6, \quad \tilde{C}_0 \xrightarrow{b} C_0, \quad \tilde{C}_i \xrightarrow{k_{dp}} \tilde{C}_{i-1} \tag{3.1}$$

$$C_i + A \underset{k_i^{Ab}}{\overset{k^{Af}}{\rightleftarrows}} AC_i \xrightarrow{k_p} C_{i+1} + A. \tag{3.2}$$

Here C_i and $\tilde{C}_i$ denote active KaiC and inactive KaiC, respectively, with i phosphorylated sites; A denotes free KaiA dimer. To study the temperature compensation of the period, we must also account for the temperature dependence of the reaction rate. Here, the rates of phosphorylation and dephosphorylation are governed by the Arrhenius equation. Then the rate constants k_{dp} and k_p are as follows:

$$k_{dp} = c_{dp} \exp(-\beta E_{dp}), \quad k_p = c_p \exp(-\beta E_p) \tag{3.3}$$

with inverse temperature β ($\beta = 1/T$) by taking the unit of Boltzmann constant as unity. We could include the temperature dependence of the rates f and b in a similar manner, but as the reaction between active and inactive states progresses faster and does not influence the period (van Zon et al., 2007), this dependence is neglected. Even if f and b are temperature-

dependent, the conclusion below does not change, as the corresponding process in [3.1] is faster than others. van Zon et al. demonstrated that temperature compensation occurs when the speed of phosphorylation and dephosphorylation is completely temperature-compensated at the level of elementary reaction process. However, it is difficult to explain why the amplitude of oscillation depends on temperature, or why entrainment to temperature cycles occurs. A compensation mechanism that works at the system level is necessary. Here, the formation and dissociation of KaiAC complexes occur at much faster rates than other reactions and so are eliminated adiabatically. Thus, the change in the concentration $[A]$ is given by

$$[A]_{total} = [A] + \sum_{i=0}^{5} \frac{[A][C_i]}{K_i + [A]} \tag{3.4}$$

where $K_i (= k_i^{Ab}/k^{Af})$ are the dissociation constants. Considering the decrease in affinity for KaiA with the number of phosphorylated sites, we set $K_i = K_0\alpha^i (\alpha > 1.0)$. We adopted the deterministic rate equation given by the mass-action kinetics, and it is simulated by using the fourth-order Runge-Kutta method.

3.2.2 Simpler model with two catalytic reactions sharing the same enzymes

Our simpler model is based on a model introduced by van Zon et al. (van Zon et al., 2007)

In this simpler model, a cyclic change in five substrates occur, as shown in Fig.3.12A. The reactions are given by,

$$S_i + E \underset{k_i^{Eb}}{\overset{k^{Ef}}{\rightleftarrows}} ES_i \xrightarrow{k_i} S_{i+1} + E \quad (i = 0, 1) \tag{3.5}$$

$$S_i \xrightarrow{k_{ps}} S_{i+1} \quad (i = 2, 3, 4) \tag{3.6}$$

Here, $K_i = k_i^{Eb}/k^{Ef}$ is the dissociation constant for the enzyme (E) binding to substrate (S_i).

The rates of each reactions are governed by the Arrhenius equation, so that the rate constants k_i and k_{ps} are given by

$$k_i = c_i \exp(-\beta E_c), \quad k_{ps} = c_{ps} \exp(-\beta E_{ps}) \tag{3.7}$$

3.2.3 Simpler model with three catalytic reactions sharing the same enzymes

Fundamental structure is same as the above model, while three reactions are catalyzed by th same enzyme (Fig.3.11A). Then, the reactions are given by,

$$S_i + E \underset{k_i^{Eb}}{\overset{k^{Ef}}{\rightleftarrows}} ES_i \xrightarrow{k_i} S_{i+1} + E \quad (i = 0, 1, 2) \tag{3.8}$$

$$S_i \xrightarrow{k_{ps}} S_{i+1} \quad (i = 3, 4) \tag{3.9}$$

3.3 Results

3.3.1 Oscillations at varied temperature

As mentioned, a KaiC allosteric model was analyzed. Specifically, we studied the case in which the activation energy for phosphorylation, E_p, is larger than that of dephosphorylation, E_{dp}. See Appendix A for other cases.

For a certain range of parameter values, we found periodic oscillations in the KaiC phosphorylation level and free KaiA abundance, as shown in the time series in Fig.3.2A. The oscillation is described by a limit-cycle attractor, as represented by the orbit in a two-dimensional plane in KaiC phosphorylation level and free KaiA abundance (Fig.3.3). As the temperature increases, the amplitude of the limit-cycle increases (Fig.3.2A). Lowering the temperature causes a decrease in the maximum amount of free KaiA and an increase in the minimum level of KaiC phosphorylation. Further lowering it, however, results in the limit-cycle changing into a stable fixed point via Hopf bifurcation. The timeseries of $[C_i](i = 0, 1, 2, .., 6)$ and the temperature dependence are shown in Fig.3.2B. With a decrease in temperature, we see an increase in $[C_5]$, that is, the abundance of KaiC with five phosphorylated residues (5P-KaiC), which leads to an increase in the minimum KaiC phosophorylation level, as shown in Fig.3.2B.

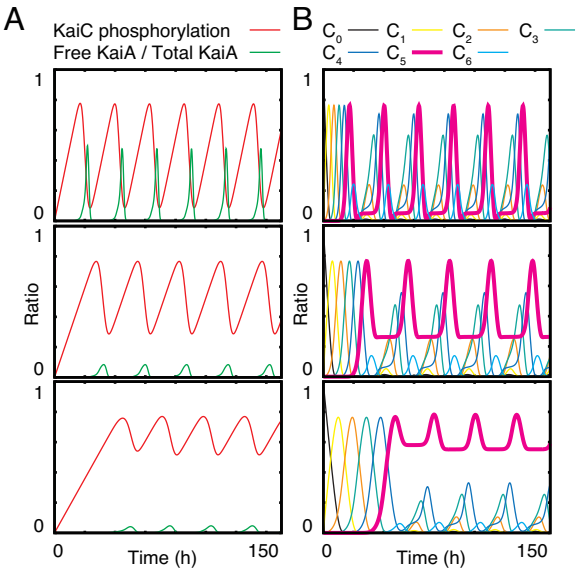

Figure 3.2: Oscillations in KaiC phosphorylation at various temperatures ($\beta = 1.0, 1.5, 2.0$). (A) Red line indicates the time series of the mean phosphorylation level defined by $\Sigma_{i=0}^{6} i[C_i]/[C]_{total}$, whereas the green line indicates that of the fraction of free KaiA, $[A]/[A]_{total}$. A decrease in temperature causes a decrease in the amplitude of the phosphorylation level. (B) Time course of the abundance of each form of KaiC, $[C_i]$. At low temperature, the basal amount of C_5 (magenta line) is remarkably high.

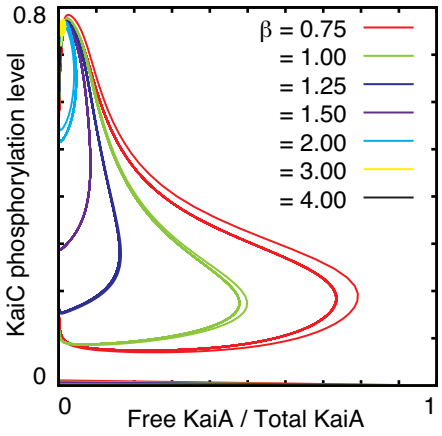

Figure 3.3: Orbits in a two-dimensional plane of KaiC phosphorylation level and free KaiA abundance for $E_p = 1.0$, $E_{dp} = 0.1$. By starting from a state with a high free KaiA abundance and a low KaiC phosphorylation level, the former suddenly decreases as KaiC phosphorylation progresses. When the KaiC phosphorylation level approaches near 0.8, the free KaiA abundance increases and KaiC starts to be dephosphorylated, which brings the system back to the start point. The limit-cycle is shrunk in the case of $E_p > E_{dp}$ by a decrease the temperature.

3.3.2 Transition to temperature compensation

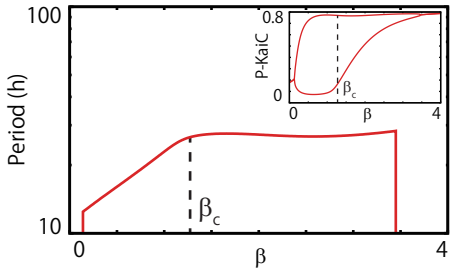

Figure 3.4: Dependence of period of oscillation on the inverse temperature $\beta = 1/T$. At high temperature (low β), the period changes exponentially with β, whereas above $\beta_c = 1/T_c \approx 1.2$, i.e., at temperatures below the critical temperature T_c, the period is nearly constant against changes in temperature. (Inset: Maximum and minimum values of mean phosphorylation level over a cycle. The maximum value is nearly constant against temperature changes, whereas the minimum value increases with β above β_c. The oscillation disappears via Hopf bifurcation at $\beta \approx 3.5$).

The transition at $\beta \simeq \beta_c = 1/T_c \approx 1.2$ is also reflected in the temperature dependence of the period. We plotted the period of oscillation as a function of (inverse) temperature, together with the maximum and minimum KaiC phosphorylation levels (see Fig.3.4). Above T_c, the temperature dependence of the period follows $\exp(\beta E_p)$, as can be naturally expected from a reaction process with a jump beyond the energy barrier. However, at lower temperature, the period is no longer prolonged exponentially and is nearly constant. Thus, the temperature compensation of the circadian period appears at lower temperature. There is also a clear difference in the amplitude of oscillation below and above T_c. At higher temperature (without temperature compensation), the amplitude of oscillation is almost constant over a large interval of temperatures. However, at lower temperature (with temperature compensation), the amplitude decreases with lower temperature; eventually, the oscillation disappears via Hopf bifurcation. This decrease in amplitude is due to the increase in the minimum value of the KaiC phosphorylation level, caused by the increase in the minimum abundances of $[C_5]$. The temperature dependences of the abundance of each KaiC and free KaiA also show distinct behaviors below and above T_c (see Figs.3.5 and 3.6). The average and minimum abundances of $[C_5]$ increase remarkably with a decrease in

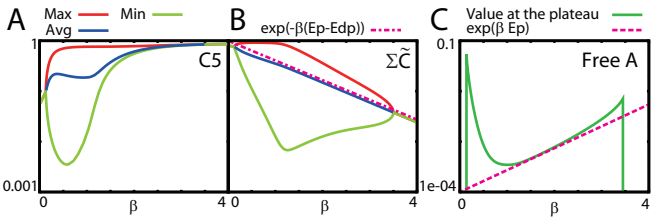

Figure 3.5: Normalized concentration of each component, $[C_5]/[C]_{total}$ (A), $\Sigma[\tilde{C}]/[C]_{total}$ (B), $[A]/[A]_{total}$ (C) plotted against the inverse temperature β. (A)(B) Maximum (red), minimum (green), and average (blue) over a cycle. (A) Note that the maximum value of $[C_5]$ is nearly constant, wheras its minimum and average increase with β beyond β_c (i.e., at lower temperature). (B) The average value of $\Sigma[\tilde{C}]/[C]_{total}$ is fitted well by the value of the unstable fixed point of the equation (magenta line), which is proportional to $\exp(-\beta(E_p - E_{dp})$. (C) The concentration of free KaiA in the plateau region of $[C_5]$ is plotted, as estimated from the time where $[C_3]$ reaches a peak. This free KaiA concentration closely follows $\exp(\beta E_p)$ (magenta line), for $\beta > \beta_c$, i.e., below the critical temperature.

temperature below T_c, whereas the maximum hardly changes with temperature (Fig.3.5A). Since the reaction from $[C_5]$ to $[C_6]$ becomes a bottleneck at lower temperature, the accumulation of $[C_5]$ occurs. However, the amplitude of the oscillation in $[C_i](0 \leq i \leq 4)$ has a peak around T_c, and the minimum value increases as the temperature decreases (Figs.3.6A–E). The value of free KaiA at the plateau increases when the temperature decreases (Fig.3.5C). The minimum inactive KaiC abundance (independent of the number of phosphorylated subunits on the KaiC hexamer) and $[C_6]$ showed behaviors similar to those of $[C_i](0 \leq i \leq 4)$, whereas the average followed $\exp(-\beta(E_p - E_{dp}))$ dependence throughout the temperature range (Figs.3.5B and 3.6G). Considering that the total amount of all KaiCs is conserved and the difference in activation energy, this dependence itself is rather natural.

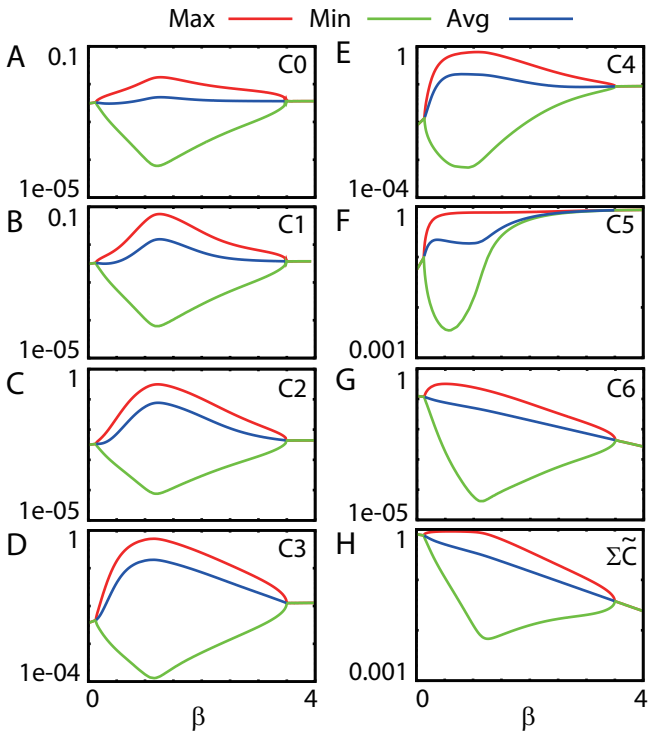

Figure 3.6: Concentration of each KaiC forms. Red line : maximum value, green line : minimum value, blue line : average value over a cycle. (A) $[C_0]$, (B) $[C_1]$, (C) $[C_2]$, (D) $[C_3]$, (E) $[C_4]$, (F) $[C_5]$, (G) $[C_6]$, (H) $\Sigma[\tilde{C}]$.

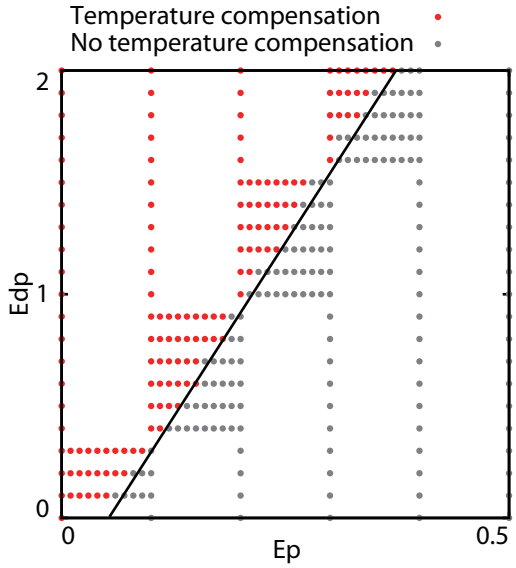

Figure 3.7: Phase diagram showing temperature dependence of the period for various E_p and E_{dp}, while A_{total} is fixed at 1.2×10^{-8}. Red: temperature-compensated oscillation satisfying $\partial\tau/\partial\beta \leq 0$ (τ : the period) below the characteristic temperature. Gray: oscillation without temperature compensation. When $0.2 < E_{dp}/E_p < 1$, the oscillation is temperature-compensated at temperatures below the characteristic temperature.

3.3.3 Proportion of free-energy of phosphorylation to that of dephosphorylation is critical for temperature compensation

Thus, the transition in the oscillation and temperature compensation behavior at low temperature is the salient feature of the present system. Next, we analyzed the conditions for E_p and E_{dp}, the activation energies for phosphorylation and dephosphorylation, respectively, to elucidate the temperature compensation. Fig.3.7 shows a plot for the region where temperature compensation appears in the parameter space of E_p and E_{dp}. From Fig. 3.7, we observe that temperature compensation appears in the regime $E_p \gtrsim 5E_{dp}$. The overall periodic behavior is determined mainly by E_{dp}/E_p, rather than the individual magnitudes. When $0.2 < E_{dp}/E_p < 1$, there still exists a transition to a regime with weaker temperature dependence on lowering the temperature, but this effect is not sufficient to produce the temperature compensation (see also Fig.3.8A). (See Appendix A for the case with $E_p < E_{dp}$.)

3.3.4 Temperature compensation depends on amounts of KaiA and KaiC

As already mentioned by van Zon et al., oscillation of KaiC abundance requires that the amount of KaiA is less than that of KaiC (van Zon et al., 2007). An increase in KaiA abundance leads to a decrease in the period, finally leading to no oscillations. The range of temperatures where oscillations exist narrows as KaiA abundance increases, and the oscillation disappears at higher temperatures. Here, the transition temperature T_c shifts to lower temperatures (see Fig.3.8B). Furthermore, the temperature compensation at $T < T_c$ is lost as KaiA abundance is increased. Although the temperature dependence of the period is weaker at $T < T_c$, the dependence $\exp(\beta\Delta E')$ still exists with $\Delta E'$ smaller than E_p. We plotted the range where temperature compensation occurs at $T < T_c$ in the two-dimensional plane comprising KaiA abundances and E_{dp}/E_p. We see that a low level of KaiA abundance is necessary for temperature compensation. Note that when $[A]_{total}$ is too small and $E_p - E_{dp}$ is too large, temperature compensation is achieved without transition, because the phosphorylation process is rate limiting throughout the temperature region of interest. Note that temperature compensation emerges for a sufficiently broad range of values for parameters E_p and E_{dp}. This is

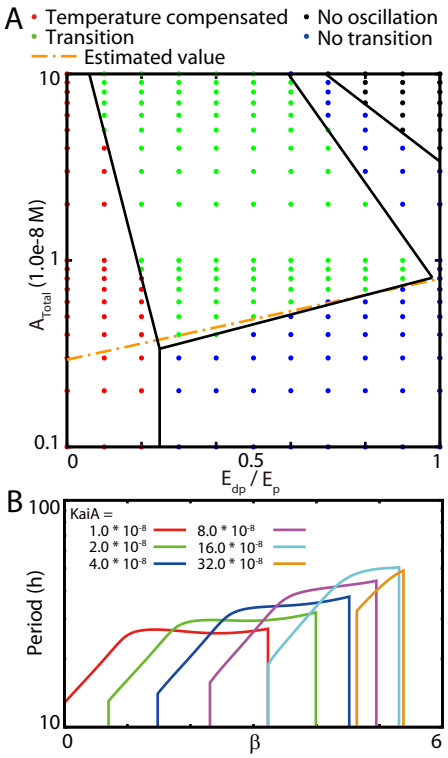

Figure 3.8: Influence of activation energy difference and the KaiA abundance on the temperature dependence of the period. (A) Diagram of the temperature dependence of the cycle against activation energy ratio (E_{dp}/E_p) and abundance of total KaiA (A_{total}). Red: Temperature-compensated oscillation with $\partial\tau/\partial\beta \sim 0$ (τ: the period) below the critical temperature. Green: Oscillation showing transition at the critical temperature. Blue: Oscillation without transition, with a simple increase with temperature following the Arrhenius form. Black: No oscillations at all. Orange dotted line: Transition line theoretically estimated from the condition at which the speeds of phosphorylation and dephosphorylation are equal. As E_{dp}/E_p increases from 0 to 1, we successively see temperature compensation, transition, and disappearance of oscillation. (For the case with $E_p < E_{dp}$, see Appendix A). As $[A]_{total}$ increases, the width of the temperature compensation region decreases. (B) Effect of KaiA increase on the period. An increase in KaiA leads to narrowing of the range of the periodic solution, and also the range of temperatures at which temperature compensation occurs.

free for other parameter values.

3.3.5 Range of temperatures where systems is temperature -compensated is narrowed by a reduction in phosphorylation sites

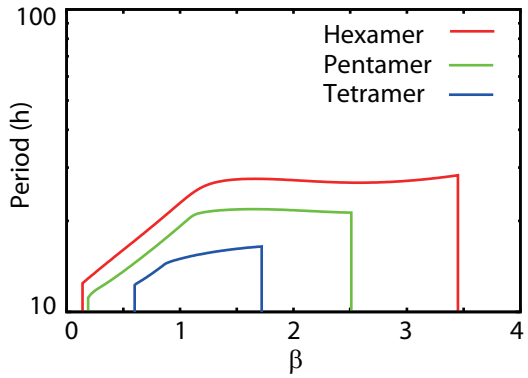

Figure 3.9: Temperature dependence of the period of reduced Kai models. The hexamer is the original model shown in Fig.3.1 containing $[C_0] \sim [C_6]$, while a pentamer and tetramer are the reduced models containing $[C_0] \sim [C_5]$ and $[C_0] \sim [C_4]$, respectively. The same parameter values are used as in the original model. Models with fewer phosphorylation sites ($i \leq 3$) cannot generate any oscillation. In the reduced models, the temperature ranges where oscillations occur and where temperature-compensated oscillations occur are both narrower, and the temperature compensation in the tetramer model is not perfect.

Since KaiC is a hexamer, we adopted six phosphorylation sites in our model. However, to understand the biological significance of this number of sites, we examine models with a reduced number of phosphorylation sites (Fig.3.9). We find that the reduction in the number of phosphorylation sites when moving from hexamer to pentamer, and then to tetramer, narrows the temperature range where oscillations exist and temperature compensation occurs. For the tetramer, temperature compensation is not observed even at

$T < T_c$.

3.3.6 KaiC phosphorylation cycle is entrained by temperature cycles

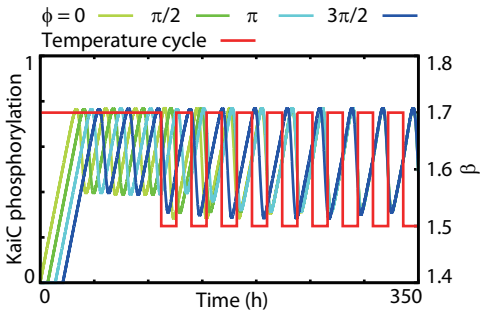

Figure 3.10: Entrainment of oscillation to externally applied thermal cycles. Oscillations with various s ($\phi = 0, \pi/2, \pi, 3\pi/2$) are entrained by the temperature cycle between $\beta = 1.5$ and 1.7 within about 10 cycles.

It has been demonstrated that KaiC's phosphorylation cycle is entrained to external temperature cycle (Yoshida et al., 2009). To examine such entrainment, we cycle the temperature between $\beta = 1.5$ and 1.7 (i.e., within the temperature compensation region) periodically in time with a period close to that of the Kai system (27 h). Within about 10 cycles, the period of oscillation of the KaiC system is entrained with that of temperature, independently of the initial period of oscillation. Thus, entrainment to the temperature cycle is achieved (see Fig.3.10).

3.4 Discussion

Here we discuss how temperature compensation is achieved. As presented in the Results section, there are two stages: transition in the temperature dependence of the period, and complete temperature compensation of the period at lower temperature. As seen in Fig.3.8A, the former requires that E_p is sufficiently larger than E_{dp}, which, as will be shown, means that the phosphorylation process is rate limiting. For the latter, the abundance of

KaiA should be sufficiently small so that there is limited free KaiA that can be used for phosphorylation (i.e., competition for free KaiA). As will be shown below, the abundance of free KaiA decreases as the temperature increases, which compensates for the increase in the rate constant of the reaction.

1. Transition: When there is a difference between the energy barriers for phosphorylation and dephosphorylation, the temperature dependence of the rate of each process is different. Roughly speaking, the time scale for the phosphorylation process changes in proportion to $[A]\exp(\beta E_p)$, whereas dephosphorylation has $\exp(\beta E_{dp})$, where $[A]$ is the concentration of free KaiA. Thus, there exists a critical temperature at which the two rates are comparable; the rate-limited reaction switches at this temperature, where the transition to temperature dependence occurs. Thus, $\beta_c \simeq \log[A]/(E_p - E_{dp})$ where $[A]$, the concentration of free KaiA, is estimated from the steady-state solution of our model to afford $[A] \simeq K_5[A]_{total}/K_5 + [C_5]$ if $[A]_{total} \ll K_5$ and $[A] \simeq [A]_{total}$ if $[A]_{total} \gg K_5$.

Thus, a sufficient difference in activation energy is necessary for the transition-like behavior because the critical temperature will diverge as $E_p \simeq E_{dp}$. If the difference is small, the critical temperature goes below the temperature for the onset of oscillation and the transition never occurs. If A_{total} is too large or too small, the critical temperature is lower or higher than the range where the oscillation exists, and thus for both the cases, the transition disappears. These estimates are consistent with Fig.3.8A.

2. Temperature compensation by autonomous regulation of the KaiA concentration: As mentioned, the reaction from $[C_5]$ to $[C_6]$ becomes a bottleneck at lower temperature, and the amount of active and inactive KaiC is mainly determined via $[C_5]$ and $\Sigma[\tilde{C}]$. When the temperature is lower than the transition temperature, the phosphorylation process takes more time, and $[C_5]$ accumulates before dephosphorylation from $[C_6]$ progresses, as already discussed (see Fig.3.2B). The increase in the abundance of active KaiC leads to competition for KaiA, and thus a decrease in free KaiA. If the total KaiA abundance is limited, the system reaches a stage where phosphorylation almost stops. This leads to the plateau in the time course of $[C_5]$, as observed in Fig.3.2B. This drastic slow-down of the phosphorylation process occurs when $[A]$ is decreased to the level at $K_p[A] \lesssim 1$. Thus, during the plateau in $[C_5]$, this approximate estimate gives, $[A] \propto 1/K_p \propto \exp(\beta E_p)$. Thus, the temperature dependence of the phosphorylation rate $K_p[A]$ is compensated for by the decrease in $[A]$. This

plateau region is rate-limited in the circadian cycle, making the whole period independent of temperature.

In more detail, this compensation is also estimated as follows. The abundances of the inactive forms of KaiC decrease with an increase in $[C_5]$. Considering the differences in speed between phosphorylation and dephosphorylation, the total inactive KaiC abundance (at the fixed point) is estimated as

$$\Sigma[\tilde{C}]^* \propto \exp(-\beta(E_p - E_{dp})) \tag{3.10}$$

which is consistent with Fig. 3.5. The flow from inactive KaiC is thus estimated by $k_{dp}\Sigma[\tilde{C}]^* \propto \exp(-\beta E_p)$.

This flow starts the phosphorylation processes from $[C_0]$, but is slowed down at some number of phosphorylated subunits on the KaiC hexamer, m. In the present model, this slow down starts at $m \approx 2 \sim 3$ due to the paucity of free KaiA. Following the above estimate of flow, the maximum $[C_m]$ is estimated to be proportional to $\exp(-\beta E_p)$. Now from eq.(3.4) and $K_m \ll K_i$ $(i > m)$ and $[C_j] \ll [C_m]$ $(j < m)$ at this time, the abundance of free KaiA can be estimated approximately as $[A] \simeq [A]_{total} - ([A][C_m])/(K_m + [A])$ When $[A]_{total}$ is small enough, the minimum free KaiA abundance is smaller than K_m,thus $[A] \simeq [A]_{total} - ([A][C_m])/(K_m)$.

$$[A] \simeq \frac{[A]_{total}}{1 + [C_m]/K_m} \simeq \frac{[A]_{total}K_m}{[C_m]} \propto \exp(\beta E_p). \tag{3.11}$$

Therefore, when $[A]_{total}$ is small enough and E_p is sufficiently greater than E_{dp}, the time scale of the phosphorylation process is $k_p[A]$, and the period of the cycle is temperature-compensated. Indeed, as shown in Fig.3.6, the maximum $[C_1]$ (and $[C_2]$) values show $\exp(-\beta E_p)$ dependence, whereas free KaiA shows approximately $\exp(\beta E_p)$ dependence when phosphorylation is slowed down.

Below T_c, the process stops for a long time at the limited process, phosphorylation from $[C_5]$ to $[C_6]$. Hence, accumulation of $[C_5]$ occurs, which leads to a qualitative change in the amplitude.

In essence, the temperature compensation mechanism requires two properties: difference in activation energy between phosphorylation and dephosphorylation processes, and a limited abundance of enzyme KaiA. The former is essential to the transition, and the latter to the compensation for the

Arrhenius-type temperature dependence of the individual reactions. As long as these conditions are met, the period is temperature-compensated at low temperature, without the need for fine tuning of the parameters of the system. This "*enzyme-limited competiton* (ELC) mechanism" is important for understanding temperature compensation.

These two properties generally appear if there are two types of processes with different activation energy, with one type catalyzed by a common enzyme and the other not being catalyzed by the common enzyme or at all. If the enzyme abundance is limited, the competition for the enzyme will lead to temperature compensation in cyclic reaction systems. In particular, if the main component of the chemical reactions has allosteric structure like KaiC, the competition for enzymes will occur naturally.

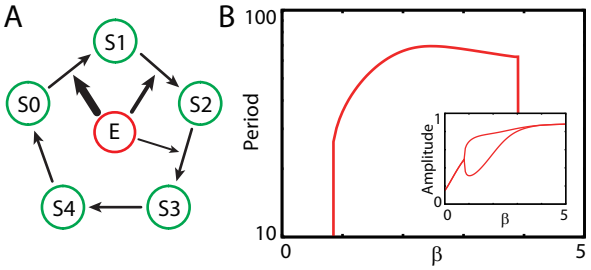

Figure 3.11: Temperature compensation of period in a simpler model with enzyme competition. (A) Scheme of the simpler model. The substrate has five forms, and reactions $S_0 \to S_1, S_1 \to S_2, S_2 \to S_3, S_3 \to S_4$ are catalyzed by the same enzyme E, but the other reactions are not. The affinity between S_i and E weaken as i increases. (B) The period, plotted against the inverse temperature β. The oscillation is temperature-compensated over a specific range of temperatures, although the transition is not as sharp as in the Kai model. (Inset: Maximum and minimum values of $[S_2]$ over a cycle).

As an example, we consider the cyclic process shown in Fig.3.11, where a cyclic change in five substrates occurs. Three processes—$S_0 \to S_1 \to S_2 \to S_3$—have a high activation energy barrier, and are catalyzed by the common enzyme E. In this case, the period of the oscillation in the concentration of each substrate is temperature-compensated at low temperature. If the number of reactions with the common enzyme is decreased to two, compensation still appears, but it is weaker, as shown in Fig.3.12. This example demonstrates the generality of the ELC mechanism, and opens the possibility of

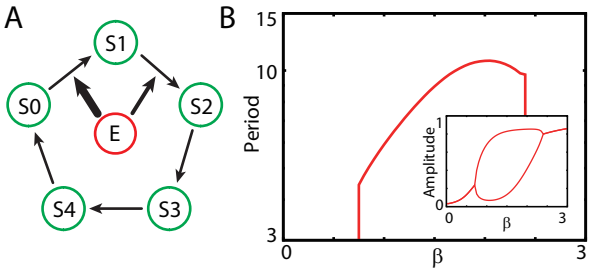

Figure 3.12: Temperature compensation in a simpler model with just two catalytic reactions sharing the same enzyme. (A) Scheme of the model. The reactions between $S_0 \to S_1, S_1 \to S_2, S_2 \to S_3$ are catalyzed by the same enzyme E, and other reactionsare not. The affinity between S_0 and E is higher than that between S_1 and E. (B) the period, plotted as a function of the inverse temperature β. The range with temperature compensation is narrower, and the compensation is not perfect. (Inset: Maximum and minimum values of $[S_1]$ over a cycle).

applications to temperature compensation in other biochemical oscillations as well.

Regulation of reaction speed by limitation of catalysts, as proposed here, should be important, not only for the temperature compensation of circadian clocks in general, but also for other biological processes. For example, we expect that the ELC mechanism could work even for steady-state fluxes in an open flow system instead of a closed oscillation circuit, if a common enzyme is shared and competed for among several reactions (Bullock, 1955; Ruoff et al., 2007).

Recall that as a consequence of our mechanism, the temperature dependence of the rate of the reactions of interest is compensated for by the change in the concentration of the available enzyme. Hence, when our mechanism works, it may be observed that some "balance" also occurs. In this regard, in some systems that are so far regarded as being examples of the "balance mechanism," it may in fact be the ELC mechanism that underlies the balance. By studying, in more detail, the dynamics of enzyme concentrations, our mechanism may be unveiled therein.

The regulation of reaction process by autonomous changes in enzyme concentration, as proposed here, was previously pointed out by Awazu and

Kaneko, who reported that relaxation to equilibrium slows down when the concentrations of substrate and enzymes are negatively correlated (Awazu and Kaneko, 2009). Excess substrate hinders the enzymatic reaction, leading to a plateau in relaxation dynamics. In the present model, the total concentration of KaiA as an enzyme is a conserved quantity but the fraction of free KaiA available is reduced when there is abundant active KaiC so that the speed of phosphorylation slows down dramatically. In this sense, several other Kai models that adopt competition for KaiA as a driving force for synchronization of each KaiC hexamer should fit well with our scheme. For example, our mechanism may work in the model by Mehra et al (Mehra et al., 2006).

Now we briefly discuss the relevance of the present results to experiments on the Kai protein circadian system. In our model, it is assumed that KaiC's affinity to KaiA depends on the phosphorylation levels. This assumption is necessary not only for the emergence of temperature compensation but also for the existence of the oscillation itself.

In the actual circadian clock comprising Kai proteins, KaiB is also involved besides KaiA and KaiC. However, as mentioned, an increase in KaiB abundance has minor influence on the clock (Nakajima et al., 2010). Earlier it was suggested that KaiB binds to KaiAC complexes strongly and restricts the concentration of free KaiA (van Zon et al., 2007). Thus, the inclusion of KaiB is expected to not alter the present temperature compensation mechanism, but to facilitate it by strengthening the limitation of enzyme availability. Note that previously reported temperature compensation at the element level—KaiC's ATPase activity (Terauchi et al., 2007) and autodephosphorylation activity (Tomita et al., 2005) — is also relevant to our model; the former to achieve fast equilibration between KaiA and the KaiA complex used for eq.(3.4), and the latter to provide $E_{dp} \ll E_p$.

It is known that the amplitude of KaiC oscillation decreases as the temperature is lowered (Nakajima et al., 2005), which agrees well with our results (Fig.3.2A). Indeed, as described already, this decrease in amplitude is tightly coupled with the temperature compensation mechanism. It is also interesting to note that in many circadian clocks, the period does not depend on the temperature, although the amplitude decreases with temperature (Nakajima et al., 2005). If every elementary step of the circadian clock were temperature compensated at the single-molecule level, this temperature dependence of the amplitude would not be possible. Furthermore, the entrainment of the KaiC oscillation to imposed temperature cycles, as observed in a recent experiment

naturally appears without further tuning the model (Yoshida et al., 2009).

Our mechanism for temperature compensation depends on the paucity of KaiA—increasing the KaiA concentration leads to loss of compensation. We expect that this prediction will be directly confirmed in a future experiment.

Appendix A : Behaviors in a Region for $E_p < E_{dp}$

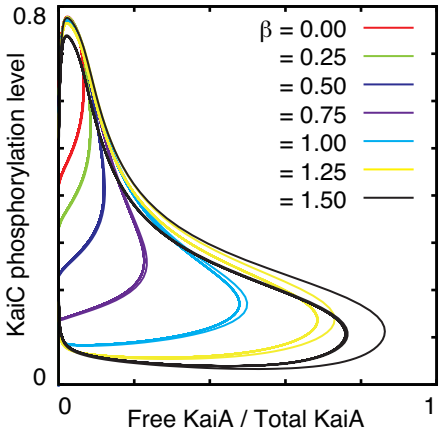

Figure 3.13: Orbits in a two-dimensional plane of KaiC phosphorylation level and free KaiA abundance for $E_p < E_{dp}$ ($E_p = 0.1$, $E_{dp} = 1.0$). By starting from a state with a high free KaiA abundance and a low KaiC phosphorylation level, the former suddenly decreases as KaiC phosphorylation progresses. When the KaiC phosphorylation level approaches about 0.8, the free KaiA abundance increases and KaiC starts to be dephosphorylated, which brings the system back to the start point. The limit cycle is extended when $E_p < E_{dp}$ by a decrease the temperature.

In the region where $E_p < E_{dp}$, the oscillation is described by a limit-cycle attractor, as represented in the orbit in a two-dimensional plane representing KaiC phosphorylation level and free KaiA abundance (Fig.3.13). We plotted the period of oscillation as a function of (inverse) temperature, together with the maximum and minimum KaiC phosphorylation levels (Fig.3.14) and diagram of the temperature dependence of the cycle against the activation

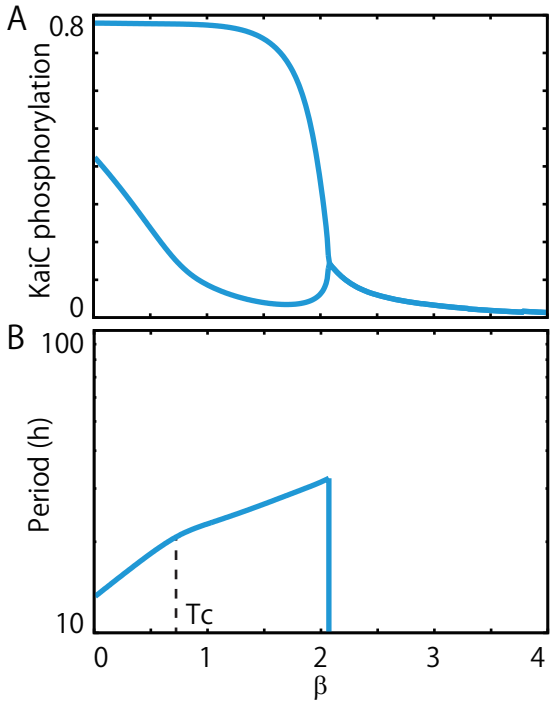

Figure 3.14: Temperature dependence of the amplitude and period of oscillation for $E_p < E_{dp}$ ($E_p = 0.1$, $E_{dp} = 1.0$). (A) Maximum and minimum mean phosphorylation levels over a cycle. The maximum value is nearly constant against temperature changes. The minimum value increases with β for $\beta > \beta_c = 1/T_c \approx 0.7$, and is nearly constant below β_c. The oscillation disappears at $\beta \approx 2.0$. (B) Period of oscillation. The period changes with the Arrhenius form, i.e., in an exponential manner over the whole range of temperature, while the slope changes below and above T_c. Below T_c (beyond β_c), the temperature dependence of the period is about $\exp(\beta E_{dp})$, and is $\exp(\beta \Delta E')$ with $\Delta E'$ larger than E_{dp} at $T > T_c$ ($\beta < \beta_c$).

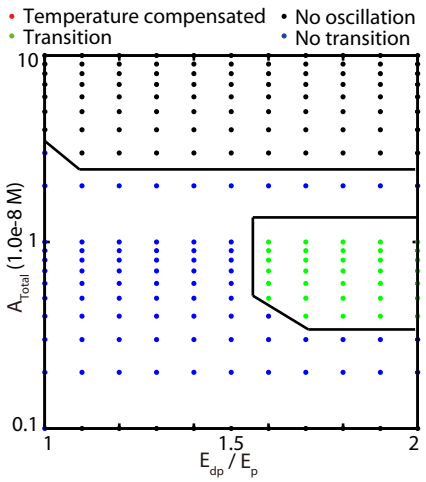

Figure 3.15: Diagram of the temperature dependence of the cycle against the activation energy ratio (E_{dp}/E_p) and the abundance of total KaiA ($[A]_{total}$) in the region where $E_p < E_{dp}$. Green: oscillation showing transition at the critical temperature. Blue: oscillation without transition, with a simple increase with temperature of the Arrhenius form. Black: no oscillations at all. In the region where $E_p < E_{dp}$, the temperature compensation region never appears. As $[A]_{total}$ increases, oscillation disappears. As $|E_{dp}/E_p|$ increases from 1 to 2, we can see the transition region.

energy ratio (E_{dp}/E_p) and the abundance of total KaiA (Fig.3.15). In this region, the temperature dependence of period is $\exp(\beta\Delta E')$ with $\Delta E'$ larger than E_{dp} at $T > T_c$ ($\beta < \beta_c$). Such "temperature sensitiveness" is thought to be a converse phenomenon of temperature compensation.

Appendix B : Models and Settings

The Kai protein model

In the simulation of the main text, we adopted the parameter values in Table.3.1. Still, our temperature compensation mechanism does not rely on these specific values.

c_p	13.6
c_{dp}	0.908
f	0.908 h^{-1}
b	0.908 h^{-1}
k^{Af}	$3.45 \cdot 10^{13}$ $\mathrm{M}^{-1}\mathrm{h}^{-1}$
k_0^{Ab}	10 h^{-1}
α	10
$[C]_{total}$	0.58 μM
$[A]_{total}$	0.012 μM

Table 3.1: Parameter set of Kai protein model

Simpler model with two catalytic reactions sharing the same enzymes

In the simulation, we adopted the parameter values in Table.3.2.

c_0	10
c_1	500
c_{ps}	1
E_c	1.0
E_{ps}	0
K_0	0.001
K_1	1
$[S]_{total}$	1
$[E]_{total}$	0.02

Table 3.2: Parameter set of simpler model with two catalytic reactions

Simpler model with three catalytic reactions sharing the same enzymes

In the simulation, we adopted the parameter values Table.3.3.

c_0	10
c_1	30
c_2	300
c_{ps}	0.1
E_c	1.0
E_{ps}	0.05
K_0	0.0001
K_1	1
K_2	10
$[S]_{total}$	1
$[E]_{total}$	0.02

Table 3.3: Parameter set of simpler model with two catalytic reactions

Chapter 4

Reciprocity Relationship between Robustness of the Period and Plasticity of the Phase

Chapter Outiline

Robustness and plasticity seem to be incompatible at a first glance, because the former implies resistance to change and the latter implies feasibility to change. Organisms, however, can manifest both robustness and plasticity against the same stimuli. How organisms can achieve both of the two conflicting features is a principal problem. In the circadian clocks, also, both characteristics are compatible. Biological clocks are known to show temperature and nutrient compensations, which can keep the period a clock constant against changes in temperature and nutrient condition, respectively. In contrast, the period of biological clocks is known to be entrained by external cycles of both temperature and nutrient condition, by adjusting the phase of oscillation. How are both robustness of the period and plasticity of the phase against the same environmental cue achieved? In this chapter, we first show that robustness of the period is achieved by the enzyme-limited competition via change in the concentration of free catalyst as a buffer molecule, not only against temperature but also against other environmental changes such as the nutrient condition. Such change in the concentration of a buffer molecule lead

to a shift of a limit cycle orbit in the phase space, which introduces a phase shift against the change in environmental conditions. Therefore, robustness of the period and plasticity of the phase show a reciprocity relationship : higher robustness of the period will provoke higher plasticity in the period. Such reciprocity relationship is achieved in some other model with different mechanisms of circadian clocks , i.e., not only for post-translational but also for transcription-translational oscillators, and this will be a universal feature in the biological clock.

4.1 Introduction

Biochemical oscillations are commonly observed from cells to humans and provide the basic functions for the organism. To list a few examples:

- Intermediate metabolites in glycolysis show temporal oscillations (Goldbeter, 1997).
- Cells replicate themselves by periodic cell division events.
- Insulin is released from a pancreas periodically (Bergsten and Hellman, 1993).
- Individuals can quickly adapt to daily environmental changes by means of the circadian clock (Bell-Pedersen et al., 2005).

These oscillations are thought to work as pacemakers, and the maintenance of their characteristic period to a constant value against changes in external conditions is important. To date, it is known that some of such oscillators show homeostasis against external changes (Bell-Pedersen et al., 2005; Bergsten and Hellman, 1993).

Indeed, circadian clocks, one of the most important biological oscillators, are known to be resistant against various types of stimuli. The most prominent example is temperature compensation, i.e., robustness of the period against temperature changes. In addition to temperature compensation, circadian clocks show robustness against changes in trophic conditions (e.g., the concentration of glucose or adenosine triphosphate (ATP)), which is called nutrient compensation (Phong et al., 2013; Sancar et al., 2012; Terauchi et al., 2007). Such homeostatic features (i.e., temperature and nutrient compensation) are known to be universally conserved across a wide range of

organisms, and their mechanisms have been investigated. Moreover, the relationship among different homeostatic responses of clocks have been also discussed (McDaniel et al., 1974; Pittendrigh et al., 1973). However, the question how various homeostatic responses of the period are achieved simultaneously remains unsolved.

Incidentally, homeostasis of the period is not sufficient to adapt to environmental changes. Plasticity of the phase is also needed. For example, circadian clocks which cannot be entrained by diurnal cycles (e.g., light-dark, temperature, and metabolic cycles) are useless to predict and adapt to daily events.

Although these two criteria, robustness of the period and plasticity of the phase, seem to be hard to go together, they are compatible in the actual clocks in living organisms (Bell-Pedersen et al., 2005; Zimmerman et al., 1968). Mechanism of the compatibility is one of the most important problems to be resolved. Here, we introduce a general mechanism and condition for the homeostasis of the period of post-translational biochemical oscillation against various environmental changes. Moreover, we discuss that there is a reciprocity relationship between robustness of the period and plasticity of the phase against external changes, i.e., higher robustness is associated with higher plasticity. This reciprocity is a natural consequence of the mechanism of robustness of the period.

Here, we propose a general mechanism and suggest a condition for homeostasis of the period of post-translational biochemical oscillation against various environmental changes. The post-translational oscillation, which consists of modification and demodification reactions of proteins without *de novo* transcription and translation, is one of the basic mechanisms of circadian clocks. Indeed, the Kai-protein system, which constitutes a cyanobacterial post-translational clock, has been investigated in depth as a basic model. Kondo and his colleagues succeeded in the *in vitro* reconstruction of the cyanobacterial clock by mixing three proteins, KaiA, KaiB, and KaiC, with ATP as the energy source (Nakajima et al., 2005). KaiC has a hexameric structure with six monomers, each of which has two phosphorylation sites (Kageyama et al., 2003). Furthermore, it has both auto-phosphorylation and auto-dephosphorylation activities; however, since the auto-dephosphorylation activity is usually stronger, the protein is spontaneously dephosphorylated (Nishiwaki et al., 2000; Xu et al., 2003). The binding of the dimer of KaiA (Kageyama et al., 2003) to KaiC enhances KaiC's auto-phosphorylation activity, leading to its phosphorylation (Iwasaki et al., 2002; Xu et al., 2003),

while KaiB inhibits the activity of KaiA (Williams et al., 2002; Xu et al., 2003). This phosphorylation/dephosphorylation process of KaiC constitutes a circadian rhythm.

In the previous chapter focused on a model of the KaiC system, we showed that the temperature compensation of biochemical oscillators is achieved by enzyme-limited competition (ELC). The model consisted of catalytic phosphorylation reactions and non-catalytic dephosphorylation reactions for KaiC modification sites, with KaiA as the catalyst. Each phosphorylation reaction competes for the limited abundance of the catalyst. When the external temperature is increased, the competition for the catalyst among the substrates increases, leading to a decrease of the amount of free catalysts. We showed that the decrease of the amount of free catalyst, indeed, could counterbalance the temperature-induced increase in the rate of elementary reactions, when two conditions are met:
1. The amount of the catalyst is not high.
2. The activation energies of the catalytic reactions are higher than those of the non-catalytic reactions.
The first condition is required to limit the amount of enzyme, while the second condition is needed for the catalytic reactions to be rate limiting. Hence, the speed of a catalytic process is more sensitive than that of a non-catalytic process, because the rate constant depends on the temperature according to the Arrhenius's law: $k \propto \exp(-E_\alpha/kT)$ where E_α is the activation energy and T is the temperature.

Although the temperature is one of the key factors that alter the speeds of biochemical reactions, other factors can also play a role. For example, rate constants depend on the changes in the concentrations of donor substrates (e.g., ATP for phosphorylation, S-adenosyl methionine for methylation, and acetyl-CoA for acetylation) following mass-action kinetics or Michaelis-Menten type kinetics. Osmotic pressure and pH also affect the rate constants because of protein denaturalization. However, it is unknown whether there is a mechanism that commonly compensates the period against such changes in the reaction speeds.

Here, we show that the ELC can work as a general framework for homeostasis of the period of biochemical oscillators. As an example, we show that the nutrient compensation of the period is achieved by ELC. Because the nutrient compensation at the level of organisms may involve more complicated mechanisms, it is important to first understand the mechanism at the molecular level. At the molecular level, changes in nutrient conditions

lead to drastic changes in the concentration of the donor substrates through metabolic networks and, thus, alter the speed of modification reactions. In spite of such changes, circadian clocks tick with almost the same period. Indeed, the reconstructed Kai system showed homeostasis of the period against changes in the concentration of ATP (Phong et al., 2013; Terauchi et al., 2007). Therefore, to understand the mechanism of nutrient compensation at the molecular level, we should consider the homeostatic response against changes in the concentration of donor substrates. Here, we will show that such nutrient compensation can be achieved by ELC at low metabolic condition.

Secondarily, we will demonstrate that biological clock with robustness of period against changes in an environmental factor can be easily entrained by a cyclic change in the factor, because of a large phase shift induced by stimuli. We show that environmental changes can alter the period little and can cause a large phase shift when a difference in reaction speeds between catalytic and non-catalytic reactions is large, while the period is strongly altered and the phase is shifted little if the difference in the speed is smaller. It suggest a reciprocity relationship between the change in the period and that in the phase. Because of such relationship, biochemical oscillators can easily adapt to the changes in external environments. Interestingly, such reciprocity relationship is also true in a quite different model. We discuss why such reciprocity relationship is achieved in biochemical oscillators.

4.2 Model

4.2.1 KaiC protein model

We again choose the KaiC phosphorylation clock, adopted in Chapter.3.

Here, to discuss not only temperature compensation but also nutrient compensation, we slightly extend the model to be responsive both to temperature and nutrient conditions. The rates of phosphorylation and dephosphorylation depend on external environment such as temperature and nutrient conditions. Rates of phosphorylation and dephosphorylation reactions depend on temperature, following the Arrhenius kinetics as $k_p \propto \exp(-\beta E_p)$ and $k_{dp} \propto \exp(-\beta E_{dp})$, where the β is inverse temperature by taking the unit of Boltzmann constant as unity and E_p and E_{dp} are activation energies of phosphorylation and dephosphorylation reactions, respectively. In this

Chapter, we study two types of reactions, the mass-action kinetics and the Michaelis-Menten kinetics as for the dependence of reaction speed on the ATP concentration is given. In the former case, phosphorylation reactions immediately process when ATP binds to KaiA-KaiC complex, while in the latter case, a binding reaction between ATP and KaiA-KaiC complex is faster than a phosphorylation reaction so that the ratio of KaiA-KaiC complex to KaiA-KaiC-ATP complex approach the equilibrium ratio immediately. The speed of reactions are given as $k_p \propto [ATP]$ and $k_p \propto [ATP]/([ATP]+K_{ATP})$, for the mass-action kinetics and the Michaelis-Menten kinetics, respectively. Note that we assumed that only the phosphorylation reaction rate depends on the concentration of ATP because dephosphorylation reactions do not need ATP as a donor substrate.

4.2.2 Transcription-translation feedback model

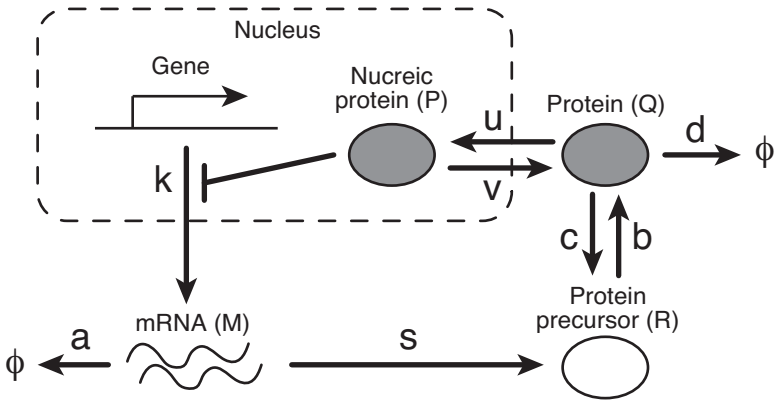

Figure 4.1: The schematic representation of a transcription-translation feedback model.

Recent studies have suggested that the present circadian clocks roughly classified into two types, a post-translational oscillator and a transcription-translation feedback oscillator (Gallego and Virshup, 2007; Qin et al., 2010; Zwicker et al., 2010). Whereas the post-translational oscillator consists only of protein-protein interactions, the transcription-translation feedback oscillator includes both transcription and translation processes.

In the transcription-translation feedback model, first a clock-related gene is transcribed and translated, and later such translated protein represses an

expression of its own gene with a time-delay. When a transcription rate decreases, the amount of such protein also decreases, which weakens the suppression of the clock-related gene expression, so that such gene is transcribed again. It is a prototype of the transcription-translation feedback oscillator.

The Kai protein model in 4.2.1 was one of prominent example of the post-translational oscillator. As a typical example of the translation-transcription feedback model, we choose here a model of a fruit fly's circadian clock by (Kurosawa and Iwasa, 2005), schematically illustrated in Fig.4.1, The governing differential equations are described below:

$$\begin{aligned}
\frac{d[M]}{dt} &= \frac{k}{h+[P]} - \frac{a[M]}{a'+[M]} \\
\frac{d[R]}{dt} &= \frac{s[M]}{s'+[M]} - \frac{b[R]}{b'+[R]} + \frac{c[Q]}{c'+[Q]} \\
\frac{d[Q]}{dt} &= \frac{b[R]}{b'+[R]} - \frac{c[Q]}{c'+[Q]} - \frac{d[Q]}{d'+[Q]} \\
&\quad - \frac{u[Q]}{u'+[Q]} + \frac{v[P]}{v'+[P]} \\
\frac{d[P]}{dt} &= \frac{u[Q]}{u'+[Q]} - \frac{v[P]}{v'+[P]}
\end{aligned} \tag{4.1}$$

where, M is a mRNA of clock-related gene (*per* mRNA), R is a protein precursor of a clock-related protein (PER protein), Q and P are an extranuclear protein and a nucleic protein, respectively, and $[x]$ denotes the concentration of x. k, a, s, b, c, d, u, and v are rate constants, and h, a', s', b', c', d', u', and v' are dissociation constants.

In (Kurosawa and Iwasa, 2005), it was reported that a and k are especially important to decide the length of the period. Following this report, we set a rate constant of mRNA degradation as $a \propto \exp(-\beta E_a)$ and other kinetic constants as $\propto \exp(-\beta E_k)$. By fixing E_k and varying E_a, we analyze the relationship between temperature compensation and phase shift.

4.3 Result

4.3.1 The biochemical oscillator shows nutrient compensation

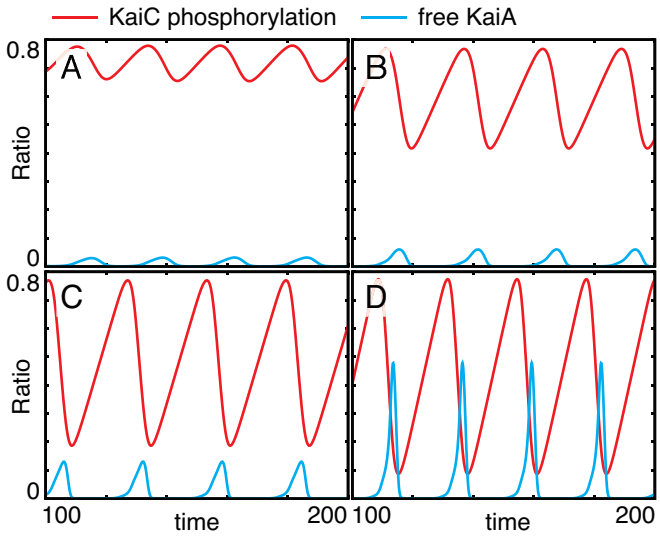

Figure 4.2: Oscillation in the phosphorylation level of KaiC and in the ratio of free KaiA at various ATP concentrations. The time evolutions of KaiC phosphorylation level ($\Sigma[C_i]/[C]_{total}$) and the normalized concentration of free KaiA ($[A]_{free}/[A]_{Total}$) are plotted according to the mass-action model. (A) $[ATP] = 0.25$, (B) $[ATP] = 0.5$, (C) $[ATP] = 0.75$, (D) $[ATP] = 1.0$. For (A)-(C) the period is almost identical, while for (D) it is slightly decreased.

First, we analysed the Kai protein model following the mass-action kinetics. This model shows oscillations in KaiC phosphorylation levels over a wide range of ATP concentration (Fig.4.2). Since the speed of the phosphorylation reactions changes with the concentration of ATP linearly, the period is expected to decrease with the inverse of ATP concentration. Indeed, the period decreases roughly in such a manner when the concentration of ATP is high. In the low ATP concentration regime, however, the phosphorylation clock ticks with approximately the same period over a broad range of ATP concentrations (Fig.4.3A). Thus, the post-translational clock shows

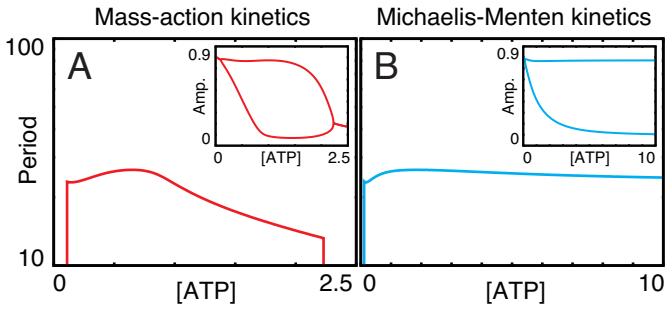

Figure 4.3: Dependence of the period on the concentration of ATP and the maximum and minimum values of the mean phosphorylation level over a cycle of the mass-action model and the Michaelis-Menten model. (A) The period for the mass-action model is nearly constant against changes in $[ATP]$ in the low ATP concentration regime, while it changes roughly with the inverse of $[ATP]$ in the high ATP concentration regime. (Inset) The minimum value decreases with $[ATP]$ at a low ATP concentration, while it is almost constant at a high ATP concentration. (B) The period for the Michaelis-Menten model is almost constant over the full range of ATP concentration. (Inset) The maximum value is nearly constant against $[ATP]$ change, whereas the minimum value decreases with $[ATP]$ at low ATP concentration.

nutrient compensation when the concentrations of donor substrates are not too high. However, the amplitude of the phosphorylation level drastically changes when the nutrient compensation is achieved, while the amplitude changes slightly in the high ATP concentration region (inset of Fig.4.3A). A similar relationship between the period and amplitude has been already observed in the temperature compensation : when the period is kept constant, the amplitude changes, and when the period changes, the amplitude changes only slightly (see Chapter 3).

In an experiment on KaiC phosphorylation clock, in agreement with our results, it was found that the period remained constant against the change in ATP concentration, while the amplitude drastically depended on ATP concentration (Phong et al., 2013; Terauchi et al., 2007). However, the experimental result shows that nutrient compensation occurred at high ATP concentration, while the amplitude did not change at such concentrations.

4.3.2 ELC and Michaelis-Menten kinetics work independently to achieve global nutrient compensation

In general, the speed of the modification reactions does not ceaselessly increase with the concentration of donor substrates, but starts to saturate following the Michaelis-Menten kinetics or Hill kinetics, because of fast binding rates and slow modification rates. When the concentration of donor substrates is too high, the speed of the modification reactions approaches a plateau. This behaviour is regarded as a mechanism of nutrient compensation at too high donor substrate concentrations. Actually, the model following the Michaelis-Menten kinetics shows approximately a constant period over a much broader concentration range than the mass-action kinetics model (Fig.4.3B), indicating that the nutrient compensation mechanism by Michaelis-Menten kinetics and by ELC work independently in the low and high ATP concentration regions, respectively.

In contrast to the ELC mechanism, the Michaelis-Menten kinetics change the speed of the reaction at an elemental level, so that, not only the period but also the amplitude becomes insensitive to the ATP concentration (see Fig.4.3B). These features of the period and the amplitude agree well with previously reported experimental results (Phong et al., 2013; Terauchi et al., 2007) and indicate that nutrient compensation in actual post-translational

oscillators is achieved both by system-level and element-level mechanisms, i.e., at low ATP concentration by the system-level ELC, and at high ATP concentration, by the elemental enzymatic-reaction level.

4.3.3 Nutrient compensation is caused by the autonomous regulation of the catalyst concentration

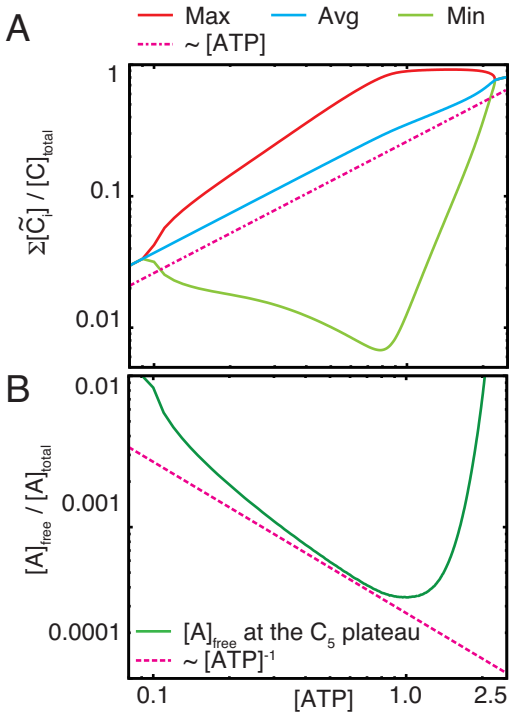

Figure 4.4: Dependence of the normalized concentrations of the components in the mass-action Kai protein model upon the concentration of ATP. (A) The maximum value (red line), the minimum value (blue), and the value averaged over a cycle (green line) of total concentration of inactive KaiCs are plotted. The average value of $\Sigma[\tilde{C}]/[C]_{total}$ is roughly proportional to $[ATP]$ (pink dashed dotted line). (B) The concentration of free KaiA computed when $[C_5]$ reaches a plateau, as estimated from the time where $[C_3]$ reaches a peak (see also Fig.3.5 of Chapter 3). This free KaiA concentration closely follows $[ATP]^{-1}$ (pink dotted line) at low ATP concentrations.

To explain how ATP concentration compensation functions by ELC, we analysed the abundance of available enzyme against ATP concentration. As shown in Fig.4.4A, as the ATP concentration increases, the average value of the summation of inactive KaiCs ($\Sigma[\tilde{C}]$) increases following $\Sigma[\tilde{C}] \propto [ATP]$. The flow from the inactive KaiC is thus estimated as $k_{dp}\Sigma[\tilde{C}]^* \propto [ATP]$ with $[\tilde{C}]^*$ as its fixed point (stationary) concentration. Because the phosphorylation reactions process in a step-by-step manner, the amount of active KaiC with m modification sites, $[C_m]$ ($m = 0 \sim 4$), follows $[C_m] \propto k_{dp}\Sigma[\tilde{C}]^* \propto [ATP]$. Therefore, the binding of C_m to the enzyme increases accordingly and causes the decrease of the amount of free KaiA, which can be estimated approximately as $[A]_{free} \simeq [A]_{total} - ([A]_{free}[C_m])/(K_m + [A]_{free})$. When $[A]_{total}$ is small enough, the minimum free KaiA abundance is smaller than K_m and, thus, $[A]_{free} \simeq [A]_{total} - ([A]_{free}[C_m])/K_m$. Accordingly, $[A]_{free} \simeq \frac{[A]_{total}}{1+[C_m]/K_m} \simeq \frac{[A]_{total}K_m}{[C_m]} \propto [ATP]^{-1}$ (see Fig.4.4B). Therefore, the amount of free KaiA counterbalances the altered speed of phosphorylation by increasing ATP concentration.

This mechanism of compensation is essentially the same as that previously proposed for temperature compensation (see Chapter 3). In general, homeostasis of the period against various environmental changes is achieved, as long as the following two criteria are satisfied:
1. The amount of the catalyst is small enough
2. The catalytic reactions rate-limit the total process, and their speed depends more sensitively on an external parameter than that of non-catalytic reactions
In the case of nutrient compensation, the second requirement is satisfied when the modification reactions consume more donor substrates than the demodification reactions. On the other hand, for temperature compensation, modification reactions require larger activation energy than demodification reactions. The mechanism of temperature compensation can be generally applied to the robustness of the oscillation period to a variety of external parameters.

Assume that the speed of the catalytic reaction is given by $F_{cat}(\{a\}) \times [A]$, which rate-limits the process where $\{a\}$ is control parameters that sensitively changes the catalytic process. If $F_{cat}(\{a\})$ increases with the parameter a_i, $[A] \propto F_{cat}^{-1}(\{a\})$ generally follows according to the above ELC mechanism. Thus, the period, which is mainly determined by the speed of the catalytic reaction, is unchanged against the changes in the parameter a_i. In this

manner, homeostasis of the period is generally achieved.

4.3.4 Relationship between nutrient compensation and temperature compensation

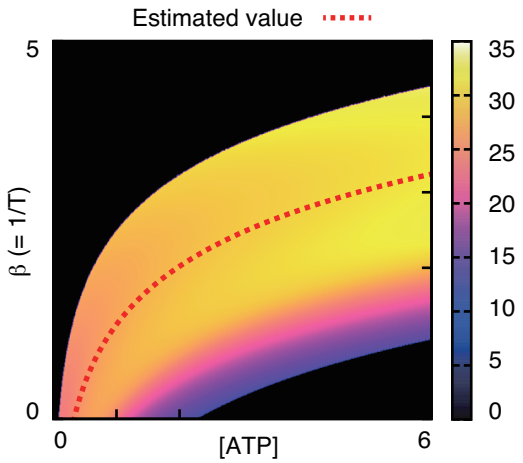

Figure 4.5: Relationship between nutrient and temperature compensation. Plot of the dependence of the period on the concentration of ATP and temperature. The activation energies of the modification and demodification reactions are given by $E_p = 1.0$ and $E_{dp} = 0.1$, respectively. The dotted line indicates the estimated value of the time scales at which the phosphorylation and dephosphorylation are balanced. Beyond the line where the period is almost unchanged, the catalytic phosphorylation reaction is rate-limiting (see the main text).

To analyse how nutrient and temperature compensation relate to each other, we calculated the period over a broad range of temperatures and ATP concentrations (Fig.4.5). It is evident that the range of ATP concentration for nutrient compensation and of temperature for temperature compensation mutually depend on each other. The region in which the period is insensitive to the temperature or ATP concentration is roughly estimated when the catalytic phosphorylation reaction is rate limiting. At low temperature, the speed of the phosphorylation reactions is much slower than that of the dephosphorylation reactions, and the phosphorylation reaction can be rate

limiting over a broad range of ATP concentrations; at high temperature, a lower ATP concentration is needed to reduce the speed of phosphorylation.

The region for nutrient and temperature compensation is roughly estimated from the condition in which the phosphorylation process is rate-limiting, i.e., $c_p \exp(-\beta E_p)[ATP][A][C_i]/([C_i] + K_i) < c_{dp} \exp(-\beta E_{dp})[\tilde{C}]$. Here, the rate-limiting process of the phosphorylation is given by its last step C_5, at which the amount of inactive KaiC is estimated to be equal to $[C_5]$. As a rough estimate for the phosphorylation rate, we adopt $[C_5] \sim K_5$ and $[A] \sim [A]_{total}$. Under these assumptions, the condition for nutrient and temperature compensation is estimated as $\beta \gtrsim (\ln(c_p[A]_{total}/(2c_{dp}K_5)) + \ln[ATP])/(E_p - E_{dp})$. The curve estimated taking into account this condition is plotted as a dotted line in Fig.4.5. Although this is a rough estimate, it basically captures the region for homeostasis of the period and suggests that homeostatic responses in the period against different external factors occur when the catalytic reaction is rate limiting.

4.3.5 The reciprocity relationship between robustness of the period and plasticity of the phase in the Kai model

We demonstrated that the homeostasis of the period against various environmental changes is achieved by enzyme-limited competition. In contrast, plasticity of the phase is needed to adapt accurately to diurnal cycles, i.e., the circadian clock has to be entrained quickly by external environmental cycles (e.g, light-dark, temperature, and metabolic cycles). Robustness of the period and plasticity of the phase seem to be incompatible at a glance, because robustness implies resistance to change and plasticity implies feasibility to change. Here, we analyze a relationship between robustness of period and plasticity of the phase, by varying the difference in the dependences of phosphorylation and dephosphorylation reactions upon external conditions. Then, we chose temperature as the external conditions, because the degree of temperature compensation is easily controlled by change the difference in activation energies.

First, we computed a phase response curve by transiently changing temperature from β_1 to β_2 for the duration of 1.0 of time (Fig.4.6). The maximum of $\Sigma i[C_i]$ is defined as $\phi = 0, 2\pi$, and the phase is defined by normalizing a time between two peaks by 2π. Then, we measured the minimum value of

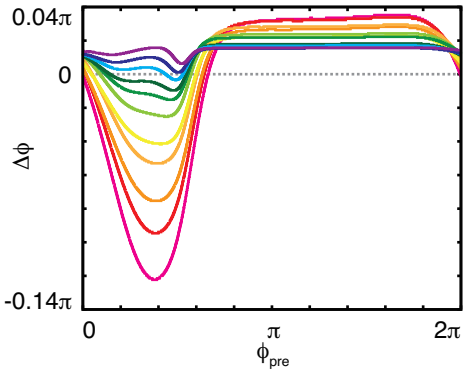

Figure 4.6: Phase response curve of the Kai model under various E_{dp} and fixed E_p.

a phase response curve ($\Delta\phi$) as an indicator of plasticity of the phase and the difference of periods at two different temperature conditions (ΔT) as an indicator of robustness of the period for various values of E_{dp} with fixing E_p. Dependence of $\Delta\phi$ and ΔT on E_{dp} is plotted in Fig.4.7A. When E_{dp} is low, i.e., temperature dependence of phosphorylation reaction is week, ΔT is small and $\Delta\phi$ is large. In contrast, when E_{dp} is high, i.e., temperature dependence of phosphorylation reaction is strong, ΔT is large and $\Delta\phi$ is small. When we chose β_1 and the KaiA concentration as control parameters, similar results are obtained (see Figs.4.8 and 4.9). It indicates that a biochemical oscillator with the homeostatic period against some environmental change can easily shift its own phase under the same environmental change, while as the homeostasis in period is weaker, the phase is hard to be shifted. This suggests that robustness of the period and plasticity of the phase are compatible, rather they cannot be separated.

Then we analyzed an entrainability, which is an indicator how fast oscillation can be entrained by external cycle, As already shown in Fig.3.10, the phosphorylation rhythm can be entrained by temperature cycles when the temperature compensation is achieved (E_{dp} is ranging from 0 to 0.35), whereas the clock never shows perfect entrainment at the other range where the period strongly depends on temperature (see Fig.4.7B). Moreover, at a small E_{dp} value where temperature compensation becomes nearly perfect ($E_{dp} = 0.05$), the oscillation shows faster entrainment than other E_{dp}. These results indicate that a biochemical oscillator with a homeostatic period against environmental changes is easily entrained by the same change. This

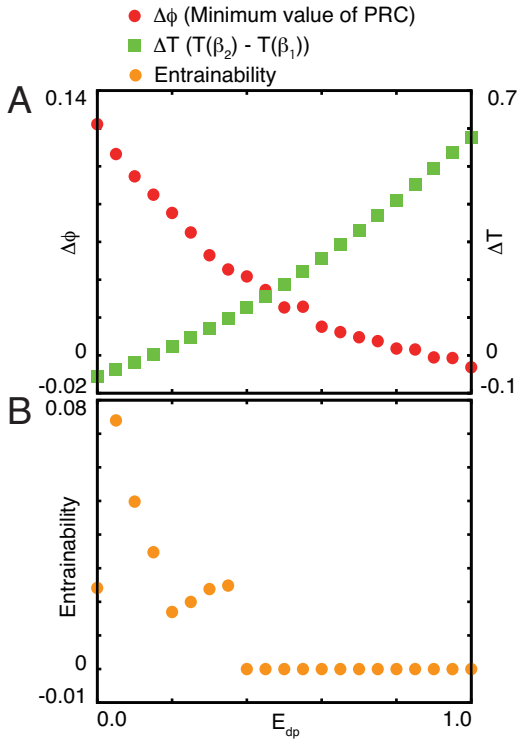

Figure 4.7: Reciprocity relationship between robustness of the period and plasticity of the phase and an entrainability in the Kai model. (A) Difference of periods at two temperatures ($\beta_1 = 1.0$ and $\beta_2 = 1.5$) (ΔT, green square) and the minimum value of phase response curve against a transient jump of temperature from β_1 to β_2 ($\Delta\phi$, red circle) are plotted against various E_{dp} and fixed $E_p = 1.0$. ΔT is normalized by the period at β_1, and $\Delta\phi$ is defined as the maximum value of magnitude of a phase advance. ΔT and $\Delta\phi$ seem to be inversely-correlated across a all range of E_{dp}. (B) Entrainability is plotted against various E_{dp}. Entrainability is defined as the inverse of the number of cycles required for the oscillator phase to entrain the external oscillation of temperature. Here, the temperature cycle is applied as a square wave between β_1 and β_2 with equal interval, which is initially half-period out-of-phase with the Kai oscillator.

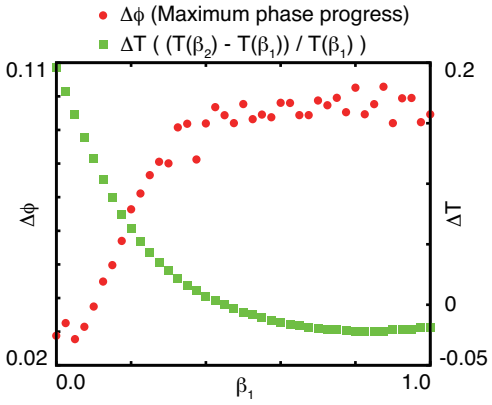

Figure 4.8: Reciprocity relationship between robustness of the period and plasticity of the phase in the Kai model under various temperature. Difference of periods at two temperatures (β_1 and $\beta_2 = \beta_1 + 0.5$) (ΔT, green square) and the minimum value of phase response curve against a transient jump of temperature from β_1 to β_2 ($\Delta\phi$, red circle) are plotted against various β_1. ΔT and $\Delta\phi$ are calculated in a similar way to Fig.4.7.

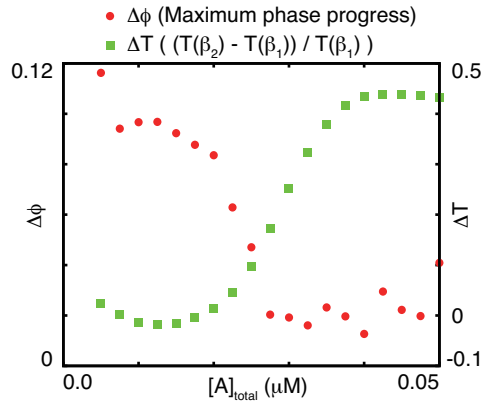

Figure 4.9: Reciprocity relationship between robustness of the period and plasticity of the phase in the Kai model under various concentration of KaiA. Difference of periods at two temperatures ($\beta_1 = 1.0$ and $\beta_2 = 1.5$) (ΔT, green square) and the minimum value of phase response curve against a transient jump of temperature from β_1 to β_2 ($\Delta\phi$, red circle) are plotted against various concentration of KaiA. ΔT and $\Delta\phi$ are calculated in a similar way to Fig.4.7.

is useful to adapt to external conditions.

4.3.6 The reciprocity relationship between robustness of the period and plasticity of the transcription-translation feedback model

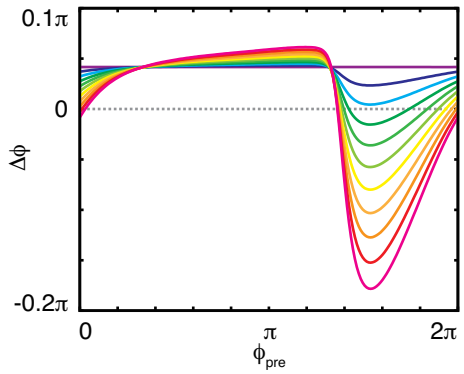

Figure 4.10: Phase response curve of the transcription-translation feedback model under various E_a and fixed E_k.

We found the reciprocity relationship between robustness of the period and plasticity of the phase in the Kai model as an example of the post-translational oscillator, which is one of the two major classes of circadian clocks. Here, we analyze such reciprocity relationship in the other class of circadian clocks, a transcription-translation feedback model. We measured $\Delta\phi$ and ΔT by the same procedure as the Kai model. The phase response curve in this case is given in Fig.4.10 Then, we define $\Delta\phi$ as the minimum value of the phase response curve. In the transcription-translation feedback model, ΔT is low and $\Delta\phi$ is high under a low E_a value, and ΔT is high and $\Delta\phi$ is low under a high E_a value. As shown in Fig.4.11, ΔT and $\Delta\phi$ is negatively correlated with approximately with a linear relationship, as in the Kai model. Then, the reciprocity relationship is achieved in not only the post-translational oscillator but also the transcription-translation feedback model.

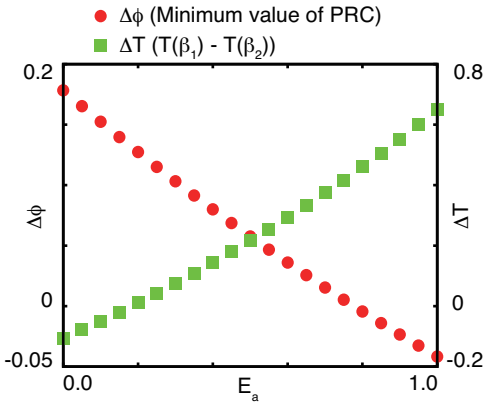

Figure 4.11: Reciprocity relationship between robustness of the period and plasticity of the phase in the transcription-translation feedback model. Difference of periods at two temperature ($\beta_1 = 0.0$ and $\beta_2 = 0.5$) (ΔT, green square) and the minimum value of phase response curve against a transient jump of temperature from β_1 to β_2 ($\Delta\phi$, red circle) are plotted against E_a while fixing $E_k = 1.0$. ΔT and $\Delta\phi$ are negatively correlated across a all range of E_{dp}, in same way as the Kai protein model.

4.4 Discussion

4.4.1 Basis of robustness of the period via ELC

Here, we showed that the ELC provides a general mechanism for homeostasis of the period of the post-translational biochemical oscillator. If the catalytic modification reaction is a rate-limiting process and the abundance of the catalyst is limited, the competition for the enzyme leads to compensation against parameter changes that sensitively alter the speed of the catalytic (phosphorylation) reaction rather than that of the non-catalytic (dephosphorylation) reaction. Therefore, the period is robust to parameter changes such as temperature or metabolic conditions. Experimentally, it is known that the circadian clocks show robustness of the period against changes in various environmental factors such as the temperature or ATP concentration (Nakajima et al., 2005; Phong et al., 2013; Terauchi et al., 2007).

In contrast, it is reported that some external cues can change the period of the clocks. For example, it is known that the administration of heavy water (D_2O) changes the period of the circadian clocks of various organisms

ranging from unicellular algae to vertebrates (Bruce and Pittendrigh, 1960; Enright, 1971; McDaniel et al., 1974). Indeed, this is consistent with our theory, because the mechanism that we propose requires selective change of the speed of the catalytic reaction, suggesting that external stimuli, which alter the speeds of the modification and demodification reactions equally, can change the period drastically.

The model of KaiC protein, which has six phosphorylation sites, used in this study seems to be complicated. However, it is reported that simpler models with a few phosphorylation sites show temperature compensation of the period according to the present ELC mechanism (see Chapter 3 and (Jolley et al., 2012)), while in the absence of multiple phosphorylation sites, oscillations with homeostatic periods are not available. Our theory, then, shows the general relevance of multimeric proteins to the homeostatic response of post-translational oscillators. Indeed, there are extensive studies on the possible roles of protein modification rhythms on the circadian clocks, to which our mechanism will be generally applicable.

We expect that ELC provides a general mechanism of robustness of the period of biological oscillators against external changes, which will be verified experimentally and will facilitate our understanding of homeostasis in organisms.

4.4.2 The reciprocity relationship between robustness of the period and plasticity of the phase

We demonstrated reciprocity relationship between robustness of the period and plasticity of the phase in two models, the KaiC protein model and the translational-transcriptional feedback model. To answer such relationship is achieved, we have to first discuss about universality in homeostasis of the period of biological clocks. In a study by François and coworkers, they computationally evolved a biochemical reaction network to achiev a homeostatic oscillator (François et al., 2012). In their simulation, external changes affect only a few kinetic parameters and others are insensitive to an external environment. Under such condition, they found that homeostatic oscillators have a buffer molecule, which can counterbalance changes in external environments by altering its own concentration. Because such buffer molecule takes care of environmental changes in the same way as a well-known adaptation mechanism (Segel et al., 1986), other parts of the systems are kept

constant, so that the period of such oscillator shows homeostatic response against environmental changes. In this case, a limit-cycle orbit of such oscillators shifts in a phase space of molecular concentrations along a direction of a concentration of such buffer molecule.

Both of the two models we studied here are distinguishable from the above model, because all of kinetic constant are environment-dependent. Still, in the Kai protein model, homeostasis of the period is achieved by a spontaneous change in the amount of the free enzyme. In this case, the free enzyme works as a buffer molecule and a homeostatic feature is achieved as a result of adaptation.

When the perfect homeostatic response achieved, the concentration of a buffer molecule x should be altered by the change in external environment. If the change in the concentration is Δx, the limit-cycle orbit will be shifted in the direction of changing the concentration of a buffer molecule and the magnitude of such shift will be $O(\Delta x)$. When this shift is small, the phase shift is due to the shift in limit-cycle, and thus $\Delta\phi \propto \Delta x$. On the other hand, when the change in a concentration of a buffer molecule is not sufficient to counterbalance the environmental stimulus, the concentrations of other molecules will change. Let us represent the concentration of x needed for a perfect adaptation as Δx^*. Then the change in concentration of the other molecule of the lowest order is proportional to $\Delta x^* - \Delta x$ The period also changes accordingly, so that $\Delta T \propto \Delta x^* - \Delta x$ is expected. Even if the number of buffer molecule species is not one, the above discussion can be adapted by considering a vector of the concentrations of buffer molecules $\{x_i\}$. By combining the two proportionally relationships, we get $a\Delta\phi + b\Delta T = \Delta x^*$ with proportional coefficients a and b. This relationship is consistent with the results of simulations of the two models. Thus the reciprocity relationship between robustness of the period and the plasticity of the phase can be explained by the above buffering mechanism for adaptation.

A molecular mechanism of homeostasis of the period of biological clocks cannot be derived by the reciprocity relationship, and itself depends on a particular target system. Conversely, such relationship may be universally achieved regardless of the molecular species of a buffer molecules. In ELC, the free enzyme is expected to work generally as a buffer.

Note that there could be a exception that shows homeostasis of the period without the phase shift : consider a biochemical oscillator that consists only of chemical reactions all of which are insensitive to changes in environment, i.e., the speed of whole reactions in the oscillator is not altered externally.

In this case, both the period and the phase (and also the oscillation amplitude) are not changed by an environmental factor, because of insensitivity of whole reactions. However, we do not have to think such case, because usual environmental factors, e.g., temperature and a concentration of a nutrient, should alter the speed of chemical reactions. Moreover, in this case, the clock cannot be entrained to external cycles, which means that the clock cannot adapt to environment and will not survive under selection pressure in evolution. Thus, the present biochemical oscillator's homeostatic response to environmental changes is expected to achieved by an adaptation mechanism and follow the reciprocity relationship universally.

We have shown that such reciprocity relationship is achieved also in the transcription-translational feedback model. François *et al.* (François et al., 2012) suggested that a Goldwin model, which is also a transcription-translation feedback model simiraly to the model adopted here, shows temperature compensation by adaptation. Then, it is natural that the reciprocity relationship is achieved in the transcription-translation feedback model by the same mechanism as the post-translational oscillator as described above. Therefore, it is expected that the reciprocity relationship can be achieved universally in broad circadian clocks, which, so far, are either the post-translational or the transcription-translation oscillator. Since and the reciprocity relationship is found in both of two classes, we expected that the relationship will be confirmed in experiments.

Appendix : Models and settings

The Kai protein model

In the simulation of the main text, parameter values are same as the parameters in the previous chapter.

Transcription-translation feedback model

In the simulation, we adopted the parameter values Table.4.1.

k	25.1
h	5.0
a	1.66
a'	0.1
s	503.0
s'	100.0
b	503.0
b'	100.0
c	5.03
c'	0.1
d	50.3
d'	0.1
u	503.0
u'	100.0
v	5.03
v'	0.1
E_k	1.0

Table 4.1: Parameter set of simpler model with two catalytic reactions

Part III

Memory

Chapter 5

Kinetic Memory Based on Enzyme-Limited Competition

Chapter Outline

Cellular memory, which allows cells to retain information from their environment, is important for a variety of cellular functions, such as adaptation to external stimuli, cell differentiation, and synaptic plasticity. While posttranslational modifications have received much attention as a source of cellular memory, mechanisms directing such alterations have not been fully uncovered. It may be possible to embed memory in multiple stable states in dynamical systems governing modifications. However, several experiments on modifications of proteins suggest long-term relaxation depending on experienced external conditions, without explicit switches over multi-stable states. As an alternative to a multistability memory scheme, we propose "kinetic memory" for epigenetic cellular memory, in which memory is stored as a slow-relaxation process far from a stable fixed-state. Information from previous environmental exposure is retained as the long-term sustainment of a cellular state, rather than switches over fixed-states. To demonstrate this kinetic memory, we study several models in which multimeric proteins undergo catalytic modifications (e.g., phosphorylation, methylation), and find that a slow relaxation process of the modification state, logarithmic in time, appears when the concentrations of a catalyst (enzyme) involved in the modification reactions are lower than that of the substrates. Sharp transitions from a normal fast-relaxation phase into this slow-relaxation phase are re-

vealed, and explained by enzyme-limited competition among modification reactions. The slow-relaxation process is confirmed by simulations of several models of catalytic reactions of protein modifications, and allows for the memorization of external stimuli, as its time course depends crucially on the history of the stimuli. This kinetic memory provides a novel insight to a broad class of cellular memory and functions. In particular, applications to long-term potentiation are discussed, including dynamics of modifications of calcium-calmodulin kinase II and cAMP-response element-binding protein, which are essential to synaptic plasticity.

5.1 Introduction

The importance of cellular memory, in which information from experienced environmental exposures can be preserved within cellular states, has received a great deal of attention in recent years. The capability of cells to translate environmental exposures into cellular memory has been reported in various organisms, ranging from bacteria to unicellular protozoa and multicellular vertebrates (Bliss and Gardner-Medwin, 1973; Bliss and Lomo, 1973; Guan et al., 2012; Jennings, 1906; Wolf et al., 2008). Such examples of cellular memory are thought to result from stored epigenetic changes, which are not restricted to histone modifications, but include long-term modifications (e.g., phosphorylation, methylation, and acetylation) of any proteins or DNAs that can regulate gene expression and affect cellular states. In a general context, cellular epigenetic memory is regarded as a phenomenon that occurs more slowly than biochemical reactions without resorting to any change in genome sequence, and is considered to be important for a variety of cellular functions, such as adaptation to external stimuli, cell differentiation, and synaptic plasticity (Bliss and Gardner-Medwin, 1973; Bliss and Lomo, 1973; Chickarmane et al., 2006; Sasagawa et al., 2005; Wolf et al., 2008).

One of the most prominent examples of cellular memory is long-term potentiation (LTP) for synaptic plasticity, whereby persistent phosphorylation of Ca^{2+}/calmodulin-dependent protein kinase II (CaMKII) is known to be important in early LTP (Lisman et al., 2002; Sweatt, 1999). Phosphorylation levels of CaMKII are elevated by transient increases in concentrations of Ca^{2+}, and are sustained even after decreases in concentrations of Ca^{2+}. Similarly, in late LTP, the persistent phosphorylation of transcription factors such as cyclic AMP-response element-binding protein (CREB) is important (Silva

et al., 1998; Sweatt, 1999). Another important example of cellular memory is seen in the determination of cell fates. For example, nerve growth factor is administrated to PC12 cells, extracellular-signal-regulated kinase (ERK) shows persistent phosphorylation and transmits information into downstream molecules, which finally lead to cell differentiation (Sasagawa et al., 2005).

Such cellular memory consists of three events: induction, maintenance, and expression. Signaling input can change the modification state of the molecule in concern, which can be maintained over a long time span (e.g., minutes to days), longer than the timescale of normal biochemical reactions. Such modifications can result in changes in expression or the activation of other molecules. In this study, we focus on the question of how modified states are maintained over a long timescale.

One possible avenue for addressing this question could be the use of the attractor concept. This concept includes the "memories-as-attractors" viewpoint, whereby dynamical systems governing the modification of states have multiple attractors (steady states), in each of which memory is stored as a stable modification state of the substrates (Crick, 1984; Dodd et al., 2007; Lisman, 1985; Thomson and Gunawardena, 2009). For example, models for the persistent phosphorylation of CaMKII have been proposed, in which the phosphorylation can take on two stable states, so that there appears hysteresis against the change in Ca^{2+} (Lisman and Goldring, 1988; Lisman and Zhabotinsky, 2001; Zhabotinsky, 2000). In an *in vitro* experiment, however, CaMKII did not show bistability, but only ultrasensitivity against the change in Ca^{2+} (Bradshaw et al., 2003). There have been reports that modification levels are shifted continuously upon stimulation, rather than taking only a few discrete states (Bradshaw et al., 2003) (see also (De Koninck and Schulman, 1998)); this continuity of modification states cannot be explained by the multistability model. Furthermore, the relaxation time: ~ 20 minutes after inhibition of CaMKII in ref (Sanhueza et al., 2011) suggests long-term dynamics, without resorting to the bistability discussed therein. In addition, the inclusion of positive feedback processes in gene expression dynamics, which are necessary for the maintenance of multiple states, requires energy, and as a result, memory retention incurs housekeeping costs. In summary, the stability of time-invariant attractors is important in some cases, but in others cannot be explained by the "memories-as-attractors" viewpoint.

Thus, it will be important to identify other forms of memory that allow for very slow changes of cellular states and adaptations to transient stimuli. We propose a "kinetic memory hypothesis" for epigenetic cellular

memory. In this scheme, memory is stored as a slow relaxation process far from an attractor, in which slowness allows for long-term sustainment of an embedded state. When cells are stimulated, their cellular states are shifted continuously, and are kept apart from attractors, and relaxation occurs more slowly than under a normal chemical reaction timescale. With this slowness in relaxation, stimulus-induced excited states are memorized over long time spans. This is in strong contrast to the memory-as-attractor scheme, in which new stable states are generated, or different attractors are selected in order to store memory of the stimuli. In kinetic memory, states can be changed continuously depending on the magnitude of the stimulus, and thus epigenetic kinetic memory is more flexible than attractor-memory. However, to date, an explicit biochemical model that realizes kinetic memory has not been proposed. In this study, we apply the kinetic memory scheme to model processes underlying cellular memory.

5.2 Models

5.2.1 Chained modification model

We introduce a chained modification model showing very slow kinetics (Fig.5.1). This model consists of a substrate with N modification sites and a catalyst, where the total abundance of each are conservation quantities given as $[S]_{total}$ and $[C]_{total}$, respectively. The use of 'modification' here refers to phosphorylation, methylation, and so forth. We assume that the catalyst can only facilitate each demodification reaction of the substrate. For simplicity, we assumed that enzymes for modification reactions are always maintained at sufficiently high levels so as not to be rate-limiting. In addition, some autocatalytic reactions (e.g., CaMKII phosphorylation reactions) also can be described as first order kinetics. Furthermore, even though both the modification and demodification reactions follow Michaelis-Menten kinetics, the same results can be obtained as described below in the kinase-phosphatase model. This yields,

$$S_i \xrightarrow{a_{i+1}} S_{i+1}$$

$$S_i + C \underset{k_i^-}{\overset{k_i^+}{\rightleftarrows}} CS_i \xrightarrow{b_i} S_{i-1} + C$$

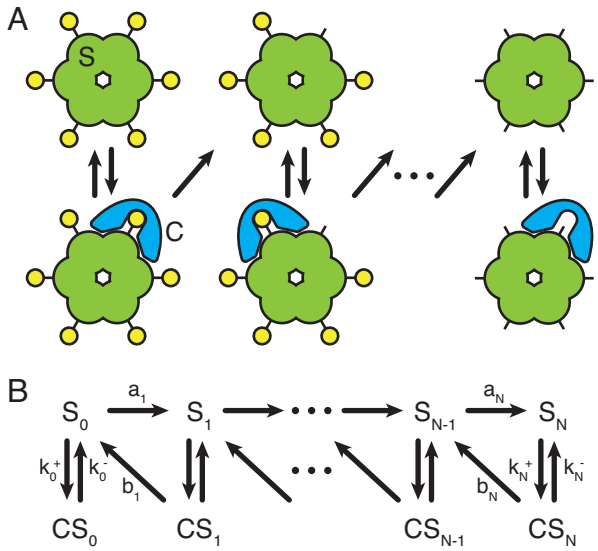

Figure 5.1: **The reaction scheme of the chained modification model.** Schematic representation (A) and reaction diagram (B) of our model. A substrate has N modification sites. Modification reactions of the substrates progress without catalyst at rates a_i and demodification reactions are facilitated by the catalyst at rates b_i.

where S_i and CS_i denote the substrates and a substrate-catalyst complex with i-th modification sites, respectively, and C denotes the catalyst.

Here, the formation and dissociation of substrate-catalyst complexes occur at much faster rates than other reactions and so are eliminated adiabatically. By denoting the concentration of free catalyst that does not form a complex as $[C]_{free}$, the model can be described as:

$$
\begin{aligned}
[\dot{S_0}] &= -a_1[S_0] + b_1 \frac{[C]_{free}[S_1]}{K_0 + [C]_{free}} \\
[\dot{S_i}] &= -a_{i+1}[S_i] + b_{i+1} \frac{[C]_{free}[S_{i+1}]}{K_{i+1} + [C]_{free}} \\
&\quad + a_i[S_{i-1}] - b_i \frac{[C]_{free}[S_i]}{K_i + [C]_{free}} \\
[\dot{S_N}] &= a_N[S_{N-1}] - b_N \frac{[C]_{free}[S_N]}{K_N + [C]_{free}} \qquad (5.1) \\
[C]_{total} &= \sum_{i=0}^{N} \frac{[C]_{free}[S_i]}{K_i + [C]_{free}} + [C]_{free} \qquad (5.2)
\end{aligned}
$$

where $K_i (= k_i^- / k_i^+)$ are the dissociation constants between S_i and C. Generally, binding energy of complex can depend on modification sites. For simplicity, we assume that a constant amount of energy is added per single modification (van Zon et al., 2007), but as long as the energy distribution is not narrow (whose condition is described below), the same results are obtained. With this simplification, the dissociation constant between C and S_i increases exponentially as $K_i = K_0 \times \gamma^i$. Input is given as the changes in speeds of modification reactions as $a_i = a(t)$ for all i. This is a simplified model for reactions with several modification sites, as discussed in the context of phosphorylation, methylation, and so forth in proteins, while several extensions will be discussed later.

5.2.2 The kinase-phosphatase model

Whole reactions are described below.

$$
\begin{aligned}
K + S_i &\underset{k_i^{K-}}{\overset{k_i^{K+}}{\rightleftarrows}} KS_i \\
P + S_I &\underset{k_i^{P-}}{\overset{k_i^{P+}}{\rightleftarrows}} PS_i \\
KS_i &\xrightarrow{a_{i+1}} K + S_{i+1} \\
PS_i &\xrightarrow{b_i} P + S_{i-1}
\end{aligned}
$$

By assuming that association and dissociation reactions are faster than others, we obtained the following equations:

$$
\begin{aligned}
[\dot{S_0}] &= -a_1[S_0]\frac{[K]_{free}/K_0^K}{1 + [K]_{free}/K_0^K + [P]_{free}/K_0^P} \\
&\quad + b_1[S_1]\frac{[K]_{free}/K_1^K}{1 + [K]_{free}/K_1^K + [P]_{free}/K_1^P} \\
[\dot{S_i}] &= -a_{i+1}[S_i]\frac{[K]_{free}/K_i^K}{1 + [K]_{free}/K_i^K + [P]_{free}/K_i^P} \\
&\quad + b_{i+1}[S_{i+1}]\frac{[K]_{free}/K_{i+1}^K}{1 + [K]_{free}/K_{i+1}^K + [P]_{free}/K_{i+1}^P} \\
&\quad + a_i[S_{i-1}]\frac{[K]_{free}/K_{i-1}^K}{1 + [K]_{free}/K_{i-1}^K + [P]_{free}/K_{i-1}^P} \\
&\quad - b_i[S_i]\frac{[K]_{free}/K_i^K}{1 + [K]_{free}/K_i^K + [P]_{free}/K_i^P} \\
[\dot{S_N}] &= a_N[S_{N-1}]\frac{[K]_{free}/K_{N-1}^K}{1 + [K]_{free}/K_{N-1}^K + [P]_{free}/K_{N-1}^P} \\
&\quad - b_N[S_N]\frac{[K]_{free}/K_N^K}{1 + [K]_{free}/K_N^K + [P]_{free}/K_N^P}
\end{aligned}
\tag{5.3}
$$

The total concentrations of the kinase and the phosphatase are conserved quantities, and thus

$$[K]_{total} = \sum_{i=0}^{N} [S_i] \frac{[K]_{free}/K_i^K}{1 + [K]_{free}/K_i^K + [P]_{free}/K_i^P} + [K]_{free} \tag{5.4}$$

$$[P]_{total} = \sum_{i=0}^{N} [S_i] \frac{[P]_{free}/K_i^P}{1 + [K]_{free}/K_i^K + [P]_{free}/K_i^P} + [P]_{free} \tag{5.5}$$

5.2.3 The extended Asakura-Honda model

The complete set of reactions in the extended Asakura-Honda model (see (Asakura and Honda, 1984) for the original Asakura-Honda model) is given as follows:

$$\begin{aligned}
C + T_i &\underset{k_i^{T-}}{\overset{k_i^{T+}}{\rightleftarrows}} CT_i \\
C + S_i &\underset{k_i^{S-}}{\overset{k_i^{S+}}{\rightleftarrows}} CS_i \\
T_i &\underset{k_i^{Sf}}{\overset{k_i^{Tf}}{\rightleftarrows}} S_i \\
CT_i &\underset{k_i^{Sf}}{\overset{k_i^{Tf}}{\rightleftarrows}} CS_i \\
CS_i &\xrightarrow{a_{i+1}} C + S_{i+1} \\
CT_i &\xrightarrow{b_i} C + T_{i-1}
\end{aligned}$$

Assuming that catalyst association and dissociation reactions, as well as flip-flop reactions between S and T are much faster than modification reactions, they can be eliminated adiabatically, so that the model can be

described as:

$$\begin{aligned}
[\dot{P_0}] &= -\frac{a_1[C]_{free}[S_0]}{[C]_{free}+K_0^S} + \frac{b_1[C]_{free}[T_1]}{[C]_{free}+K_1^T} \\
[\dot{P_i}] &= \frac{-a_{i+1}[C]_{free}[S_i]}{[C]_{free}+K_i^S} + \frac{b_{i+1}[C]_{free}[T_{i+1}]}{[C]_{free}+K_{i+1}^T} + \frac{a_i[C]_{free}[S_{i-1}]}{[C]_{free}+K_{i-1}^S} - \frac{b_i[C]_{free}[T_i]}{[C]_{free}+K_i^T} \\
[\dot{P_N}] &= \frac{a_N[C]_{free}[S_{N-1}]}{[C]_{free}+K_{N-1}^S} - \frac{b_N[C]_{free}[T_N]}{[C]_{free}+K_N^T}
\end{aligned} \tag{5.6}$$

Where $[P_i] = [S_i] + [T_i]$ and $[S_i] = [P_i]L_i/(1+L_i), [T_i] = [P_i]/(1+L_i)$. Here, $[C]_{free}$ is the free catalyst that is not bound to T or S, which satisfies,

$$[C]_{total} = \sum_{i=0}^{N}\left(\frac{[C]_{free}[S_i]}{[C]_{free}+K_i^S} + \frac{[C]_{free}[T_i]}{[C]_{free}+K_i^T}\right) + [C]_{free}, \tag{5.7}$$

where, K_i^S and K_i^T are dissociation constants between C and S_i or T_i, respectively. We assumed that the affinities between the catalyst and the substrate decrease exponentially with the number of modified sites in the substrate, that is, the dissociation constants K_i^S and K_i^T increase exponentially. Exponential increases of K_i^S and K_i^T are required for perfect adaptation, when the amount of the catalyst is sufficiently small (see Appendix). In addition, we assumed that the dissociation constants are not different between the S form and the T form, so that the dissociation constants are described as $K_i^S = K_i^T = K_0 \times \gamma^i$; this is only for simplicity, and is not essential. Stimuli are given as changes in L_i, identical to the original A-H model.

5.3 Results

5.3.1 The chained modification model shows slow "glassy" relaxation

In order to analyze relaxation processes from a highly modified state to a low modified state, we set the initial condition as $[S_N] = [S]_{total}$ and $a_i = 0$ for all i. Then, only demodification reactions progress. Under this condition, a modification level ($= \sum_{i=0}^{N} \frac{i[S_i]}{N[S]_{total}}$) relaxes from 1 to 0 in a single direction. When concentrations of the catalyst are sufficiently high (i.e., in the limit $[C]_{total} \to \infty$), the behavior of this model is same as the first-order reactions,

so that fast exponential relaxation occurs.

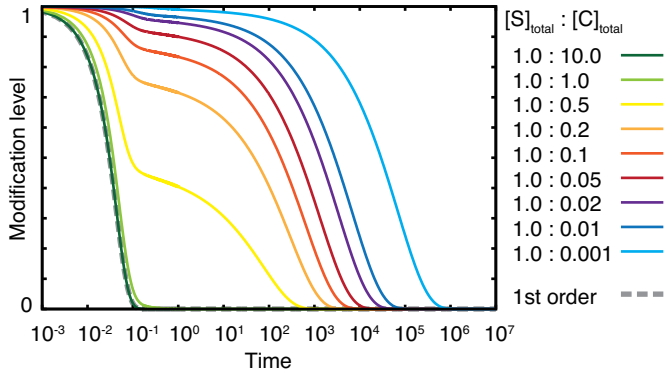

Figure 5.2: **The slow logarithmic relaxation of the chained modification model.** Initial condition is set as $[S_N] = [S]_{total}$ and $[S_i] = 0.0$ for other i, and the relaxation process of the modification level is computed without input ($a_i = 0$). The parameters are given as $N = 6$, $\gamma = 5.0$, and $K_0 = 0.1 \times \gamma^{-6}$. Plotted are the time courses of the modification level, for different values of the catalyst concentration, 0.001, 0.01, 0.02, 0.05, 0.1, 0.2, 0.5, 1.0, and 10.0 with different colors, where the concentration of S is fixed at 1.0. Although exponential relaxation is observed as in first-order reactions (dotted line) when the concentration of the catalyst is sufficiently large, the relaxation is drastically slowed down as the concentration of the catalyst becomes smaller than that of the substrate.

At low catalyst concentrations, however, the relaxation process is quite different. In this case, as shown in Fig.5.2, the modification level relaxes more slowly; it is fitted by logarithmic relaxation in time. Moreover, when the concentration of the catalyst is in some range, the relaxation process shows a plateau. Indeed, such logarithmic relaxation processes and an emergence of a plateau have been shown to exist in glasses, and studied in kinetic constraint models of glasses (Awazu and Kaneko, 2009).

5.3.2 The chained modification model shows transition from slow relaxation to fast relaxation

As shown in Fig.5.2, the relaxation process shows transition from a fast exponential relaxation phase to a slow logarithmic relaxation phase, as catalyst

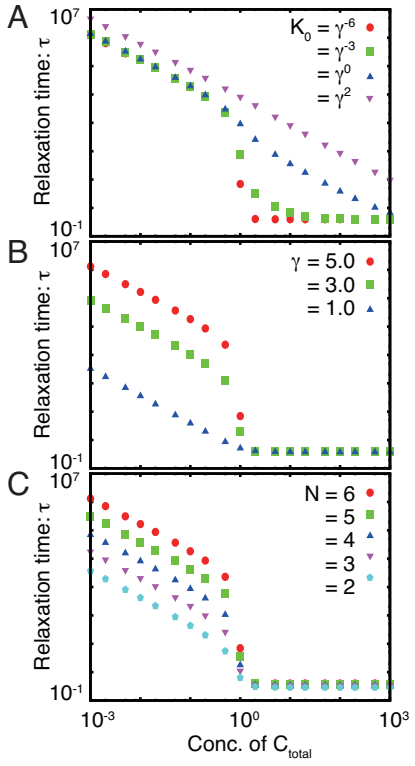

Figure 5.3: **Change in the catalyst dependence on the relaxation time τ against K_0, the dissociation constant (A) against γ, heterogeneity of the dissociation constant (B), and against N. the number of modification sites (C).** τ is plotted against $[C]_{total}$; τ is defined as the time when summation of all of $|[S_i] - [S_i]^*|$ falls below the threshold value(10^{-12}) without input, started from the initial condition ($[S_N] = [S]_{total}$). (A) $K_0 = 0.1 \times \gamma^{-6}, 0.1 \times \gamma^{-3}, 0.1 \times \gamma^0, 0.1 \times \gamma^2$, $\gamma = 5.0$, $N = 6$. (B) $\gamma = 1.0, 3.0, 5.0$, $K_0 = 0.1 \times \gamma^{-6}$, $N = 6$. (C) $N = 2, 3, 4, 5, 6$, $K_0 = 0.1 \times \gamma^{-N}$, $\gamma = 5.0$.

concentration is decreased. To examine this transition quantitatively, we analyzed the dependence of relaxation time τ on the concentration of the catalyst. In Fig.5.3, dependence of τ upon the total concentration of catalyst $[C]_{total}$ is plotted. It shows a sudden increase of τ with the decrease of $[C]_{total}$ below the concentration of total substrates $[S]_{total}$. Although nonlinear dependence on the catalyst concentration is expected based on Michaelis-Menten kinetics, this sharp increase in τ near the critical point is due to the limitation of catalyst.

Here, by slightly decreasing the concentration of the catalyst below that of the substrate or by increasing that of the substrate beyond that of the catalyst, the relaxation time suddenly increases by several orders of magnitude. In other words, the relaxation time becomes much longer than the original chemical timescale, so that the modification state remains almost at the original level. Hence, the modification state is "memorized" over a long timescale, and storing or erasing memory is processed by slightly changing the ratio of catalyst to substrate below and beyond the critical value. In summary, our model exhibits a transition from fast exponential relaxation to slow logarithmic relaxation, providing kinetic memory.

5.3.3 Continuous memory as input dependence of the relaxation time

When kinetic memory is formed via logarithmic relaxation, the relaxation time is not constant, but is instead further increased with the ratio between the concentrations of the substrate and catalyst. Relaxation time increases continuously with the magnitude and the duration of stimuli given as $a(t) = A$ for $-\tau_{pre} < t < 0$ and $a(t) = 0$ for $0 \leq t$, as shown in Fig.5.4. Thus, information of the input stimulus (i.e., magnitude and duration) is "memorized" as the difference in relaxation time. This continuous memory is in contrast to the on-off type attractor memory.

5.3.4 Condition for kinetic memory

In this section, we discuss the condition for the existence of sharp transition to memorized states.

(i) The binding affinity should be small – condition for K_0

First, we analyzed the dependence of τ on K_0 (Fig.5.3A). When K_0 is small, the catalyst easily binds to substrates, whereas when K_0 is large, the

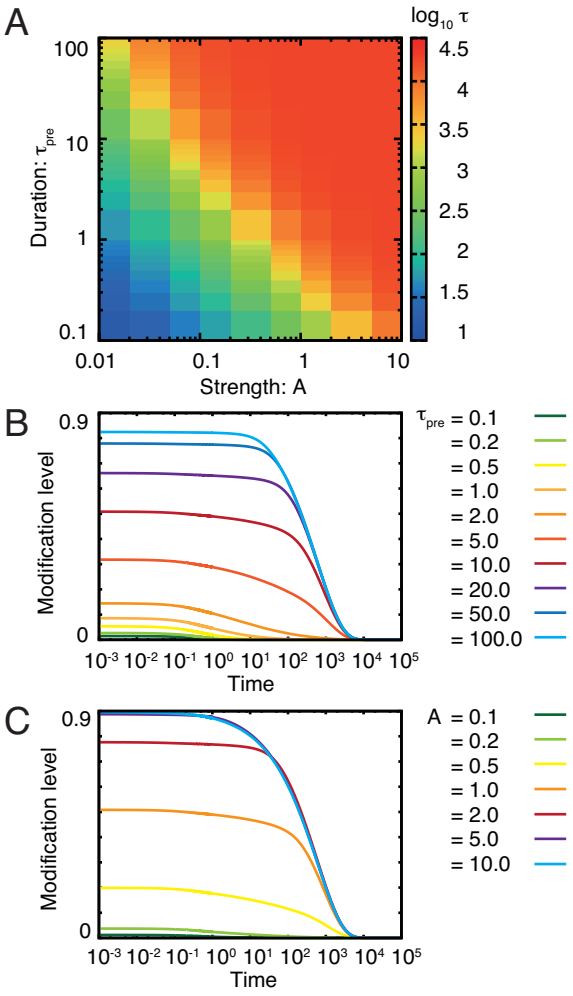

Figure 5.4: **Dependence of the relaxation process τ on the magnitude and duration of a stimulus.** (A) The relaxation time after exposure to the stimulus with various magnitudes and durations is plotted as a color map. The initial condition is given as $[S_0] = [S]_{total}$ and $[S_i] = 0.0$ for other i, and input is given as $a(t) = A$ for $-\tau_{pre} < t < 0$ and $a(t) = 0$ for $0 \leq t$. When the magnitude (A) and duration of the stimulus (τ_{pre}) increases, τ increases continuously over an order of magnitude. The catalyst concentration is set at 1/10 of the substrate concentration. (B) Dependence of the relaxation process on the duration of stimulus exposure. The duration of stimulus exposure is changed while the magnitude is fixed at $A = 1.0$. Here, the relaxation time almost increases exponentially with the increase in duration for the some extent small τ_{pre}. When τ_{pre} is long enough, different modification level is maintained for long time. (C) Dependence of the relaxation process of the chained modification model on the magnitude of the stimulus. The magnitude of the stimulus is changed while the duration is fixed as $\tau_{pre} = 10.0$. The increase of the magnitude has a weaker effect on the relaxation time than the duration.

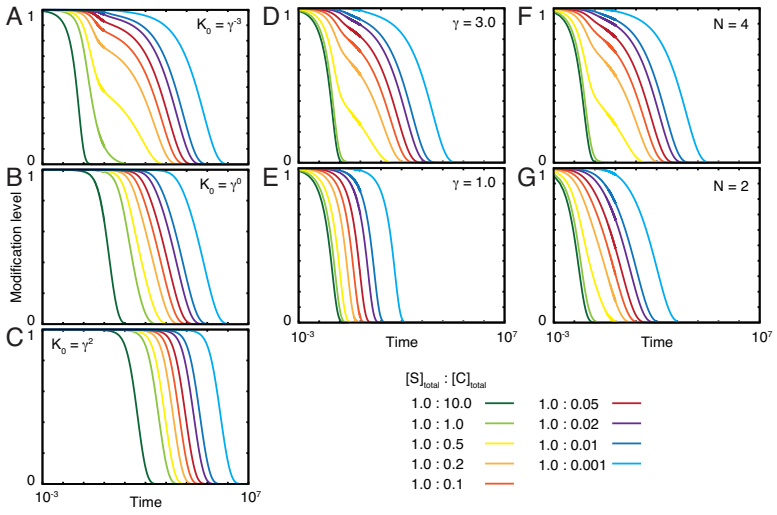

Figure 5.5: The relaxation process of the chained modification model for $K_0 = 0.1 \times \gamma^{-3}$ (A), $0.1 \times \gamma^0$ (B), $0.1 \times \gamma^2$ (C) and $\gamma = 5.0$, $N = 6$, $\gamma = 3.0$ (D), $\gamma = 1.0$ (E) and $K_0 = 0.1 \times \gamma^{-6}$, $N = 6$, $N = 4$ (F), $N = 2$ (G) and $K_0 = 0.1 \times \gamma^{-N}$, $\gamma = 5.0$. The time course of the phosphorylation level is plotted. The initial condition is the same as in Fig. 5.2. Plotted for different values of $[C]_{total}$ with different colors. The transition from fast exponential to slow logarithmic relaxation is sharp for low K_0 . For the low γ, slow logarithmic relaxation becomes similar to fast exponential relaxation, and finally slow logarithmic relaxation disappears when $\gamma = 1.0$. When the number of modification sites is small, slow logarithmic becomes unclear.

catalyst tends to be free. Hence, as K_0 is increased, the threshold concentration of the catalyst at saturation is decreased, and for larger values of K_0, a sharp transition of τ against the catalyst concentration disappears, as shown in Fig.5.3A. Indeed, in the case of $K_0 = 0.1 \times \gamma^0 = 0.1$, the relaxation process is slowed down gradually by decreasing the catalyst concentration, and there is no sharp transition.

As K_0 is decreased, the transition becomes sharper (see Fig.5.3A for $K_0 = 0.1 \times \gamma^{-3}$ and $0.1 \times \gamma^{-6}$). Indeed, for $K_0 = 0.1 \times \gamma^{-6}$ (Fig.5.2), the transition from exponential to logarithmic relaxation occurs with the decrease in the catalyst concentration below the critical concentration, $[C]^*_{total}$. This critical value always remains at the total substrate concentration, as long as a sharp transition occurs. Below the critical concentration, τ is proportional to $[C]^{-1}_{total}$, which is almost independent of K_0.

(ii) The difference in the dissociation constants is important for slow logarithmic relaxation – condition for γ

The relaxation behavior also crucially depends on the value of γ (Fig.5.3B). For large γ, τ drastically changes at around the critical concentration of the catalyst. With the increase in γ, the slope of the logarithmic relaxation becomes smaller (Fig.5.5), resulting in much slower relaxation. Above the critical concentration, τ is independent of $[C]_{total}$, and below the critical concentration, $\tau \propto [C]^{-1}_{total}$. This transition is distinctively sharper than that of Michaelis-Menten type dynamics and is regarded as an example of ultrasensitivity (McCarrey and Riggs, 1986).

In contrast, as γ becomes smaller, the change in τ is reduced, and at $\gamma = 1$, the logarithmic relaxation does not appear at all (Fig.5.5E) even at the low concentration of the catalyst. The relaxation time gradually decreases with the increase in the catalyst concentration and is almost constant if the catalyst concentration is larger than that of the substrate.

(iii) With an increase in the number of modification sites, relaxation occurs more slowly – condition for N

When the number of modification sites, N, is increased, the gap in the relaxation time between the fast relax phase and the slow relax phase is increased (Fig.5.3C). Indeed, in the fast exponential relaxation phase, the relaxation time is almost independent of N, while it increases with N, in the slower logarithmic relaxation phase. For $N = 2$, the relaxation process deviated from logarithmic relaxation, but occurred more slowly than in exponential relaxation (Fig.5.5G). For $N > 3$, relaxation time increased exponentially with N.

5.3.5 The order of relaxation reverses under the logarithmic relaxation regime

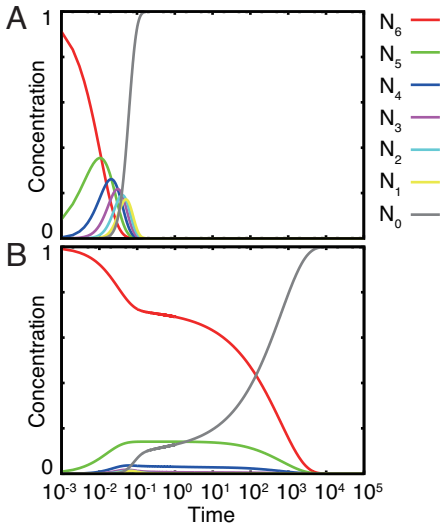

Figure 5.6: **Relaxation process of each $[S_i]$.** The time course of $[S_i]$ for each i is plotted by setting the initial condition as already described. (A) $[C]_{total} = 2.0$ $[S_i]$'s relax in descending order, in the same manner in the first-order reactions. (B) $[C]_{total} = 0.1$ $[S_i]$'s relax in ascending order, that is, converse to that observed for the first-order reactions. The highly modified state relaxes only after the relaxation of the lower modified $[S_i]$. The relaxation process consists of several plateaus, which are typically observed in relaxation processes of kinetic glass

The relaxation of the modification level is accompanied by changes in the modifications of substrate sites. Initially, $[S_N]$ is set larger than other values for $[S_i]$, and the relaxation process to the stationary state with $[S_0] = [S]_{total}$ was investigated. At high catalyst concentrations, $[S_i]$ relaxes in descending order (Fig.5.6A); decreases in $[S_N]$ resulted in increases of $[S_{N-1}]$, whose decrease resulted in the increase of $[S_{N-2}]$, and so forth. This ordered relaxation agrees with that of the first-order kinetic case, which is expected given that a substrate with $i+1$ modified sites is demodified to a substrate with i sites.

At low catalyst concentrations, however, the relaxation process is not ordered in such a monotonic manner. Indeed, highly modified substrates cannot relax readily (Fig.5.6B), whereas less modified substrates are able to take on modified states more easily. This relaxation of reversed order is due to the limitation of catalysts and differences in catalyst/substrate affinities by the number of modified sites i, both of which underlie slow, logarithmic relaxation.

5.3.6 The kinase-phosphatase model exhibits the same features as the chained modification model

To further demonstrate the utility of kinetic memory, we also investigated the Kinase-phosphatase (K-P) model (Fig.5.7A). This model contains three components, which are kinase K, phosphatase P, and substrate S with multiple modification sites. These modification states are characterized by S_i, which denotes the number of phosphorylated residues i. Kinase facilitates the increase of the number of phosphorylated residues, while phosphatase facilitates inverse reactions. Generally, substrate modifications lead to changes in the affinities of substrates and catalysts. The dissociation constant between K and S_i, and P and S_i increases exponentially as $K_i^K = K_0^K \times \gamma^i$ and $K_i^P = K_0^P \times \gamma^i$, respectively, identical to that observed in the chained modification model.

We studied the relaxation process of $[S_i]$ after the amount of the total kinase ($[K]_{total}$) was varied, which works as the input stimuli. We analyzed the relaxation process following the input of stimuli with a higher concentration of active kinase for a sufficient length of time. Here again, the dephosphorylation processes in the K-P model show slow logarithmic relaxations, when γ is positive. As shown in Fig.5.7B, when the total amount of phosphatase is lower than that of the substrate, the dephosphorylation process shows very slow relaxation. The transition between fast and slow relaxation occurs at the point where the amount of phosphatase and that of the substrate is balanced.

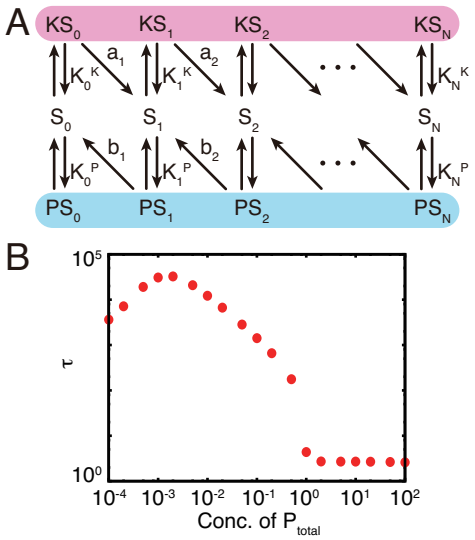

Figure 5.7: **Kinase-phosphatase model (A) and its relaxation time (B).** The relaxation times τ of the variables S_i are plotted against the total concentration of phosphatase. τ is defined as the time when summation of $|[S_i] - [S_i]^*|$ of all i falls below the threshold value, after relaxation at a kinase rich condition ($[K]_{total} = 10^4$). The model shows the transition from fast exponential relaxation to slow logarithmic relaxation at the critical point ($[P]_{total} = 1.0$). (When the amount of the phosphatase is lower than that of kinase ($[P]_{total} = 0.001$), the relaxation time itself is shorter, while the logarithmic relaxation remains. Here, the stable fixed point value of the concentration S_N changes to a higher value, and relaxation time is decreased.)

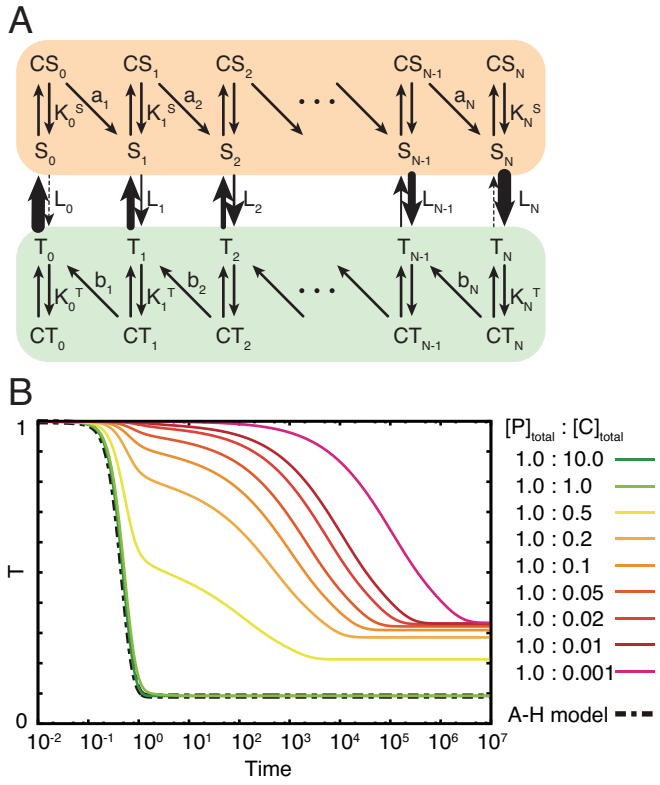

Figure 5.8: **The extended Asakura-Honda model (A) and its slow logarithmic relaxation after exposure to an environmental stimulus (B).** After the system is relaxed in the presence of the attractant as $L_i/L_i^0 = 317.23$, the system transitions to a repellant condition as $L_i/L_i^0 = 0.0032$, and the relaxation process of $T = \Sigma[T_i]$ is computed. The parameters are given as $N = 6$, $\gamma = 5.0$, and $K_0 = 0.1 \times \gamma^{-6}$. Plotted are the time courses of T, for different values of the catalyst concentration, 0.001, 0.01, 0.02, 0.05, 0.1, 0.2, 0.5, 1.0, and 10.0 with different colors, where the concentration of S is fixed at 1.0. Although exponential relaxation is observed as in the original A-H model (dotted line) when the concentration of the catalyst is sufficiently large, the relaxation is drastically slowed down as the concentration of the catalyst becomes smaller than that of the substrate.

5.3.7 The extended Asakura-Honda model shows the same behavior as the chained modification model

As another example, we studied an extended version of Asakura-Honda (A-H) model. The original A-H model was introduced to explain processes of adaptation to changes in the concentration of external signal molecules (attractant and repellant) in chemotactic behavior (Asakura and Honda, 1984). This model represents a two-state receptor with multiple modification sites. Receptors of different states are recognized by distinct enzymes, which facilitate an increase and a decrease in the number of modified sites. In the model, the enzymes are always maintained at sufficient levels so as to not be rate-limiting. This A-H model consists only of first-order reactions, without Michaelis-Menten type reactions. Here, to discuss kinetic memory, we explicitly took dynamics of co-factor as a catalyst into account that catalyzes each modification reaction (Fig.5.8A).

We analyzed the adaptation process after the input stimulus is applied to change the fraction of two states, to find that the extended A-H model shows that the slow logarithmic relaxation occurs when the abundance of catalyst is limited, as observed in the chained modification model (Fig.5.8B). The modified state memorizes the input amplitude and duration, in the time course of adaptation, and the conditions for this kinetic memory are essentially identical with those of the chained modification model (see Fig.5.9-5.11). It is noted that a slow process exists only in the relaxation in the adaptation, while the response remains fast independent of the parameters and the abundance of catalysts. The timescales of response and relaxation are separated, and independently controlled by tuning dissociation constants between substrates and a catalyst.

5.4 Discussion

5.4.1 Transition to the long-term kinetic memory

In the present chapter, we studied three models, the chained modification model, the kinase-phosphatase model and the extended A-H model, which consist of a substrate with multi-modification sites and a catalyst that facilitate modification of the substrate's sites. As shown in Fig.5.3 and Fig.5.7B and Fig.5.10, all of these models reveal the transition from fast exponential

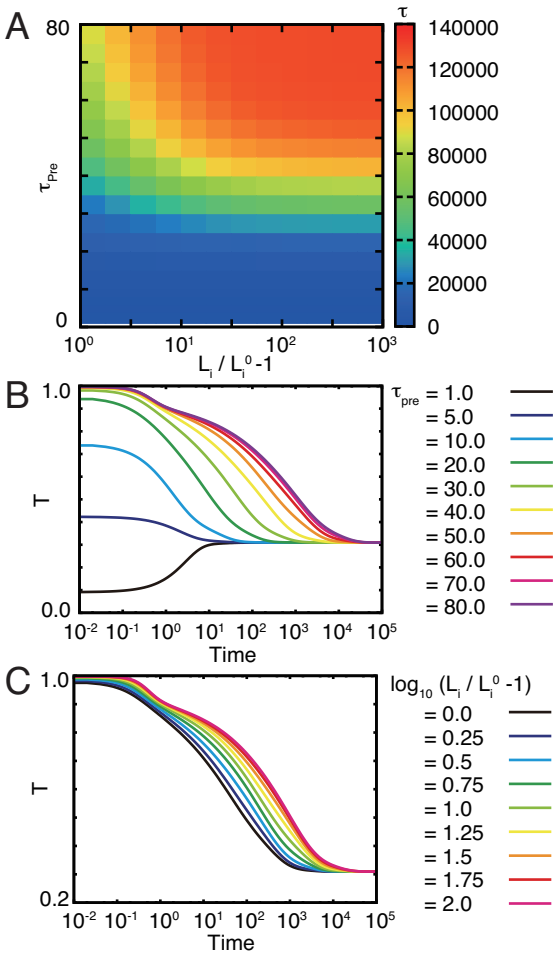

Figure 5.9: Dependence of the relaxation process of the extended A-H model on the magnitude and duration of a stimulus. (A) The relaxation time after exposure to the stimulus with various magnitudes and durations is plotted as a color map. The initial condition is given as $[S_0] = [S]_{total}$ and $[S_i] = [T_i] = 0.0$ for other i. When the magnitude (L_i) and duration of the stimulus increases, relaxation time τ increases continuously over an order of magnitude. The catalyst concentration is set at 1/10 of the substrate concentration. (B) Dependence of the relaxation process on the duration of stimulus exposure. The duration of stimulus exposure is changed while the magnitude is fixed at $L_i/L_i^0 = 11$. Here, the relaxation time almost increases exponentially with the increase in duration. (C) Dependence of the relaxation process on the magnitude of the stimulus. The magnitude of the stimulus is changed while the duration is fixed as $\tau_{pre} = 50.0$. The increase of the magnitude has a weaker effect on the relaxation time than the duration.

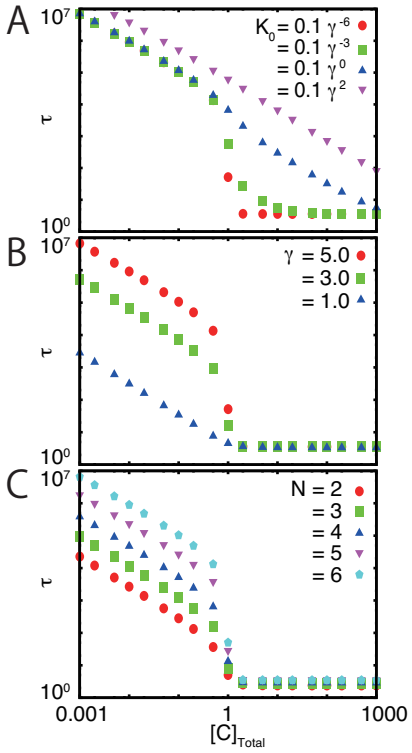

Figure 5.10: Change in the catalyst dependence of the extended A-H model on the relaxation time τ against K_0, the dissociation constant (A) against γ, heterogeneity of the dissociation constant (B), and against N, the number of modification sites. τ is plotted against C_{Total}; τ is defined as the time when summation of all of $|[S_i] - [S_i]^*|$ and $|[T_i] - [T_i]^*|$ falls below the threshold value(10^{-12}) at the repellant condition ($L_i/L_i^0 = 0.0032$), after a relaxation at the attractant condition ($L_i/L_i^0 = 317.23$). (A) $K_0 = 0.1 \times \gamma^{-6}, 0.1 \times \gamma^{-3}, 0.1 \times \gamma^0, 0.1 \times \gamma^2$, $\gamma = 5.0$, $N = 6$. (B) $\gamma = 1.0, 3.0, 5.0$, $K_0 = 0.1 \times \gamma^{-6}$, $N = 6$. (C) $N = 2, 3, 4, 5, 6$, $K_0 = 0.1 \times \gamma^{-N}$, $\gamma = 5.0$.

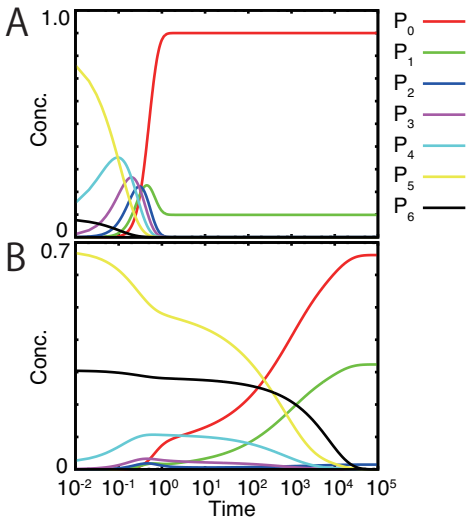

Figure 5.11: Relaxation process of each $[P_i]$ of the extended A-H model. The time course of $[P_i]$ for each i is plotted by setting the initial condition as already described. (A) $[C]_{total} = 10.0$ $[P_i]$'s relax in descending order, in the same manner as in the original A-H model. (B) $[C]_{total} = 0.1$ $[P_i]$'s relax in ascending order, that is, converse to that observed for the original A-H model. The highly modified state relaxes only after the relaxation of the lower modified $[P_i]$. The relaxation of the highly modified $[P_i]$'s plateau, a prominent feature of kinetic glass.

relaxation to slow logarithmic relaxation at the point where concentration of the catalyst falls below that of the substrate.

The conditions for this transition are summarized as follows: There must be heterogeneity in binding affinity of catalysts that depends on the number of modified sites, so that the affinity for highly modified substrates should be sufficiently small. This leads to two requirements in our model in which the dissociation constant is set at $K_0\gamma^i$ for the modification sites i.
(i) low K_0 value: this supports a high affinity for substrates, so that the competition for catalysts among substrates is induced. To satisfy this requirement, K_i should be smaller than the substrate concentration $[S]$ for all i, then the upper limit of K_0 is restricted as $K_0 \leq \gamma^{-N}[S]$.
(ii) $\gamma > 1$: affinity depends on the number of modified sites on the substrates. When the above conditions are not satisfied, the relaxation time follows that of the Michaelis-Menten equation. In contrast, when K_0 is small and $\gamma > 1$, relaxation changes drastically at the point where the concentrations of the substrate and the catalyst coincide. This change is much sharper than that expected from the Michaelis-Menten equation, and is an example of ultrasensitivity.

When the concentration of the substrate ($[S]$) is lower than that of the catalyst ($[C]$), the concentration of a catalyst-substrate complex ($[CS]$) becomes the about the same concentration as the substrate ($[CS] \sim [S]$), while $[C] < [S]$, $[CS]$ approaches $[C]$. When the concentrations of catalysts decreases to levels below that of substrates, various modification forms of the substrate compete for the catalysts. As a result, the transition to the slow relaxation occurs, induced by this enzyme-limited competition.

5.4.2 The mechanism of the logarithmic relaxation

Recall that the slowing down of relaxation was initially proposed for chemical glass in catalytic networks, in which a catalyst is consumed as a substrate for other chemical reactions and relaxation slows due to catalyst depletion. Here again, logarithmic relaxation is observed when the reaction coefficients are distributed exponentially (Awazu and Kaneko, 2009).

In our case, reaction speeds r_i are also distributed exponentially as $r_i \propto \exp(-\beta i)$, as the speeds of modifying reactions are proportional to the dissociation constant as $\frac{[C][S]}{[C]+K_i} \sim \frac{[C][S]}{K_i} \propto K_i^{-1}$ for low catalyst concentrations, while K_i is increased exponentially with the number of the modification sites i. When the reaction speed is distributed exponentially, the logarithmic re-

laxation is expected from the previous study (Awazu and Kaneko, 2009): The relaxation processes are approximately written as the superposition of $\exp(-e^{-\beta i}t)$ over i. By replacing the summation with an integral, and by assuming that there is a sufficient number of modification sites, logarithmic relaxation will occur (Fig.5.2).

The slowing down of relaxation due to the competition of the catalyst is also intuitively understood. When the n-th modified molecules are demodified, the amount of $(n-1)$-th modified molecules will increase. Because these n-th modified molecules have lower affinity for the catalyst than the $(n-1)$-th ones, they cannot effectively bind to the catalyst, and thus relaxation involving the decrease in modification is slowed down.

5.4.3 Relevance of kinetic memory to cell biology

The kinetic memory we studied here is generated by a substrate with a few modification sites and a catalyst (enzyme) shared by each of the different modification states, resulting in enzyme-limited competition (ELC) (Hatakeyama and Kaneko, 2012). Hence, multimeric proteins, for example, can provide a molecular basis for kinetic memory. A candidate for a multimeric protein bearing the kinetic memory is CaMKII, which forms a dodecameric structure with phosphorylation sites in each monomer (Lisman et al., 2002). It is known that the phosphorylation of sites on CaMKII plays a critical role in the maintenance of early LTP. CaMKII is phosphorylated with the increase in Ca^{2+} concentration and is dephosphorylated by protein phosphatase 1 (PP1). After Ca^{2+} concentration decreases, phosphorylation levels remain high, so that CaMKII stores memory in its phosphorylation state. Indeed, if PP1 is limited, ELC among CaMKII molecules is expected to lead to kinetic memory, according to our argument here. In fact, it has been reported that the concentration of PP1 is smaller than that of CaMKII in the postsynaptic density, as postulated by the condition for ELC (Lisman and Zhabotinsky, 2001). As already posed in the introduction, the phosphorylation state of CaMKII may not have multistability (Bradshaw et al., 2003).

Another candidate for kinetic memory may be CREB in brain synapses, which is known to work for potentiation by changing its phosphorylation levels. In the late LTP, CREB is phosphorylated by CaM-dependent kinase and is gradually dephosphorylated by calcineurin, while the phosphorylation of CREB leads to the activation of gene expression (Bito et al., 1996; Silva

et al., 1998). Here, it is reported that with the increase in the duration of input, the relaxation time of dephosphorylation of CREB is prolonged, as is consistent with our kinetic memory (Bito et al., 1996).

One could also expect that several other proteins with multi-modification sites may provide kinetic memory in our scheme. For example, the phosphorylation level of ERK, which has multi-phosphorylation sites, is elevated over a long time span, after a transient increase in the presence of nerve growth factor (Sasagawa et al., 2005). Such long-term phosphorylation might be a result of the logarithmic relaxation in kinetic memory.

In a multistability (attractor) model, the number of memorized states is discrete and few, since the number of attractors typically increases only linearly with the number of modification sites. In contrast, kinetic memory can store continuous information of inputs, as we have discussed. Indeed, cellular memory refers to the process by which organisms integrate information from continuous external conditions and retain it in their cells. Unicellular protozoa *P.caudatum*, when placed on a temperature gradient, accumulate in a region of the previous cultivation temperature; memory of this cultivation temperature is stored over approximately 40 min (Jennings, 1906; Nakaoka et al., 1982). Similar temperature memory in the nematode *C.elegans* over several hours has also been observed, which is suggested to be stored at the level of a single thermosensory neuron (Kimura et al., 2004). It was also reported that *C.elegans* can memorize NaCl concentration at the level of a single neuron (Oda et al., 2011; Saeki et al., 2001). The kinetic memory scheme may shed light on the understanding of such "continuous" cellular memory.

An important condition for kinetic memory is competition for catalyst. The relevance of ELC to cellular functions has recently been discussed. For example, our previous study suggested the importance of ELC for temperature compensation of a period of biological clocks (Hatakeyama and Kaneko, 2012). Both in that study and in the present study, we found that distributed affinity leads to slow dynamics, and non-linear dependence of reaction rate on substrate and catalyst concentrations is essential. There will be further applications of ELC to other cellular functions to be revealed in the near future.

Ultimately, it will be important to experimentally verify the kinetic memory hypothesis we have proposed and tested here. Steps toward this aim should include measurements of relaxation processes of protein modifications under various catalyst concentrations. In addition, the development

and use of mutant proteins that are able to mimic substrates with several modification states would allow for the testing of varying affinities between modification sites. Such experiments would not only validate our model, but would also facilitate future investigations seeking to uncover mechanisms for primitive forms of cellular memory.

Appendix : Models and Settings

The chained modification model

In the simulation, we adopted the parameter values below unless otherwise noted.

a_i	a(t)
b_i	100.0 for all i
N	6
K_0	$0.1 \times \gamma^{-N}$
γ	5.0
$[S]_{total}$	1.0

Table 5.1: Parameter set of the chained modification model

We adopted the deterministic rate equation given by the mass-action kinetics, and it is simulated by using the fourth-order Runge-Kutta method.

The kinase-phosphatase model

In the simulation, we adopted the parameter values below.

The extended Asakura-Honda model

The original Asakura-Honda (A-H) model was introduced to explain processes of adaptation to changes of the concentration of external signal molecules (attractant and repellant) in chemotactic behavior (Asakura and Honda, 1984). This model represents a two-state (S form and T form) receptor with multiple modification sites. The S and T form receptors are recognized by distinct enzymes, which catalyze an increase and a decrease in the number of modified sites, respectively. In the model, the enzymes are always

N	2
a_i	1.0 for all i
b_i	10.0 for all i
γ	10.0
K_0^K	$10^{-3}(=\gamma^{-3})$
K_0^P	$10^{-4}(=\gamma^{-4})$
$[S]_{total}$	1.0

Table 5.2: Parameter set of the kinase-phosphatase model

maintained at sufficient levels so as to not be rate-limiting. $[S_i]$ and $[T_i]$ represent the concentration of the S and T forms of receptor with i modified sites, respectively. When an external signal, such as a change in ligand concentration is applied, $L_i = [S_i]/[T_i]$, the equilibrium value of $[S_i]$ to $[T_i]$ is changed instantaneously. The equilibrium value of $[S_i]/[T_i]$ in the absence of an external signal is denoted as L_i^0, and as L_i, when in the presence of signal. L_i increases upon the administration of an attractant and decreases upon the administration of a repellant. As the number of modified sites i is increased, the receptors are assumed to take on the T form more often, so that L_i^0 decreases with the number of modification sites i.

When the ligand concentration is changed, the total ratio $S/T = \Sigma[S_i]/\Sigma[T_i]$ changes initially. As the ratio increases (decreases), the number of modified sites increases (decreases). Subsequently, the highly modified receptors again flip to the T (S) form; thus, in both cases, the S/T ratio ultimately returns to the original proportion, so that the A-H model exibits perfect adaptation. By denoting the rate $S_{i-1} \to S_i$ as a_i and $T_i \to T_{i-1}$ as b_i, the fixed point concentrations $[T_i]^*$ and $[S_i]^*$ satisfy $-a_i[S_{i-1}]^* + b_i[T_i]^* = 0$ and $\mu_i \equiv [T_i]^*/[S_{i-1}]^* = a_i/b_i$ for all i. Under perfect adaptation $\mu_i = \mu(\text{const.})$ and $L_0^0 \gg 1$ and $L_N^0 \ll 1$: In this condition, $\mu = [T_1]^*/[S_0]^* = [T_2]^*/[T_1]^* = ... = [T_N]^*/[S_{N-1}]^* = (T^* - [T_0]^*)/(S^* - [S_N]^*)$ and $[T_0]^* \sim 0$, $[S_N]^* \sim 0$, therefore $T^*/S^* \sim \mu$. At this point, perfect adaptation is achieved.

We adopt the A-H model for our study because it is a classic model for adaptation for which several modification sites can be considered. Indeed, a variety of extensions to this model have been introduced to cover a wide range of adaptation phenomena (Barkai and Leibler, 1997; Rao et al., 2004). Here, for the purpose of modeling a slower relaxation than the original A-H model, we extend the A-H model to also explicitly include the concentration

of a cofactor as a conservation quantity. Our extended A-H model has a cofactor that facilitates all reactions, acting as a catalyst, and allowing for the addition or removal of a functional (e.g., phosphate or methyl) group.

In the simulation, we adopted the parameter values below, in the case of $N = 6$. Following the original implementation of the A-H model, we initially set the system at a attractant condition (high L_i), in which the substrates were highly modified. We then exposed the system to a repellant condition (low L_i). Under these conditions, $T(= \Sigma[T_i])$, the fraction of methylated proteins increases transiently and relaxes to the original value.

a_i	1.0 for all i
b_i	10.0 for all i
L_0^0	$10^{5.5}$
L_1^0	$10^{1.5}$
L_2^0	$10^{1.0}$
L_3^0	$10^{0.5}$
L_4^0	$10^{0.0}$
L_5^0	$10^{-0.5}$
L_6^0	$10^{-4.5}$
$[P]_{total}$	1.0

Table 5.3: Parameter set of the extended Asakura-Honda model

It is important to note that in our extended model, the steady state value of T is different from that in the original A-H model, where the stable fixed point value of T is $T^* = \mu/(1+\mu) = a/(a+b)$. In the extended A-H model, however, μ_i is changed to $\mu_i' = \frac{a[C]_{free}/([C]_{free}+K_{i-1}^S)}{b[C]_{free}/([C]_{free}+K_i^T)}$. Perfect adaptation requires that μ_i' is independent of i. This is possible in the limit of $[C]_{total} \to 0$ except for in the case of $[C]_{total} \to \infty$ (original A-H model). In the case of $[C]_{total} \to 0$, $\mu_i' \sim \frac{a/K_{i-1}^S}{b/K_i^T}$. If the dissociation constants K_i^S and K_i^T increase with an exponent γi, μ_i' is independent of i as $\mu' = a\gamma/b$, and the extended A-H model shows perfect adaptation, with the change of the fixed-point value to $T^* = \mu_i/(1+\mu_i) = a\gamma/(a\gamma+b) = 1/3$. Generally, the steady-state concentration depends on the rate of free energies of the catalyst-substrate complexes, γ, except for in the case of $\gamma = 1$, where the steady state value is constant, independent of the concentration of the catalyst.

Chapter 6

Control of the Kinetic Memory

Chapter Outline

Biomolecules with multiple modification sites are often used for non-genetic memories in a cell. For example, modifications in Ca^{2+}/calmodulin kinase II (CaMKII) and cyclic AMP response element binding protein (CREB) are important for synaptic plasticity, and modifications in histone are employed for epigenetic gene regulation in a eukaryote cell. As mentioned previously, there are two candidate mechanisms for memory, a multistability and a kinetic memory. In the former case, memory is represented as a stable attractors, and in the latter case, memory is represented as a slow relaxation process achieved by the enzyme-limited competition (ELC). When only demodification reactions are in the condition of ELC, the kinetic memory is controlled by two variables, such as the speed of modification reactions and the concentration of a catalyst for the demodification reactions. If the speed of the modification reactions increases and the concentration of the catalyst is lower than that of a substrate, the substrate will be modified and such highly-modified state will be kept after decrease in the speed of the modification, for a long time. On the other hand, if the speed of the modification is low and the concentration of the catalyst transiently increases beyond that of a substrate and subsequently decreases, the substrate will be demodified and the low-modified state will be kept over a long time. Thus, we can control the kinetic memory by changing the above two variables. Here, we chose a Calcium signaling network for synaptic plasticity as an example of the network for controlling the kinetic memory. Although such network is originally

proposed for the bistable memory, the balance between the speed of modification and demodification reactions have to be finely controlled to achieve both the long-term potentiation (LTP) and depression (LTD). In contrast, by fitting this Calcium network with the kinetic memory, both LTP and LTD are flexibly achieved. Such kinetic memory shows no hysteresis against changes in the concentration of Ca^{2+}, in contrast to the bistable memory. Thus, the kinetic memory will show higher plasticity than the bistable memory. Such plasticity will be an advantage for signal propagation and successive learning in the neural network.

6.1 Introduction

In the last chapter, we demonstrated that a substrate with multiple modification sites can store a memory without multiple attractors. In such case, the memory is stored in a relaxation process rather than a stable state. We named such memory as the "kinetic memory." From the point of view of the multiple-attractor memory, memory erasure is explained as a transition from a basin of an attractor to that of another attractor. In contrast, from the point of view of the kinetic memory, erasure is explained as an increase in the speed of relaxation induced by the increase in the amount of an enzyme. The maintenance and erasure of memory work at a molecular level.

However, it still remains unclear that such molecular mechanism for the kinetic memory can work at a cellular level. Moreover, there is a question if the kinetic memory functions better than a multiple-attractor memory at a cellular level. To answer such questions, we analyzed behaviors of the kinetic memory in a cellular level network. Here, we chose a molecular network for the synaptic plasticity as a target system.

There is a pioneering theoretical work by Lisman about the memory by the synaptic plasticity in the hippocampus (Lisman, 1989). He introduced a model to explain both Hebb and anti-Hebb learning simultaneously. Such Hebb and anti-Hebb learning are though to depend on long-term potentiation (LTP) and long-term depression (LTD) at the synaptic level, respectively (Bear and Malenka, 1994). His model consists of CaMKII as a memory storage element and input that regulates its phosphorylation level, either upward and downward depending on the input strength, i.e., either phosphorylation or dephosphorylation of CaMKII occurs depending on the input strength. Then, the synaptic strength depends on a phosphorylation level of CaMKII

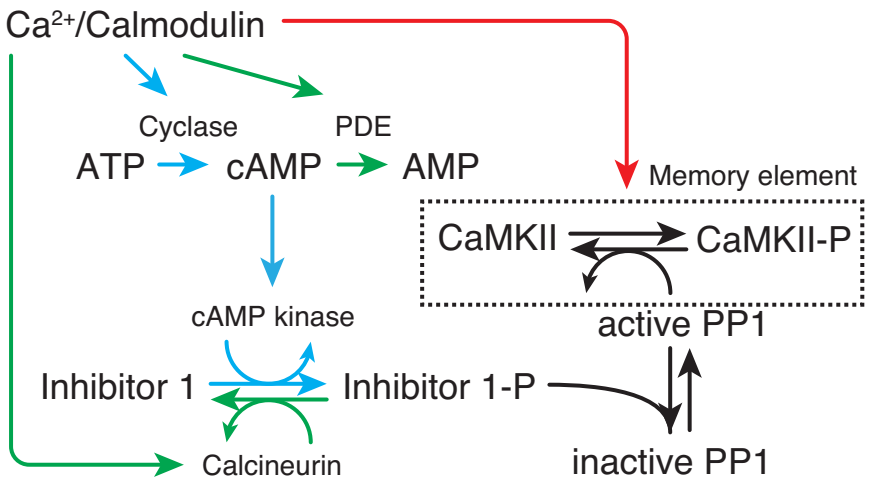

Figure 6.1: Schematic representation of CaMKII regulation network via calcium signaling and protein phosphatase 1 (modified from (Lisman, 1989)). PDE : phosphodiesterase, PP1 : protein phosphatase 1, CaMKII : Ca^{2+}/calmodulin kinese II, Inhibitor : protein phosphatase 1 inhibitor, x-P : phosphorylated x. See the main text about the meaning of colors of arrows.

through an activation of AMPA receptor.

To achieve such input dependence, first, he simplified an input pathway witch depends on the states of both presynaptic and postsynaptic cells into a single variable, the concentration of a Ca^{2+} ($[Ca]$). It is known that LTP is induced by high frequency stimulus and a subsequent rise in the concentration of intracellular Ca^{2+} in the CA1 region of hippocampal (Bear and Malenka, 1994). LDP is also thought to be caused by elevation in the concentration of Ca^{2+} after low frequency stimulus in CA1 (Mulkey and Malenka, 1992). Thus, it is reasonable that both LTP and LDP are controlled by a single input, the concentration of Ca^{2+}.

Under such simplification, there is a problem how to achieve opposite functions, LTP and LTD, by a single input variable, the concentration of Ca^{2+}. To answer this problem, he postulated existence of bidirectional pathways from the Ca^{2+} concentration to phosphorylation or dephosphorylation of CaMKII (see Fig.6.1).

Ca^{2+}-dependence of phosphorylation of CaMKII can be simply explained as a result of direct activation of CaMKII auto-phosphorylation through the binding of Ca^{2+}/calmodulin complex. On the other hand, Ca^{2+}-dependence of dephosphorylation is more complicated than that of phosphorylation. Dephosphorylation of CaMKII is directly controlled by protein phosphatase 1 (PP1), and PP1 is inhibited by phosphorylated PP1-regulatory protein inhibitor-1 (I-1) (Malenka and Bear, 2004). However, the activity of PP1 is not directly controlled by Ca^{2+} (Lisman et al., 2002, 2012). Then, a control of the activity of PP1 is explained as bidirectional controls of phosphorylation level of I-1by the Ca^{2+} concentration. I-1 is phosphorylated by cAMP-dependent kinase (Huang and Glinsmann, 1975) and dephosphorylated by calcineurin (Mulkey et al., 1994). Although the activity of calcineurin is directly controlled by Ca^{2+}/calmodulin, the activity of cAMP-dependent kinase is controlled via changes in the concentration of cAMP. Here, cAMP is made from ATP by adenylate cyclase and is changed into AMP by phosphodiesterase. Some group of adenylate cyclase families is activated by Ca^{2+} and Ca^{2+}/calmodulin complex (Cooper et al., 1995), and phosphodiesterase is also activated by Ca^{2+}/calmodulin (Goraya and Cooper, 2005). Consequently, the concentration of Ca^{2+} can control the activity of PP1, and can both progress and regress the phosphorylation level of CaMKII (see Appendix for the full version of the model in (Lisman, 1989).)

With the calcium-signaling network described above, Lisman discussed a mechanism of achieving both Hebb and anti-Hebb learning. He postulated

that the dynamics of CaMKII shows a bistable switch and CaMKII has "on" and "off" states as highly and lowly phosphorylated states, respectively. Although he did not analyze the dynamics of CaMKII, he calculated only a net phosphorylation rate for both on and off state CaMKII (see Appendix). Thus, he demonstrated that a net phosphorylation rate of on state molecule can become negative at the low concentration of Ca^{2+} and that of off state molecule can become positive at the high concentration of Ca^{2+}. Then, he advocated that both of Hebb (i.e., transition from off to on state CaMKII) and anti-Hebb (i.e., transition from on to off state CaMKII) can be caused by a calcium signaling.

Such framework of calcium signaling in (Lisman, 1989) does not depend on the nature of a memory storage element. Here, we introduce a kinetic memory element (see Chapter 5) to above calcium signaling network instead of bistable CaMKII model.

6.2 Models

6.2.1 Kinetic memory with dynamical calcium signaling

The original calcium signaling network is too much complicated with several components and parameters (see Appendix). Furthermore, Lisman studied only the static feature of the calcium signaling without dynamical-systems analysis. LTP and LDP, however, is a dynamical process. Thus, we simplify such complicated calcium signaling network, by extracting core regulations, and reconstruct the simplified network as a dynamical system. First, phosphorylation of CaMKII by Ca^{2+}/calmodulin is essential (red arrow in Fig.6.1), because there is no another pathway which upreglates CaMKII phosphorylation. Secondly, regulation of the amount of active PP1 is also important to regulate the phosphorylation level of CaMKII. There are two types of Ca^{2+}-dependent regulation of the concentration of active PP1, positive (blue arrow in Fig.6.1) and negative regulations (green arrow in Fig.6.1). Then, there are three essential regulatory pathways from Ca^{2+} concentration to CaMKII phosphorylation, i.e., direct phosphorylation, upregulation of active PP1, and downregulation of active PP1.

Hence, we simplified the calcium signaling network by extracting the above three essential paths (see Fig.6.2). We used a modified chained mod-

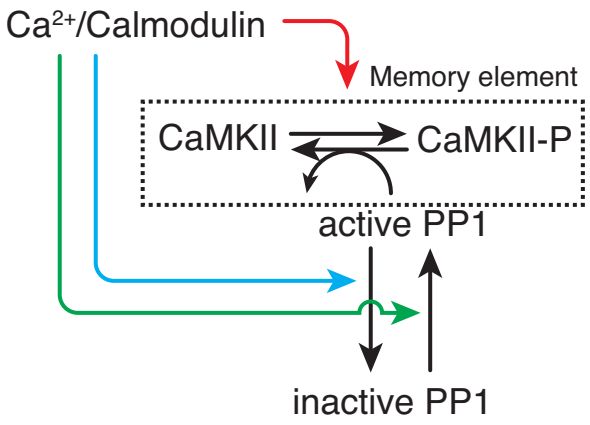

Figure 6.2: Schematic representation of simplified CaMKII regulation network. See main text about details.

ification model (see Chapter 5) as a memory storage element. Unlike the original chained modification model, in the modified model, a phosphorylation speed of the substrate depends on the concentration of Ca^{2+}. Thus, the modified chained modification model are described below:

$$
\begin{aligned}
[\dot{S}_0] &= -a\frac{[Ca]^l}{[Ca]^l + K_k^l}[S_0] + b\frac{[P_a]_{free}[S_1]}{K_0 + [P_a]_{free}} \\
[\dot{S}_i] &= -a\frac{[Ca]^l}{[Ca]^l + K_k^l}[S_i] + b\frac{[P_a]_{free}[S_{i+1}]}{K_{i+1} + [P_a]_{free}} \\
&\quad + a\frac{[Ca]^l}{[Ca]^l + K_k^l}[S_{i-1}] - b\frac{[P_a]_{free}[S_i]}{K_i + [P_a]_{free}} \\
[\dot{S}_N] &= a\frac{[Ca]^l}{[Ca]^l + K_k^l}[S_{N-1}] - b\frac{[P_a]_{free}[S_N]}{K_N + [P_a]_{free}} \qquad (6.1)
\end{aligned}
$$

$$
[P_a]_{total} = \sum_{i=0}^{N} \frac{[P_a]_{free}[S_i]}{K_i + [P_a]_{free}} + [P_a]_{free} \qquad (6.2)
$$

where, S_i is the substrate with i-th phosphorylated sites and P_a is the active phosphatase. $[Ca]$ is the concentration of Ca^{2+}, which is manipulated externally as an input. $[P_a]_{total}$ and $[P_a]_{free}$ are the total concentration of

the active phosphatase and the concentration of the free active phosphatase which is not binding to any substrates, respectively. Here, the total concentration of the phosphatase ($[P_t]$) is assumed to be constant. Then, the total concentration of the active phosphatase follows an equation described below:

$$[\dot{P}_a]_{total} = (p_p \frac{[Ca]^n}{[Ca]^n + K_{p1}^n} \frac{K_{p2}^m}{[Ca]^m + K_{p2}^m} + b_p)([P_t] - [P_a]_{total}) - d_p[P_a]_{total} \quad (6.3)$$

Here, K_k, K_{p1}, and K_{p2} are threshold values of the Ca^{2+} concentration for phosphorylation of the substrate, activation of the phosphatase, and inhibition of such activation, respectively. In the hippocampus, it is known that the high and low concentrations of Ca^{2+} cause LTP and LTD, respectively (Bear and Malenka, 1994). Then, to achieve LTP at the high Ca^{2+} concentration and LTD at the low Ca^{2+} concentration, a magnitude relationship among these threshold values should satisfy $K_{p1} < K_{p2}$ and $K_{p1} < K_k$, and we chose $K_{p2} < K_k$ here.

6.2.2 Bistable memory with dynamical calcium signaling

To compare with the kinetic memory model, we also introduced a synapse model of the simplified calcium signaling network with a bistable memory element. We used a simple bistable memory element with two phosphorylation sites modified from (Ortega et al., 2006). Note that Lisman's model does not include temporal evolution, so that we have to introduce a dynamical system model based on bistable memory here. Equations of the bistable memory model are described below:

$$\begin{aligned}
[\dot{S}_0] &= v2 - v1 \\
[\dot{S}_1] &= v1 - v2 - v3 + v4 \\
[\dot{S}_2] &= v3 - v4 \\
v1 &= k_1(\frac{[Ca]^l}{[Ca]^l + K_k^l} + b_{v1}) \frac{[S_0]/K_s}{1.0 + [S_0]/K_s + [S_1]/K_s} \\
v2 &= k_2[P_a]_{total} \frac{[S_1]/K_s}{1.0 + [S_1]/K_s + [S_2]/K_s}
\end{aligned} \quad (6.4)$$

$$v3 = k_3(\frac{[Ca]^l}{[Ca]^l + K_k^l} + b_{v3})\frac{[S_1]/K_s}{1.0 + [S_0]/K_s + [S_1]/K_s}$$

$$v4 = k_4[P_a]_{total}\frac{[S_1]/K_s}{1.0 + [S_1]/K_s + [S_2]/K_s}$$

, where b_{v1} and b_{v2} are the speeds of phosphorylation without calcium. In our simulation, we set $b_{v1} = 0$ and $b_{v3} = 0.01$, i.e., a non phosphorylated substrate is not phosphorylated and a phosphorylated is phosphorylated without calcium. Such auto-phosphorylation in the phosphorylated substrate corresponds to auto-phosphorylation in CaMKII (Lisman et al., 2002, 2012), and is helpful to maintain the highly phosphorylated state in the low concentration of Ca^{2+}. Here, we used the equation [6.3] for the dynamics of the concentration of the active phosphatase. We set the parameters for the calcium signaling as same as the kinetic memory model except b_p, which represents a basal level of the concentration of the active phosphatase. In contrast to we set $b_p = 0.5$ in the kinetic memory model, we set $b_p = 0$. Such the low concentration of the active phosphatase at the basal level is also need to maintain the phosphorylated state in the low concentration of Ca^{2+}.

6.3 Results

6.3.1 LTP and LTD are achieved in the kinetic memory with dynamical calcium signaling

First, we analyzed the time evolution of the kinetic memory model. As shown in Fig.6.3, we applied a ragged square wave of $[Ca]$ as an input (red line). When the amplitude of $[Ca]$ is sufficiently high level, the phosphorylation level of the substrate is elevated almost to its maximum, and such phosphorylation level is kept after a decrease in Ca^{2+} concentration (green line). The high phosphorylation level is not disturbed by a small increase in $[Ca]$, as the condition for kinetic memory $[P_a]_{total} < 1$ remains to be satisfied. Elevation in the phosphorylation level leads to the increase in the influx of sodium ion, and thus the elevation of phosphorylation provides a basis of LTP.

Although a small increase in $[Ca]$ cannot decrease the phosphorylation level, a larger input can decrease the elevated phosphorylation level. Such reduced phosphorylation level is also kept under decrease or small increase in $[Ca]$. Such continuous depression in the phosphorylation level of the sub-

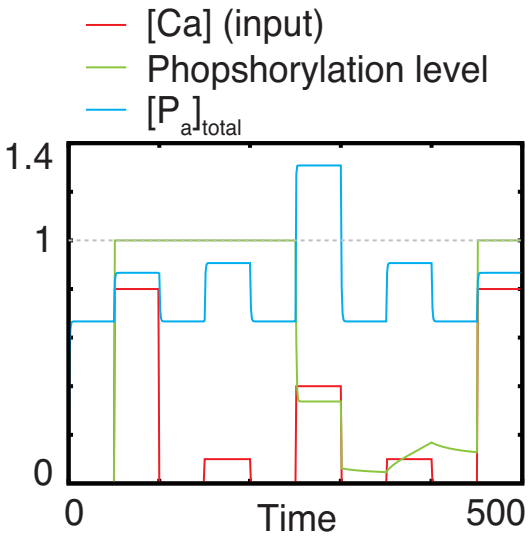

Figure 6.3: Time course of $[Ca]$ as an input (red line), a phosphorylation level of the substrate (green line), and $[P_a]_{total}$ (blue line) in the kinetic memory model. The phosphorylation level of the substrate is calculated as $\Sigma i \times [S_i]/M$, where M is the number of phosphorylation sites on the substrate. The maximum phosphorylation level is about ~ 1, while kinetic memory works when $[P_a]_{total} < 1$.

strate provides a basis of TLD. This depression is caused by the increase in $[P_a]_{total}$ (blue line) to destroy the kinetic memory. As discussed in the previous chapter, the speed of dephosphorylation reactions depends crucially on the magnitude relationship between the abandonce of the substrate and the phosphatase. When the amount of the phosphatase is lower than that of the substrate, dephosphorylation reactions are drastically slowed down by the enzyme-limited competition. In contrast, when the amount of the phosphatase becomes larger than that of the substrate, dephosphorylation reactions are accelerated. Thus, when the appropriate stimuli is administrated and $[P_a]_{total}$ turns to be larger than that of the total concentration of the substrate, then the speed of phosphorylation goes faster than that of phosphorylation and the phosphorylation level is decreased.

6.3.2 Input dependence of the phosphorylation level

Next, we plotted the altered phosphorylation level of the substrate right after continuous stimuli ($t = 100$) and after subsequent deactivation (Fig.6.4A). The stimuli are given as an increase in $[Ca]$ for the time span between 0 and 100. Then the stimuli are cut down, so that $[Ca]$ is set to 0 for $t = 100$ to 200. We computed the phosphorylation level at $t = 100$ and $t = 200$ Note that, such phosphorylation level is not same as the the steady state value.

As shown in Fig.6.4A, there are three regimes. Differences among such regimes are due to the concentration of the active phosphatase (see Fig.6.4B) and the speed of phosphorylation.

In the regime, with the concentration of Ca^{2+} from $[Ca] = 0$ to $[Ca] \simeq 0.11$, the concentration of the active phosphatase does not surpass that of the substrate (see Fig.6.4B), and the speed of dephosphorylation is very slow. Moreover, the speed of phosphorylation is also slow because the concentration of Ca^{2+} is lower than the threshold value of phosphorylation (K_k). Thus, at the steady-state phosphorylation level, where the speed of phosphorylation and dephosphorylation is balanced, relaxation dynamics to such steady-state is relatively slow (see also Fig.6.5). Under this parameter values, while the phosphorylation levels at $t = 100$ and 200 increase with $[Ca]$ slightly due to slow phosphorylation process, the steady-state value is 0.0 at $[Ca] = 0$ and is near 1.0 at other region.

In the regime II with $0.12 < [Ca] < 0.65$, the concentration of the active phosphatase surpasses that of the substrate (see Fig.6.4B), and the speed of dephosphorylation is fast. In contrast, the speed of phosphorylation is

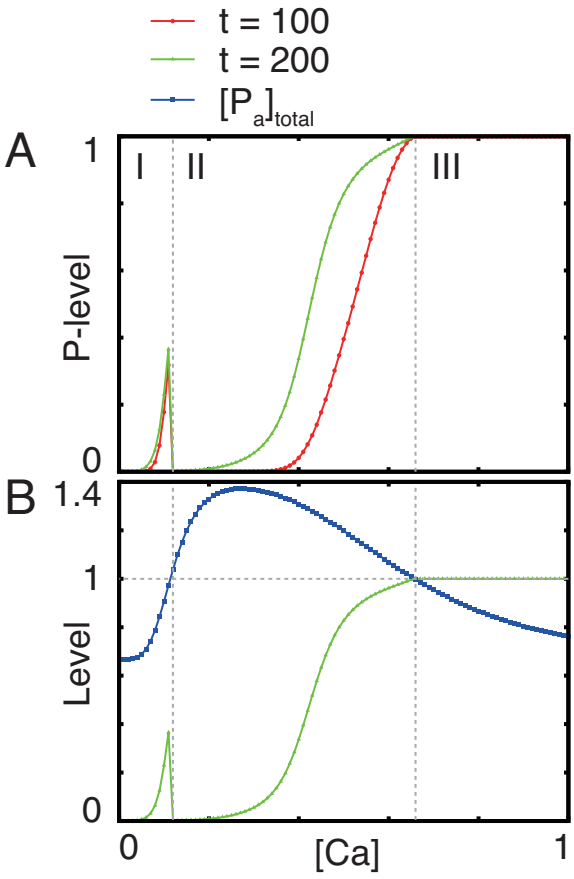

Figure 6.4: $[Ca]$ dependence of a phosphorylation level of the substrate (A) and the concentration of the active phosphatase (B). (A) Phosphorylation level of the substrate against a transient stimuli (red line) and a continuos stimuli (green line) in the kinetic memory model. An initial condition is set to $[S_0] = 1.0$ and $[S_i] = 0.0$ for $i \neq 0$. (B) The total concentration of the active phosphatase against a continuous stimuli (blue line). See main text about the regime I, II, and III.

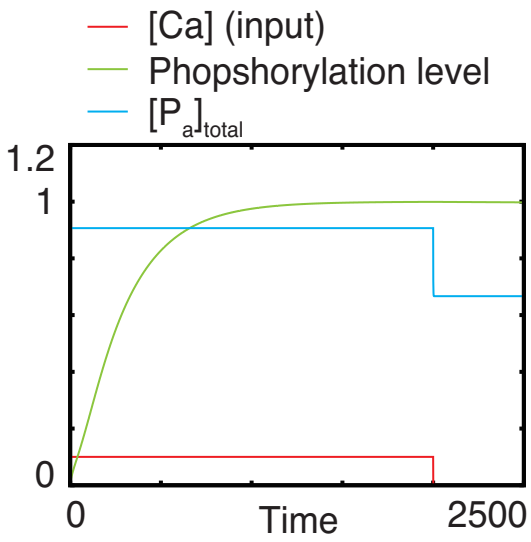

Figure 6.5: An example of the dynamics in the regime I ($[Ca] = 0.1$). Time course of $[Ca]$ as an input (red line), a phosphorylation level of the substrate (green line), and $[P_a]_{total}$ (blue line) are plotted.

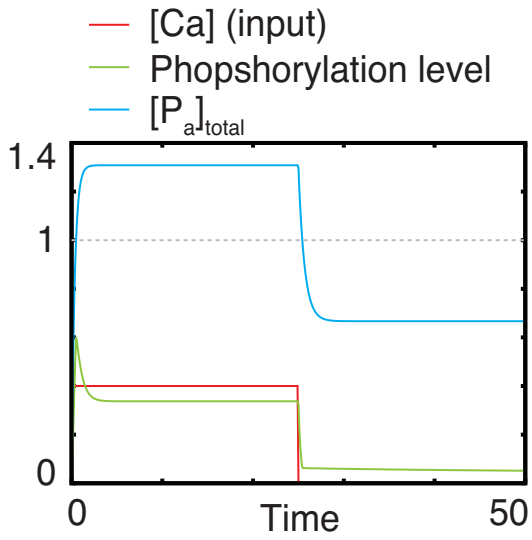

Figure 6.6: An example of the dynamics in the regime II ($[Ca] = 0.4$). Time course of $[Ca]$ as an input (red line), a phosphorylation level of the substrate (green line), and $[P_a]_{total}$ (blue line) are plotted.

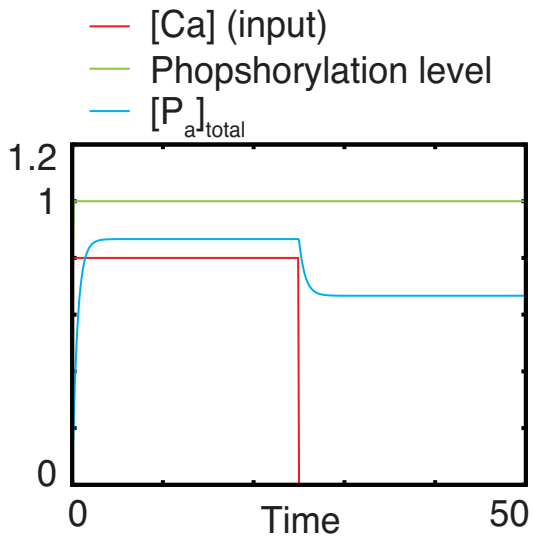

Figure 6.7: An example of the dynamics in the regime III ($[Ca] = 0.8$). Time course of $[Ca]$ as an input (red line), a phosphorylation level of the substrate (green line), and $[P_a]_{total}$ (blue line) are plotted.

slow because of a lower concentration of Ca^{2+}. Thus, the steady-state phosphorylation level tends to be low due to the fast dephosphorylation speed, and the relaxation dynamics to such steady-state is relatively fast (Fig.6.6). Note that the dynamics of the total concentration of the active phosphatase is slower than the switching of the concentration of Ca^{2+}, and thus the dephosphorylation speed is kept fast for a while after a decrease in $[Ca]$. Then, the phosphorylation level at $t = 200$ is much lower than that at $t = 100$ (see also Fig.6.4A).

In the regime III with $0.66 < [Ca]$, the concentration of the active phosphatase does not surpass that of the substrate (see Fig.6.4B), so that the kinetic memory works and the speed of dephosphorylation is very slow in the same way as the regime I. In contrast, the speed of phosphorylation is fast because of a high concentration of Ca^{2+}. Thus, the steady-state phosphorylation level reaches almost 1.0, and a relaxation dynamics to such steady-state is relatively fast (see also Fig.6.7).

LTP-like and LTD-like behaviors are due to the transition among such regimes. When the Ca^{2+} concentration increases above the border between

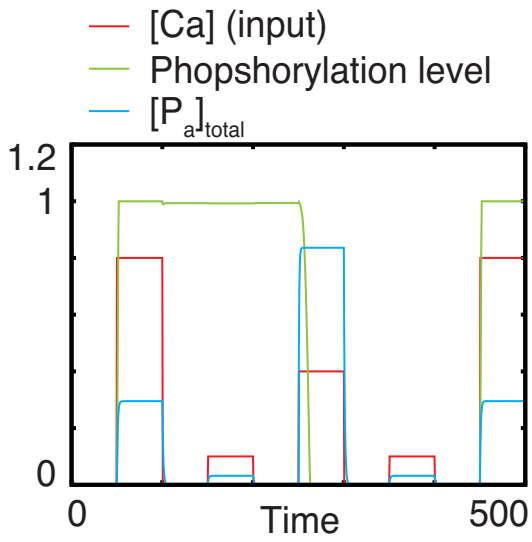

Figure 6.8: Time course of $[Ca]$ as an input (red line), a phosphorylation level of the substrate (green line), and $[P_a]_{total}$ (blue line) in the bistable memory model.

the regime II and III, the phosphorylation level is elevated. Then the Ca^{2+} concentration decreases below the border between the regime I and II, the phosphorylation level is kept approximately constant because of the slow dynamics. Such transition from the regime III to regime I is expected to be a basis of LTP. In contrast, when the Ca^{2+} concentration goes across the border between the regime I and II, the phosphorylation level is decreased. Then the Ca^{2+} concentration decreases below a border between the regime I and II, the phosphorylation level is also kept approximately constant. Such transition from the regime II to regime I will be a basis of LTD.

6.3.3 Comparison between the kinetic memory and the bistable memory

Besides the kinetic memory model, we also studied the bistable model with the dynamics of the simplified calcium signaling. We applied a ragged square wave of $[Ca]$ to the bistable model as same input as the kinetic memory model. Then, almost the same time course of the phosphorylation level of

the substrate as the kinetic memory model is obtained (green line in Fig.6.8). When the concentration of the Ca^{2+} increases sufficiently, the phosphorylation level approaches the maximum level, and such phosphorylation level is kept approximately constant after the Ca^{2+} concentration falls to zero. This is a basis of LTP in the bistable model. Although such phosphorylation level remains high under a small increase in $[Ca]$, when the concentration of Ca^{2+} increases appropriately, the phosphorylation level approaches zero. This can be a basis of LTD.

In the kinetic memory model, LTP and LTD are achieved as a fast change in the phosphorylation level and subsequent slowing down of the timescale. Thus, the relationship between the concentration of the phosphatase and the substrate is important to achieve both LTP and TLD. In contrast, in the bistable memory model, LTP and LTD are achieved as a transition from an attractor to another attractor. LTP is understood as a transition from the low phosphorylated state to the high phosphorylated, and LTD is understood as an inverse transition. In this case, the relationship between the speed of phosphorylation and the dephosphorylation, which is controlled via the concentration of the active phosphatase, is important rather than the relationship between the concentration of the phosphatase and the substrate. In the bistable model, then, both the speed of phosphorylation and the speed of the activation of the phosphatase should be fine-tuned.

The most prominent difference between the two models is existence of the hysteresis. In the bistable memory model, two attractors with low and high phosphorylation levels coexist, reached from different initial conditions, in the middle range of the Ca^{2+} concentration from $[Ca] \simeq 0.42$ to $[Ca] \simeq 0.61$ (see Fig.6.9). Such hysteresis does not exist in the kinetic memory model (Fig.6.10).

Note that, in the low concentration of Ca^{2+}, there is a difference in the phosphorylation level in both the kinetic-memory and bistable-memory models. Although the two cases look similar at a first glance, the underlying mechanism is different. In the bistable memory model, there are also bistable blanches. In contrast, in the kinetic memory model, such difference is due to slowing down of the reaction speeds of both phosphorylation and dephosphorylation.

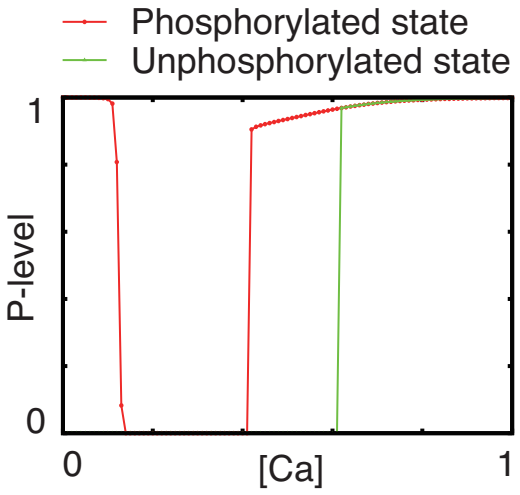

Figure 6.9: Phosphorylation level against a transient stimuli in the bistable memory model. We used two different initial conditions: $[S_0] = 1.0$ and $[S_i] = 0.0$ for $i \neq 0$ (unphosphorylated condition, green line), and $[S_M] = 1.0$ and $[S_i] = 0.0$ for $i \neq M$ (phosphorylated state, red line).

6.4 Discussion

We demonstrated that the bistable memory element can be replaced with the kinetic memory element in the calcium signaling network for the synaptic plasticity. In the bistable memory model, the balance between modification and demodification reactions should be altered for an erasure of the memory. In the kinetic memory model, the amount of the catalyst should alter for an erasure and a maintenance of the memory. Although the mechanism for the erasure and maintenance of the memory is different, the same parameters for the Ca^{2+} dynamics are adopted. Therefore, we can replace the bistable memory with the kinetic memory, if there are controlling pathways for the speed of non-catalytic reactions and the amount of the catalyst.

In a fast timescale, the kinetic memory element shows almost the same time evolution of the modification level of the substrate as the bistable model (see Fig.6.3 and 6.8). Thus, it is too hard to distinguish whether the kinetic memory from the bistable memory by a short-term observation in experiments. To distinguish the kinetic memory from the bistable memory, there are two procedures.

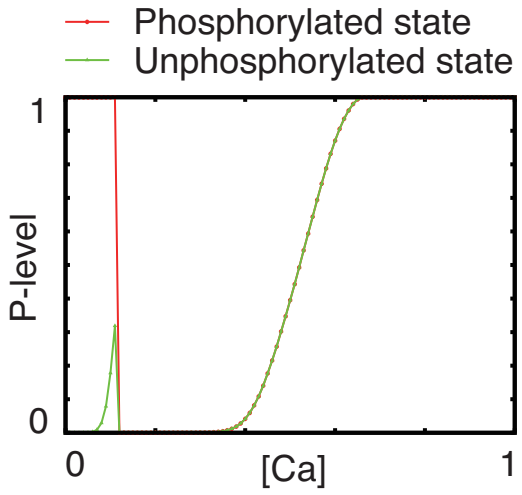

Figure 6.10: Phosphorylation level against a transient stimuli in the kinetic memory model. We used two different initial conditions: $[S_0] = 1.0$ and $[S_i] = 0.0$ for $i \neq 0$ (unphosphorylated condition, green line), and $[S_M] = 1.0$ and $[S_i] = 0.0$ for $i \neq M$ (phosphorylated state, red line).

The first one is a long-term observation. In the case of the kinetic memory, the memory is stored as a relaxation process rather than a static attracter. Although a state remain constant in a long timescale in the case of the bistable memory, in the case of the kinetic memory, the state changes in a long timescale. Then, one can distinguish the kinetic memory from the bistable memory.

The long-term observation, however, is not always possible in biological experiments. Then the second procedure is relevant, i.e., existence of the hysteresis. As shown in Fig.6.9 and 6.10, there is the hysteresis against the input change in the bistable memory, but not in the kinetic memory. Such difference is due to different characteristics as the dynamical system. Thus, analysis of the hysteresis is most relevant to distinguish the kinetic memory from the bistable memory in experiments.

Possible advantage of kinetic memory over bistable memory is the lack of hysteresis. If there is a hysteresis, synaptic connection between two neurons will be fixed for a long time when a synaptic strength is enhanced. Such fixation of the synaptic strength will decrease the plasticity in the synapse,

in which is necessary for a neural system. If a neural network consists of synapses with hysteresis, signal propagation in the network and successive learning will be difficult to be achieved because of insufficient plasticity in the single synapse. Furthermore, the homeostatic plasticity, which neurons alter their synaptic properties to maintain a target level of their activity (Turrigiano, 1999), will also be disrupted by the hysteresis in the bistable memory. In contrast, the kinetic memory may have an advantage, because higher plasticity is easily achieved.

Appendix : Full Version of Lisman's Model

In the original paper by Lisman, the dynamics of the calcium signaling network was not calculated, but only net phosphorylation rates for both "on" and "off" state of an enzyme (CaMKII) was calculated. Such net phosphorylation rates in the calcium signaling network as shown in Fig.6.1 ware calculated as follows :
First, the activity of adenylate cyclase is enhanced by Ca^{2+}/CaM (threshold value was set as $[Ca] = 0.4$) and decreased by the higher concentration of Ca^{2+} (threshold value was set as $[Ca] = 0.8$). Thus, rate of adenylate cyclase, C, reaction was described below:

$$C = \frac{0.8^4}{[Ca]^4 + 0.8^4} \frac{[Ca]^4}{[Ca]^4 + 0.4^4} + C_0 \tag{6.5}$$

where, C_0 is the basal cyclase activity. Phosphodiesterase is also activated by Ca^{2+}/CaM, and its reaction rate, D, was given by

$$D = \frac{[Ca]^4}{[Ca]^4 + 1.0^4} + D_0 \tag{6.6}$$

where, D_0 is basal reaction rate of phosphodiesterase.

Because cAMP is synthesized by adenylate cyclase and decomposed by phosphodiesterase, in the steady state, rates of adenylate cyclase and phosphodiesterase should be equivalent. Thus, the steady-state concentration of cAMP is given as :

$$[cAMP] = C/D \quad ([c\dot{A}MP] = C - D[cAMP] = 0) \tag{6.7}$$

The activity of cAMP-dependent kinase, A, depends on the concentration of cAMP (threshold value was set as $[cAMP] = 1.0$) and was described below :

$$A = 1.5\frac{[cAMP]^2}{[cAMP]^2 + 1.0^2} \tag{6.8}$$

On the other hand, the activity of calcineulin, B, depends on the concentration of Ca^{2+} (threshold value was set as $[Ca] = 0.1$), and was given by

$$B = \frac{[Ca]^4}{[Ca]^4 + 0.1^4} \tag{6.9}$$

In the steady state, phosphorylation and dephosphorylation rates should be equivalent. Thus,

$$\begin{aligned} [I1_p] - B[I1_p] &= A([I1]_{total} - [I1_p]) \\ (\dot{[I1_p]} = A([I1]_{total} - [I1_p]) - B[I1_p] &= 0) \end{aligned} \tag{6.10}$$

where, $[I1_p]$ is the concentration of phosphorylated inhibitor 1 and $[I1]_{total}$ is the total concentration of inhibitor 1. Then, the steady-state concentration of inhibitor 1 is described as

$$[I1_p] = [I1]_{total}\frac{A}{A + B} \tag{6.11}$$

Here, the fraction of PP1 which is bound to inhibitor 1, f, was described as

$$f = \frac{[I1_p]}{[I1_p] + 0.001} \tag{6.12}$$

Thus, net dephosphorylation rate, P, was postulated to be proportional to the concentration of free PP1 and given as

$$P = 1 - f \tag{6.13}$$

The net phosphorylation rate for on state, k_{on}, is given by,

$$k_{on} = k_{max} - P \tag{6.14}$$

where, k_{max} is rate for auto-phosphorylation reaction and do not depend on the concentration of Ca^{2+}.

On the other hand, the net phosphorylation rate for on state, k_{on}, is given by,

$$k_{off} = k_{max}\frac{[Ca]^4}{[Ca]^4 + 0.7^4} - P \tag{6.15}$$

In this model, it was postulated that elevation in the concentration of Ca^{2+} is required for phosphorylation of only off state enzyme.

Part IV

Concluding Remarks

Chapter 7

Conclusion and Open Questions

7.1 Enzyme-Limited Competition Re-Examined

In this doctoral thesis, first we introduced the enzyme-limited competition (ELC). Although ELC is a simple framework, which only consists of some substrates and a catalyst (enzyme), provides a variety of dynamics. For example, in Chapters 3 and 4, we demonstrated that a post-translational oscillation with robustness of the period is achieved by ELC. In Chapters 5 and 6, we demonstrated that the kinetic memory is achieved by ELC. Furthermore, it is known that a parallel ELC also provides some salient features, such as, characteristic metabolic switches (Thattai and Shraiman, 2003) , correlation in the amount of products (Cookson et al., 2011; Mather et al., 2013, 2010), and an altering stability in biological networks (Rondelez, 2012). How can such various characteristics be achieved by ELC?

Although ELC provides complex dynamics, recognizing individual functions of ELC separately will help our understanding.

First, ELC provides mutual inhibitions. When the amount of a catalyst is lower than that of substrates, substrates should compete for the limited catalyst to progress their reactions. If there are two substrates species, A and B, and affinities between the catalyst and each substrates are same, the reaction for B will be inhibited by the monopoly of the catalyst by A, if the amount of A is larger than that of B. If there is a difference in the affinities for the catalyst between A and B, such inhibition will be enhanced. Even if there are many substrates species, such mutual inhibitions should be occur.

Secondly, ELC can be a hub for several rate-limiting reactions. When the

amount of a catalyst is small, biochemical reactions which are catalyzed by such catalyst will be rate-limiting. Because of the small amount of the catalyst, speeds of such reactions are highly sensitive to changes in the catalysis amount. Moreover, such catalyst works as a hub for several reactions, speeds of reactions will be simultaneously changed by just a single manipulation on the amount of the catalyst. Thus, the dynamics of systems will be simultaneously altered by a small fluctuation or manipulation in the competed catalyst.

Furthermore, ELC can alter the speed of reactions depending on the intensity of the competition for the catalyst. It is important to think about the amount of a free catalyst for understanding the dynamics under ELC. When the amount of substrates is too large, competition for the catalyst will be severe. Then, the amount of the free catalyst, which is not bound to any substrates, will decrease. Because substrates can only use the free catalyst for their catalytic reaction, speeds of such reactions are decreased by a high competition. In a similar way, speeds of reactions are increased by relaxing the competition.

Finally, ELC provides ultrasensitivity. It is known that a small amount of catalysts leads to ultrasensitivity (Goldbeter and Koshland, 1981; McCarrey and Riggs, 1986). Especially, the buffering mechanism by (McCarrey and Riggs, 1986) is important for understanding a characteristic of ELC. The idea of buffering is very simple. When the amount of the catalyst is larger than that of the substrates, the amount of catalyst-substrate complexes approaches that of the substrates. In contrast, when the amount of the catalyst is smaller than that of the substrates, the amount of catalyst-substrate complexes approaches that of the catalyst. In systems with ELC, a transition form the former to the latter condition occurs, which alters dynamic features drastically. Note that the former and the latter conditions may correspond to underloaded and overloaded conditions in the queueing theory, respectively (Cookson et al., 2011).

In the present doctoral thesis, we demonstrated that ELC is a basis of various biochemical phenomena. Although actual biochemical reaction dynamics are complex, decomposition of such complex dynamics into the above individual basic functions of ELC facilitates us to understand the complex dynamics.

In Chapters 3 and 4, we demonstrated that a post-translational oscillation with robustness of the period is achieved by ELC. The post-translational oscillation is due to the inhibition by ELC. When a circular circuit of bio-

chemical reactions has a motif of sequential ELC, such reaction circuit must have a negative feedback loop(s) because of the mutual inhibition by ELC. Then, oscillation is universally achieved in such reaction circuits by ELC (Jolley et al., 2012; van Zon et al., 2007).

Moreover, such ELC can alter the speed of reactions via the amount of the free catalyst. Such control in the speed will provide robustness of the period of the oscillation. Furthermore, the altered amount of the free catalyst causes a phase shift. Thus, both of robustness of the period and plasticity of the phase are achieved by ELC.

In Chapters 5 and 6, we demonstrated that the kinetic memory is achieved by ELC. Such kinetic memory also depends on negative feedback loops by sequential ELC. In a model with sequential ELC, a product of one reaction will inhibit the synthesis of its own. Such feature is due to the competition for the catalyst between a substrate and its product, because such product is also a substrate. Then, drastically slow reactions are achieved by ELC and such slow reactions will work as a memory.

Moreover, a transition between states, that maintenance and erase memory, is due to an ultrasensitivity by ELC. In the memory state, the amount of the substrate is larger than that of the catalyst, and slow reactions are achieved by competition for the limited catalyst. When the amount of the catalyst exceeds that of the substrate, such competition disappears and reactions become fast. Then, the memory is erased in a faster timescale.

Although we mainly dealt with sequential ELC in the present doctoral thesis, dynamical features in parallel ELC can also be understood in the same way. For example, parallel ELC has switch characteristics (Thattai and Shraiman, 2003), which may be due to the mutual inhibition of catalytic reactions and partly due to the ultrasensitivity. It is also known that a model with parallel ELC, with two substrates catalyzed by the same catalyst, provides both of negative and positive correlations between their products (Cookson et al., 2011; Mather et al., 2013, 2010). This may be due to the mutual inhibition and a function of a hub of the limited catalyst, respectively.

As previously discussed in Chapter 2, ELC and the rate-limiting processes are inseparable. In the biological systems based on chemical reactions, some molecules will always become insufficient, because the total amount of molecules is limited, while there are abundant molecular species whose abundances are distributed. In addition, most reactions therein are catalytic. In such situation, ELC will occur at some part. We demonstrated

that ELC provides some salient characteristics : homeostasis, plasticity, and memory. Because rate-limiting processes are important to determine the dynamical feature of the whole biochemical networks, above characteristics will be achieved in complex biochemical networks via ELC. Therefore, I expect that ELC provides universal framework for basic characteristics in all living things based on enzymatic reactions.

One possible example in the application of ELC is the metabolism. A lot of catalytic reactions constitute a complex network in the metabolic systems, and it is known that some enzymes or co-enzymes are used in multiple reactions. The most prominent example is ATP, which is known to be a useful energy currency in the cell. There are many reactions which require ATP (or ADP) and these reactions can have potentially to satisfy the condition for enzyme-limited competition, but possible effects of such competition in the metabolic network is still unknown. Study in the post-translational oscillator (Chapters 3, 4) suggests a possibility that metabolic reactions can show homeostasis and plasticity by ELC. However, there is a difference between the post-translational oscillator and the metabolic reaction. In the former, concentrations of substrates and a catalyst are conservation quantities. In contrast, in the latter, concentrations of both will be altered by the metabolic reaction itself. Thus, we should analyze effects of ELC not in a closed circuit as in the post-translational oscillator but in an open flow as in the metabolic system.

Another possible example of application of ELC will be the signaling pathway. It is known that both prokaryotes and eukaryotes use successive phosphorylations as their signaling system. In such signaling network, molecules multiply phosphorylated by the same catalyst. For example, dual phosphorylation in MAPK by MAPKK is important to regulation of activity (Qi and Elion, 2005), where sequential ELC may work in a certain condition. Still, possible roles of ELC in the signal transduction are still unknown. To treat ELC in such system, we need to extend ELC with a continuous modification level to a discrete (on/off) level of modifications (phosphorylations). To uncover such problem, we should extend ELC in the continuous system to the discrete system. Here, application of information theory together with ELC may facilitate our understanding of the signal transduction systems.

In the future, we hope to unveil further properties in ELC theoretically, which will be relevant to cellular functions, while we also expect that such theoretical predictions will be directly confirmed in experiments.

7.2 Homeostasis, Plasticity, and Memory

Each of homeostasis, plasticity, and memory is an essential property common to living organisms, and its characterization have provoked a great deal of controversy. However, there is little knowledge about relationships among such properties (especially at the layer of "from molecules to cells"). In this doctoral thesis, we suggested that these features are related mutually, and sometime such relationship is reciprocal.

In Chapter 4, we demonstrated that circadian clocks show homeostasis of the period, and such homeostatic feature invokes plasticity of the period. When a clock shows the homeostatic period against an external change, the phase of this clock is easily changed by the same stimulus. In contrast, when the period of a clock is variable, the phase is hard to be changed by the same stimulus. There existes a reciprocity relationship between robustness and period. Such relationship is inherent to the mechanism to achieve homeostasis in the period, as shown in Chapter 4.

Homeostasis is not the synonym of the insensitivity. Insensitivity means that the variables in concern are not changed by external stimuli. In contrast, in the case of homeostasis, to keep dynamics of a part of variables, other relevant variables need to change as a buffer. Thus, if external environments is changed, homeostatic systems will change the buffer variables. Therefore, homeostatic systems potentially involve plasticity.

In the case of the circadian clock, plasticity is manifested as a phase shift. We expect that, in other homeostatic systems, plasticity to some other direction exists, even though it will take a different form. So far, however, we have little knowledge as yet on the form of such plasticity. Now, we should analyze possible relationships between homeostasis and plasticity in other systems and reveal the universality in such reciprocity between homeostasis and plasticity. For this purpose, the example of the circadian clock may provide a significant milestone.

We also found that the kinetic memory in the modification of a protein has higher plasticity than the bistable memory, which has a hysteresis against changes in external conditions. Although hysteresis in a single memory may provide robustness at a glance, such hysteresis will contradict robustness at the multicellular level.

Neural network provides an example to demonstrate relevance of kinetic memory. When a single synapse's memory is based on the bistable system,

activated through the modification of a protein, such higher activity will tend to be maintained for a long time against the changes in input because of a hysteresis. Similarly, synapse, once inactivated, will be kept inactivated state even against later input changes. If the neural network consists of such synapses, signal propagation in the network and successive learning will be difficult because of insufficient plasticity in the single synapse. Moreover, the homeostatic plasticity, in which neurons alter their synaptic properties to maintain a target level of their electrical activity (Turrigiano, 1999), will also be disrupted by the hysteresis in the bistable memory. Thus, homeostasis and plasticity at the neural network level will require not only robustness but also plasticity at the memory element level, which is difficult the bistable memory.

In contrast, the kinetic memory shows no hysteresis and shows sharp transition against a small change in the amount of a catalyst (Chapters 5, 6). Such features will provide higher plasticity than the bistable memory, and will give a basis of both homeostasis and plasticity at the neural network level. Now, difference in plasticity between the kinetic memory and the bistable memory is demonstrated. Through kinetic memory, one may formulate possible relationship between neural plasticity and homeostasis.

Furthermore, plasticity of synaptic plasticity, termed as metaplasticity was previously proposed to be important for homeostasis in the neural network (Abraham and Bear, 1996; Bienenstock et al., 1982). Here, metaplasticity is a change in the threshold for neural activity upon the past input, where change between LTP and LTD occurs, i.e., the change in synapse strength, either to increase or decrease the synaptic strength upon the input. Such flexible change of the plasticity will be difficult to be achieved by the bistable memory mechanism where hysteresis gives a strong resistance to change. It will be important to uncover the logic for metaplasticity based on the kinetic memory scheme.

There will be more relationships among homeostasis, plasticity, and memory, which are not treated in the present thesis. For example, a memory might provide homeostasis and plasticity against continuos and/or cyclic changes in external conditions, because the memory helps living things to store an experience of past stimulus. It will be important to uncover such relationships, to which, I hope, ELC will be relevant.

References

Abraham, W. C. and Bear, M. F. (1996). Metaplasticity: the plasticity of synaptic plasticity. Trends Neurosci. *19*, 126–30.

Adler, J. (1966). Chemotaxis in bacteria. Science *153*, 708–16.

Akman, O. E., Locke, J. C. W., Tang, S., Carré, I., Millar, A. J. and Rand, D. a. (2008). Isoform switching facilitates period control in the *Neurospora crassa* circadian clock. Mol. Syst. Biol. *4*, 164.

Alberts, B., Johnson, A., Lewis, J., Raff, M., Roberts, K., and Walter, P. (2008) Molecular Biology of the Cell, Fifth Edition. (Garland Science.)

Alberts, B. (2011). A grand challenge in biology. Science *333*, 1200.

Alon, U. (2007). Introduction to Systems Biology: And the Design Principles of Biological Networks. (CRC press.)

Andrianantoandro, E., Basu, S., Karig, D. K. and Weiss, R. (2006). Synthetic biology: new engineering rules for an emerging discipline. Mol. Syst. Biol. *2*, 2006.0028.

Asakura, S. and Honda, H. (1984). Two-state model for bacterial chemoreceptor proteins. The role of multiple methylation. J. Mol. Biol. *176*, 349–67.

Awazu, A. and Kaneko, K. (2009). Ubiquitous "glassy" relaxation in catalytic reaction networks. Phys. Rev. E *80*, 041931.

Bargmann, C. I. and Horvitz, H. R. (1991). Chemosensory neurons with overlapping functions direct chemotaxis to multiple chemicals in *C. elegans*. Neuron *7*, 729–42.

Barkai, N. and Leibler, S. (1997). Robustness in simple biochemical networks. Nature *387*, 913–7.

Bear, M. F. and Malenka, R. C. (1994). Synaptic plasticity: LTP and LTD. Curr. Opin. Neurobiol. *4*, 389–399.

Bell-Pedersen, D., Cassone, V. M., Earnest, D. J., Golden, S. S., Hardin, P. E., Thomas, T. L. and Zoran, M. J. (2005). Circadian rhythms from multiple oscillators: lessons from diverse organisms. Nat. Rev. Genet. *6*, 544–56.

Benzinger, T. H. (1969). Heat regulation: homeostasis of central temperature in man. Physiol. Rev. *49*, 671–759.

Bergeron, L. J. and Perreault, J.-P. (2005). Target-dependent on/off switch increases ribozyme fidelity. Nucleic Acids Res. *33*, 1240–8.

Bergsten, P. and Hellman, B. (1993). Glucose-induced amplitude regulation of pulsatile insulin secretion from individual pancreatic islets. Diabetes *42*, 670–4.

Bienenstock, E. L., Cooper, L. N. and Munro, P. W. (1982). Theory for the development of neuron selectivity: orientation specificity and binocular interaction in visual cortex. J. Neurosci. *2*, 32–48.

Bird, A. (2007). Perceptions of epigenetics. Nature *447*, 396–8.

Bito, H., Deisseroth, K. and Tsien, R. W. (1996). CREB phosphorylation and dephosphorylation: A Ca^{2+} - and stimulus duration-dependent switch for hippocampal gene expression. Cell *87*, 1203–14.

Blattner, F. R., Plunkett, G., Bloch, C. A., Perna, N. T., Burland, V., Riley, M., Collado-Vides, J., Glasner, J. D., Rode, C. K., Mayhew, G. F., Gregor, J., Davis, N. W., Kirkpatrick, H. A., Goeden, M. A., Rose, D. J., Mau, B. and Shao, Y. (1997). The complete genome sequence of *Escherichia coli* K-12. Science *277*, 1453–62.

Bliss, T. V. and Gardner-Medwin, A. R. (1973). Long-lasting potentiation of synaptic transmission in the dentate area of the unanaesthetized rabbit following stimulation of the perforant path. J. Physiol. *232*, 357–74.

Bliss, T. V. and Lomo, T. (1973). Long-lasting potentiation of synaptic transmission in the dentate area of the anaesthetized rabbit following stimulation of the perforant path. J Physiol. *232*, 331–56.

Bradshaw, J. M., Kubota, Y., Meyer, T. and Schulman, H. (2003). An ultrasensitive Ca^{2+}/calmodulin-dependent protein kinase II-protein phosphatase 1 switch facilitates specificity in postsynaptic calcium signaling. Proc. Nat. Acad. Sci. USA *100*, 10512–7.

Brettschneider, C., Rose, R. J., Hertel, S., Axmann, I. M., Heck, A. J. R. and Kollmann, M. (2010). A sequestration feedback determines dynamics and temperature entrainment of the KaiABC circadian clock. Mol. Syst. Biol. *6*, 389.

Bruce, V. G. and Pittendrigh, C. S. (1960). An effect of heavy water on the phase and period of the circadian rhythm in euglena. J. Cell. Comp. Physiol. *56*, 25–31.

Bullock, T. H. (1955). Compensation for Temperature in the Metabolism and Activiy of Poikilotherms. Biol. Rev. *30*, 311–342.

Chickarmane, V., Troein, C., Nuber, U. A., Sauro, H. M. and Peterson, C. (2006). Transcriptional dynamics of the embryonic stem cell switch. PLoS Comp. Biol. *2*, e123.

Clodong, S., Dühring, U., Kronk, L., Wilde, A., Axmann, I., Herzel, H. and Kollmann, M. (2007). Functioning and robustness of a bacterial circadian clock. Mol. Syst. Biol. *3*, 90.

Cochrane, J. C. and Strobel, S. A. (2008). Catalytic strategies of self-cleaving ribozymes. Accounts of chemical research *41*, 1027–35.

Cohen, P. (2000). The regulation of protein function by multisite phosphorylation–a 25 year update. Trends Biochem. Sci. *25*, 596–601.

Cookson, N. A., Mather, W. H., Danino, T., Mondragón-Palomino, O., Williams, R. J., Tsimring, L. S. and Hasty, J. (2011). Queueing up for enzymatic processing: correlated signaling through coupled degradation. Mol. Syst. Biol. *7*, 561.

Cooper, D. M., Mons, N. and Karpen, J. W. (1995). Adenylyl cyclases and the interaction between calcium and cAMP signalling. Nature *374*, 421–4.

Crick, F. (1984). Neurobiology: Memory and molecular turnover. Nature *312*, 101–101.

De Koninck, P. and Schulman, H. (1998). Sensitivity of CaM kinase II to the frequency of Ca^{2+} oscillations. Science *279*, 227–30.

Dodd, I. B., Micheelsen, M. A., Sneppen, K. and Thon, G. (2007). Theoretical analysis of epigenetic cell memory by nucleosome modification. Cell *129*, 813–22.

Dutt, A. K. and Mueller, S. C. (1993). Effect of stirring and temperature on the Belousov-Zhabotinskii reaction in a CSTR. J. Phys. Chem. *97*, 10059–10063.

Enright, J. (1971). Heavy Water Slows Biological Timing Processes. Zeitschrift für vergleichende Physiologie *16*, 1–16.

François, P., Despierre, N. and Siggia, E. D. (2012). Adaptive Temperature Compensation in Circadian Oscillations. PLoS Comp. Biol. *8*, e1002585.

Gallego, M. and Virshup, D. M. (2007). Post-translational modifications regulate the ticking of the circadian clock. Nat. Rev. Mol. Cell Biol. *8*, 139–48.

Gerisch, G. (1982). Chemotaxis in *Dictyostelium*. Annu. Rev. Physiol. *44*, 535–52.

Gnad, F., Ren, S., Cox, J., Olsen, J. V., Macek, B., Oroshi, M. and Mann, M. (2007). PHOSIDA (phosphorylation site database): management, structural and evolutionary investigation, and prediction of phosphosites. Genome biology *8*, R250.

Goldbeter, A. and Koshland, D. E. (1981). An amplified sensitivity arising from covalent modification in biological systems. Proc. Nat. Acad. Sci. USA *78*, 6840–4.

Goldbeter, A. (1997). Biochemical oscillations and cellular rhythms. (UK: Cambridge University Press.)

Goraya, T. A. and Cooper, D. M. F. (2005). Ca^{2+}-calmodulin-dependent phosphodiesterase (PDE1): current perspectives. Cellular signalling *17*, 789–97.

Guan, Q., Haroon, S., Bravo, D. G., Will, J. L. and Gasch, A. P. (2012). Cellular memory of acquired stress resistance in *Saccharomyces cerevisiae*. Genetics *192*, 495–505.

Hastings, J. and Sweeney, B. (1957). On the mechanism of temperature independence in a biological clock. Proc. Nat. Acad. Sci. USA *43*, 804.

Hatakeyama, T. S. and Kaneko, K. (2012). Generic temperature compensation of biological clocks by autonomous regulation of catalyst concentration. Proc. Nat. Acad. Sci. USA *109*, 8109–14.

Hibino, K., Shibata, T., Yanagida, T., and Sako, Y. (2011). Activation Kinetics of RAF Protein in the Ternary Complex of RAF, RAS-GTP, and Kinase on the Plasma Membrane of Living Cells SINGLE-MOLECULE IMAGING ANALYSIS. J. Biol. Chem. *286*, 36460–36468.

Hill, A. (1910). The possible effects of the aggregation of the molecules of hæmoglobin on its dissociation curves. J. Physiol. *40*, iv–vii.

Hong, C. I., Conrad, E. D. and Tyson, J. J. (2007). A proposal for robust temperature compensation of circadian rhythms. Proc. Nat. Acad. Sci. USA *104*, 1195–200.

Hong, C. I. and Tyson, J. J. (1997). A proposal for temperature compensation of the circadian rhythm in *Drosophila* based on dimerization of the per protein. Chronobiology international *14*, 521–9.

Huang, F. L. and Glinsmann, W. H. (1975). Inactivation of rabbit muscle phosphorylase phosphatase by cyclic AMP-dependent kinas. Proc. Nat. Acad. Sci. USA *72*, 3004–8.

Ishiura, M., Kutsuna, S., Aoki, S., Iwasaki, H., Andersson, C. R., Tanabe, A., Golden, S. S., Johnson, C. H. and Kondo, T. (1998). Expression of a gene cluster kaiABC as a circadian feedback process in cyanobacteria. Science *281*, 1519–23.

Isojima, Y., Nakajima, M., Ukai, H., Fujishima, H., Yamada, R. G., Masumoto, K.-h., Kiuchi, R., Ishida, M., Ukai-Tadenuma, M., Minami, Y., Kito, R., Nakao, K., Kishimoto, W., Yoo, S.-H., Shimomura, K., Takao, T., Takano, A., Kojima, T., Nagai, K., Sakaki, Y., Takahashi, J. S. and Ueda, H. R. (2009). CKIϵ/δ-dependent phosphorylation is a temperature-insensitive, period-determining process in the mammalian circadian clock. Proc. Nat. Acad. Sci. USA *106*, 15744–9.

Iwasaki, H., Nishiwaki, T., Kitayama, Y., Nakajima, M. and Kondo, T. (2002). KaiA-stimulated KaiC phosphorylation in circadian timing loops in cyanobacteria. Proc. Nat. Acad. Sci. USA *99*, 15788–93.

Jablonka, E., Lachmann, M. and Lamb, M. J. (1992). Evidence, mechanisms and models for the inheritance of acquired characters. J. Theor. Biol. *158*, 245–268.

Jennings, H. S. (1906). Behavior of the lower organisms. (New York: The Colombia University press.)

Johnson, C. H., Mori, T. and Xu, Y. (2008). A cyanobacterial circadian clockwork. Curr. Biol. *18*, R816–R825.

Jolley, C. C., Ode, K. L. and Ueda, H. R. (2012). A design principle for a posttranslational biochemical oscillator. Cell reports *2*, 938–50.

Kageyama, H., Kondo, T. and Iwasaki, H. (2003). Circadian formation of clock protein complexes by KaiA, KaiB, KaiC, and SasA in cyanobacteria. J. Biol. Chem. *278*, 2388–95.

Kaneko, K. (2006). Life: an introduction to complex systems biology. (Berlin: Springer.)

Kimura, K. D., Miyawaki, A., Matsumoto, K. and Mori, I. (2004). The *C. elegans* thermosensory neuron AFD responds to warming. Curr. Biol. *14*, 1291–5.

Komatsu, S. (1972). "Tsugu no wa dare ka?" (in Japanese) (Hayakawa Shobo)

Koshland, D. E. (1958). Application of a Theory of Enzyme Specificity to Protein Synthesis. Proc. Nat. Acad. Sci. USA *44*, 98–104.

Kurosawa, G. and Iwasa, Y. (2005). Temperature compensation in circadian clock models. J. Theor. Biol. *233*, 453–68.

Langton, C. G. (Ed.). (1989). Artificial life. (Redwood City, CA: Addison-Wesley Publishing Company.)

Langton, C. G. (Ed.). (1992). Artificial life II. (Redwood City, CA: Addison-Wesley Publishing Company.)

Langton, C. G. (Ed.). (1994). Artificial life III. (Redwood City, CA: Addison-Wesley Publishing Company.)

Leloup, J. C. and Goldbeter, A. (1997). Temperature compensation of circadian rhythms: control of the period in a model for circadian oscillations of the per protein in *Drosophila*. Chronobiology international *14*, 511–20.

Lisman, J. (1989). A mechanism for the Hebb and the anti-Hebb processes underlying learning and memory. Proc. Nat. Acad. Sci. USA *86*, 9574–8.

Lisman, J., Schulman, H. and Cline, H. (2002). The molecular basis of CaMKII function in synaptic and behavioural memory. Nat. Rev. Neurosci. *3*, 175–90.

Lisman, J., Yasuda, R. and Raghavachari, S. (2012). Mechanisms of CaMKII action in long-term potentiation. Nat. Rev. Neurosci. *13*, 169–82.

Lisman, J. E. (1985). A mechanism for memory storage insensitive to molecular turnover: a bistable autophosphorylating kinase. Proc. Nat. Acad. Sci. USA *82*, 3055–7.

Lisman, J. E. and Goldring, M. a. (1988). Feasibility of long-term storage of graded information by the Ca^{2+}/calmodulin-dependent protein kinase molecules of the postsynaptic density. Proc. Nat. Acad. Sci. USA *85*, 5320–4.

Lisman, J. E. and Zhabotinsky, A. M. (2001). A Model of Synaptic Memory: A CaMKII/PP1 Switch that Potentiates Transmission by Organizing an AMPA Receptor Anchoring Assembly. Neuron *31*, 191–201.

Liu, Y., Merrow, M., Loros, J. J. and Dunlap, J. C. (1998). How temperature changes reset a circadian oscillator. Science *281*, 825–9.

Lynch, M. (2012). The evolution of multimeric protein assemblages. Mol. Biol. Evol. *29*, 1353–66.

Lynch, M. (2013). Evolutionary diversification of the multimeric states of proteins. Proc. Nat. Acad. Sci. USA *110*, E2821–8.

Majercak, J., Sidote, D., Hardin, P. E. and Edery, I. (1999). How a Circadian Clock Adapts to Seasonal Decreases in Temperature and Day Length. Neuron *24*, 219–230.

Malenka, R. C. and Bear, M. F. (2004). LTP and LTD: an embarrassment of riches. Neuron *44*, 5–21.

Mather, W., Hasty, J., Tsimring, L. and Williams, R. (2013). Translational Cross Talk in Gene Networks. Biophys. J. *104*, 2564–2572.

Mather, W. H., Cookson, N. A., Hasty, J., Tsimring, L. S. and Williams, R. J. (2010). Correlation resonance generated by coupled enzymatic processing. Biophys. J. *99*, 3172–81.

McCarrey, J. R. and Riggs, A. D. (1986). Determinator-inhibitor pairs as a mechanism for threshold setting in development: a possible function for pseudogenes. Proc. Nat. Acad. Sci. USA *83*, 679–83.

McDaniel, M., Sulzman, F. M. and Hastings, J. W. (1974). Heavy water slows the Gonyaulax clock: a test of the hypothesis that D2O affects circadian oscillations by diminishing the apparent temperature. Proc. Nat. Acad. Sci. USA *71*, 4389–91.

Mehra, A., Hong, C. I., Shi, M., Loros, J. J., Dunlap, J. C. and Ruoff, P. (2006). Circadian rhythmicity by autocatalysis. PLoS Comp. Biol. *2*, e96.

Merrow, M., Brunner, M. and Roenneberg, T. (1999). Assignment of circadian function for the *Neurospora* clock gene frequency. Nature *399*, 584–6.

Michaelis, L. and Menten, M. (1913). Die Kinetik der Invertinwirkung. Biochem Z *49*, 333–369.

Monod, J., Wyman, J. and Changeux, J. P. (1965). On the Nature of Allosteric Transitions: a Plausible Model. J. Mol. Biol. *12*, 88–118.

Mulkey, R. M., Endo, S., Shenolikar, S. and Malenka, R. C. (1994). Involvement of a calcineurin/inhibitor-1 phosphatase cascade in hippocampal long-term depression. Nature *369*, 486–8.

Mulkey, R. M. and Malenka, R. C. (1992). Mechanisms underlying induction of homosynaptic long-term depression in area CA1 of the hippocampus. Neuron *9*, 967–75.

Nakajima, M., Imai, K., Ito, H., Nishiwaki, T., Murayama, Y., Iwasaki, H., Oyama, T. and Kondo, T. (2005). Reconstitution of circadian oscillation of cyanobacterial KaiC phosphorylation in vitro. Science *308*, 414–5.

Nakajima, M., Ito, H. and Kondo, T. (2010). In vitro regulation of circadian phosphorylation rhythm of cyanobacterial clock protein KaiC by KaiA and KaiB. FEBS Lett. *584*, 898–902.

Nakaoka, Y., Tookui, H., Gion, Y., Inoue, S. and Oosawa, F. (1982). Behavioral Adaptation of *Paramecium caudatum* to Environmental Temperature. Proc. Jap. Acad. Ser. B *58*, 213–217.

Nishiwaki, T., Iwasaki, H., Ishiura, M. and Kondo, T. (2000). Nucleotide binding and autophosphorylation of the clock protein KaiC as a circadian timing process of cyanobacteria. Proc. Nat. Acad. Sci. USA *97*, 495–9.

Oda, S., Tomioka, M. and Iino, Y. (2011). Neuronal plasticity regulated by the insulin-like signaling pathway underlies salt chemotaxis learning in *Caenorhabditis elegans*. J. Neurophysiol. *106*, 301–8.

Oosawa, F. (2000). The loose coupling mechanism in molecular machines of living cells. Genes Cells *5*, 9–16.

Oosawa, F. and Hayashi, S. (1986). The loose coupling mechanism in molecular machines of living cells. Advances in biophysics *22*, 151–83.

Ortega, F., Garcés, J. L., Mas, F., Kholodenko, B. N. and Cascante, M. (2006). Bistability from double phosphorylation in signal transduction. Kinetic and structural requirements. FEBS J. *273*, 3915–26.

Pennisi, E. (2012). Genomics. ENCODE project writes eulogy for junk DNA. Science *337*, 1159, 1161.

Phillips, R., Kondev, J., Theriot, J., Garcia, H., and Chasan, B. (2010). Physical biology of the cell. (American Journal of Physics.)

Phong, C., Markson, J. S., Wilhoite, C. M. and Rust, M. J. (2013). Robust and tunable circadian rhythms from differentially sensitive catalytic domains. Proc. Nat. Acad. Sci. USA *110*, 1124–9.

Pittendrigh, C. S. (1954). On Temperature Independence in the Clock System Controlling Emergence Time in *Drosophila*. Proc. Nat. Acad. Sci. USA *40*, 1018–29.

Pittendrigh, C. S., Caldarola, P. C. and Cosbey, E. S. (1973). A differential effect of heavy water on temperature-dependent and temperature-compensated aspects of circadian system of *Drosophila pseudoobscura*. Proc. Nat. Acad. Sci. USA *70*, 2037–41.

Pocket Monster (Pokémon) [Game Boy]. (1996). (Kyoto, Japan: Nintendo.)

Qi, M. and Elion, E. A. (2005). MAP kinase pathways. J Cell Sci. *118*, 3569–72.

Qin, X., Byrne, M., Xu, Y., Mori, T. and Johnson, C. H. (2010). Coupling of a core post-translational pacemaker to a slave transcription/translation feedback loop in a circadian system. PLoS Biol. *8*, e1000394.

Rao, C. V., Kirby, J. R. and Arkin, A. P. (2004). Design and diversity in bacterial chemotaxis: a comparative study in *Escherichia coli* and *Bacillus subtilis*. PLoS Biol. *2*, E49.

Rondelez, Y. (2012). Competition for Catalytic Resources Alters Biological Network Dynamics. Phys. Rev. Lett. *108*, 1–5.

Ruoff, P. (1992). Introducing temperature - compensation in any reaction kinetic oscillator model. Journal of Interdisciplinary Cycle Research *23*, 92–99.

Ruoff, P., Zakhartsev, M. and Westerhoff, H. V. (2007). Temperature compensation through systems biology. FEBS J. *274*, 940–50.

Rust, M. J., Markson, J. S., Lane, W. S., Fisher, D. S. and O'Shea, E. K. (2007). Ordered phosphorylation governs oscillation of a three-protein circadian clock. Science *318*, 809–12.

Saeki, S., Yamamoto, M. and Iino, Y. (2001). Plasticity of chemotaxis revealed by paired presentation of a chemoattractant and starvation in the nematode *Caenorhabditis elegans*. J. Expe. Biol. *204*, 1757–64.

Sancar, G., Sancar, C. and Brunner, M. (2012). Metabolic compensation of the *Neurospora* clock by a glucose-dependent feedback of the circadian repressor CSP1 on the core oscillator. Genes Dev. *26*, 2435–42.

Sanhueza, M., Fernandez-Villalobos, G., Stein, I. S., Kasumova, G., Zhang, P., Bayer, K. U., Otmakhov, N., Hell, J. W. and Lisman, J. (2011). Role of the CaMKII/NMDA receptor complex in the maintenance of synaptic strength. J. Neurosci. *31*, 9170–8.

Sasagawa, S., Ozaki, Y.-i., Fujita, K. and Kuroda, S. (2005). Prediction and validation of the distinct dynamics of transient and sustained ERK activation. Nat. Cell Biol. *7*, 365–73.

Savir, Y. and Tlusty, T. (2007). Conformational proofreading: the impact of conformational changes on the specificity of molecular recognition. PloS one *2*, e468.

Schrödinger, E. (1944). What Is Life? (Cambridge University Press)

Segel, L. A., Goldbeter, A., Devreotes, P. N. and Knox, B. E. (1986). A mechanism for exact sensory adaptation based on receptor modification. J. Theor. Biol. *120*, 151–79.

Silva, A. J., Kogan, J. H., Frankland, P. W. and Kida, S. (1998). CREB and memory. Annu. Rev. neurosci. *21*, 127–48.

Sweatt, J. D. (1999). Toward a Molecular Explanation for Long-Term Potentiation. Learning & Memory *6*, 399–416.

Szostak, J. W., Bartel, D. P. and Luisi, P. L. (2001). Synthesizing life. Nature *409*, 387–90.

Terauchi, K., Kitayama, Y., Nishiwaki, T., Miwa, K., Murayama, Y., Oyama, T. and Kondo, T. (2007). ATPase activity of KaiC determines the basic timing for circadian clock of cyanobacteria. Proc. Nat. Acad. Sci. USA *104*, 16377–81.

Thattai, M. and Shraiman, B. I. (2003). Metabolic switching in the sugar phosphotransferase system of *Escherichia coli*. Biophys. J. *85*, 744–54.

Thomson, M. and Gunawardena, J. (2009). Unlimited multistability in multisite phosphorylation systems. Nature *460*, 274–7.

Tomita, J., Nakajima, M., Kondo, T. and Iwasaki, H. (2005). No transcription-translation feedback in circadian rhythm of KaiC phosphorylation. Science *307*, 251–4.

Turrigiano, G. G. (1999). Homeostatic plasticity in neuronal networks: the more things change, the more they stay the same. Trends Neurosci. *22*, 221–7.

Vale, R. D. and Oosawa, F. (1990). Protein motors and Maxwell's demons: does mechanochemical transduction involve a thermal ratchet? Adv. Biophys. *26*, 97–134.

van Zon, J. S., Lubensky, D. K., Altena, P. R. H. and ten Wolde, P. R. (2007). An allosteric model of circadian KaiC phosphorylation. Proc. Nat. Acad. Sci. USA *104*, 7420–5.

"Life." Wikipedia: The Free Encyclopedia. (Wikimedia Foundation, Inc. 16.Nov.2013 updated, 09.Dec.2013 viewed.)

Williams, S. B., Vakonakis, I., Golden, S. S. and LiWang, A. C. (2002). Structure and function from the circadian clock protein KaiA of *Synechococcus elongatus*: a potential clock input mechanism. Proc. Nat. Acad. Sci. USA *99*, 15357–62.

Wolf, D. M., Fontaine-Bodin, L., Bischofs, I., Price, G., Keasling, J. and Arkin, A. P. (2008). Memory in microbes: quantifying history-dependent behavior in a bacterium. PloS one *3*, e1700.

Xu, Y., Mori, T. and Johnson, C. H. (2003). Cyanobacterial circadian clockwork: roles of KaiA, KaiB and the kaiBC promoter in regulating KaiC. EMBO J. *22*, 2117–26.

Yoda, M., Eguchi, K., Terada, T. P. and Sasai, M. (2007). Monomer-shuffling and allosteric transition in KaiC circadian oscillation. PloS one *2*, e408.

Yoshida, T., Murayama, Y., Ito, H., Kageyama, H. and Kondo, T. (2009). Nonparametric entrainment of the in vitro circadian phosphorylation rhythm of cyanobacterial KaiC by temperature cycle. Proc. Nat. Acad. Sci. USA *106*, 1648–53.

Zhabotinsky, A. M. (2000). Bistability in the Ca^{2+}/calmodulin-dependent protein kinase-phosphatase system. Biophys. J. *79*, 2211–21.

Zimmerman, W. F., Pittendrigh, C. S. and Pavlidis, T. (1968). Temperature compensation of the circadian oscillation in *Drosophila pseudoobscura* and its entrainment by temperature cycles. J. Insect Physiol. *14*, 669–84.

Zwicker, D., Lubensky, D. K. and ten Wolde, P. R. (2010). Robust circadian clocks from coupled protein-modification and transcription-translation cycles. Proc. Nat. Acad. Sci. USA *107*, 22540–5.

Acknowledgements

Professor Kunihiko Kaneko introduced me into complex systems biology. I wish to express my gratitude to him for creative and unique advices, stimulating discussions, and essential supports. Most of the present thesis comes from the collaborative studies with him. Through these researches, I have studied many things from him and my view of life have been sophisticated.

Dr. Shuji Ishihara, Dr. Atushi Kamimura, Dr. Nen Saito, Dr. Tomoki Kurikawa, and Dr. Nobuto Takeuchi gave me opportunities of exciting discussions and useful comments for my researches.

Professor Hideo Iwasaki introduced me into the research field of the biological science. Choice of the circadian clock as a subject of my study was mainly due to him.

Dr. Akinori Awazu motivated some of my researches and gave me useful comments.

Dr. Chikara Furusawa, Dr. Yasushi Okada, Dr. Yoriko Murayama, and Dr. Takuma Sugi gave me fruitful comments for my papers, which are basis of this thesis.

Dr. Koichi Fujimoto, Dr. Yuichi Togashi, Dr. Tetsuya Kobayashi, Dr. Yutaka Shikano, Dr. Hiroshi Ito, Dr. Masayo Inoue, and Dr. Hiroshi Kori gave me useful comments in conferences or colloquiums.

All members of Kaneko laboratory gave me a lot of supports whether business or personal. Especially, Motoko Miura gave me critical supports through office jobs. Takahiro Kohsokabe gave me chocolates and some fruits. Hironobu Noguchi rent me comic books (but I cannot read such books yet).

On a final note, I would like to thank my family for a lot of supports.